Expanding the Reach of Electrocorticographic Brain-Computer Interfaces: A Bimanual Approach

Devapratim Sarma

A dissertation
submitted in partial fulfillment of the
requirements for the degree of

Doctor of Philosophy

University of Washington
2017

Reading Committee:

Dr. Rajesh P.N. Rao, Co-Chair
Dr. Jeffrey G. Ojemann, Co-Chair
Dr. Eric H. Chudler

Program Authorized to Offer Degree:
Bioengineering

University of Washington

Abstract

Expanding the Reach of Electrocorticographic Brain-Computer Interfaces: A Bimanual Approach

Devapratim Sarma

Chair of the Supervisory Committee:

Professor and Director Rajesh Rao
Computer Science & Engineering; Center for Sensorimotor Neural Engineering

Professor and Division Chief Jeffrey Ojemann
Neurological Surgery

Brain-computer interface (BCI) technologies have traditionally been designed under the assumption that BCI users are patients who no longer exhibit any significant motor control abilities, due in part to deficits resulting from neuromuscular disease. Of particular interest is the activity that occurs in motor related areas of the brain during precise, dexterous movements of the hand. Previous studies of the central and peripheral motor nervous systems suggest the presence of synergistic activations of musculoskeletal groups during coordinated movement, however the existing clinical technology has not been sufficient for accurate exploration. Among the many features of the cortical response measured by electrocorticography (ECoG), we find that high gamma (75-200Hz) activity in primary motor cortex shows high spatial preference for individual digit movements during overt finger flexions. In contrast, the average spatial activity during object grasping appears to show little unique spatial organization relative to the grasps performed. To investigate this discrepancy, we explore the difference of spatial distribution of activity during dexterous hand movement between traditional (10mm-spacing) and high resolution (3mm) ECoG grids. We find that the informational

density present at the higher scale underscores the potential of synergistic dimensionality reduction as a possible model of prosthetic control. Complicating the gains from resolution, however, is the remnant hand motor function present in a large population of patients interacting with BCIs. This presents a challenge for real-world implementation of these systems for therapy and rehabilitation. Thus, an important question that had yet to be systematically studied within the BCI control architecture is: can subjects use BCIs simultaneously coordinated with overt motor activity? We explored this question by testing if patients could effectively learn to perform and coordinate bimanual control. Patients implanted with ECoG electrodes were trained to interact with a 2-D BCI center-out cursor task in which one dimension of control was modulated by neural activation related to motor imagery and the other dimension was controlled by overt natural movement. Over the course of multiple sessions and days, the subjects gained levels of proficiency and demonstrated accurate control. In addition, this system was implemented for a test case subject with lifelong hemiparesis and significantly impaired bilateral motor abilities brought on by a perinatal stroke. Especially in the stroke case, the subject demonstrated significant proficiency and accurate control, despite confounding ipsilateral and contralateral neural activations. As control improved, activation patterns changed across related cortical areas but without any significant observable changes in the overt motor behavior. In gestalt, this work provides steps and a framework towards adapting ECoG-based BCIs for patients with similar cortical deficits for the purpose of dexterous coordinated hand control.

TABLE OF CONTENTS

LIST OF FIGURES

LIST OF TABLES

ACKNOWLEDGEMENTS

Due to the highly collaborative nature of the burgeoning field of neural engineering in addition to the ethos of the greater scientific community at the University of Washington, I have had the great pleasure and good fortune to work with and learn from a great number of talented and truly amazing individuals throughout my graduate career.

I would first like to thank my advisors Dr. Rajesh P.N. Rao and Dr. Jeffrey Ojemann, the least of which for their unwavering patience and fortitude over perhaps few years too many, as well as my supervisory committee members Dr. Eric Chudler, Dr. Tom Daniel, Dr. Colin Studholme, Dr. Chet Moritz, and Dr. Eberhardt Fetz, for their guidance, advice, conversation, and humanity during my studies.

In addition, the author would like to acknowledge the help and support of members of the GRIDlab & Neural Systems lab who toiled arduously in solidarity: Jeremiah Wander, Lise Johnson, Kurt Weaver, Jared Olson, Felix Darvas, Melissa Smith, Tim Blakely, David Su, Andrew Ko, Kai Miller, Hai Sun, Kelly Collins, James Wu, Nile Wilson, Jeneva Cronin, David Caldwell, Kaitlyn Casimo, Willy Cheung, and Mike Chung. In particular, I would like to underscore the role Miah, Kurt, Jared, and Lise had in shaping my experience and providing much needed mentorship in times of need. Their time and consideration has always been deeply appreciated and valued, especially in the darker moments.

I would also like to thank the Center for Sensorimotor Neural Engineering whose members are a constant source of support, insight and spontaneous collaboration, in particular: Tyler Libey, Brian Mogen, Charlie Matlack, Stavros Zanos, Aiva Ievins, Mark Wronkiewicz, and Tim Brown. In addition, I would like to thank the material and patient support of the members of the University Washington Regional Epilepsy Center. The mentoring and advising of many of the members, past and present, of the Centers and labs were critical in the creation and direction of this document.

DEDICATION

This document is dedicated first to my parents, without whom I would have never thought; to my siblings, without whom I would never be; and to my particular friends and soul family, without whom I would have never made it through. Thank you all for your love and support all these long years.

Thank you to my maternal grandfather, Dr. Harendra Nath Sarma, who passed away as I took my qualifying exam, for teaching me that creativity, passion for learning, and the gusto for life knows no age limit. Also, thank you for not accidentally killing me when "teaching" me how to ride a bike.

Thank you to my paternal uncle, the Honorable Justice Jitendra Nath Sarma, who passed away as I considered applying to graduate school, for showing me the meaning of familial responsibility, for creating a sense of belonging for an immigrant child from America, and for having unwavering faith and conviction in a kid he barely knew. Jai Maa Kali!

Chapter 1: Specific Aims

With nearly two million people in the U.S. suffering from severe neuromuscular deficits resulting from stroke (Grensham, Stason and Duncan, 1995; Wolpaw et al., 2002; Birbaumer, 2006; Leuthardt, Schalk, et al., 2006; Bejot et al., 2008; National Institutes of Health, 2009; Gomez-Rodriguez, Grosse-Wentrup, et al., 2010), central nervous system (CNS) trauma (Wolpaw et al., 2002; Amorim, Isableu and Jarraya, 2006; Leuthardt, Schalk, et al., 2006; Sheets, Stein and Manetz, 2006; Faul et al., 2010; NSCISC, 2010; Coronado et al., 2011; Eng et al., 2011; Of, 2013), amyotrophic lateral sclerosis or ALS (Grensham, Stason and Duncan, 1995; Wolpaw et al., 2002; Birbaumer, 2006), and other neurodegenerative disorders (Wolpaw et al., 2002; Leuthardt et al., 2004; Birbaumer, 2006; Demain et al., 2013), there has been considerable interest in brain-computer interfaces (BCIs) for cognitive and motor rehabilitation (Wolpaw and McFarland, 1994; Wolpaw, McFarland and Vaughan, 2000; Wolpaw et al., 2002; Leuthardt et al., 2004). Using a host of hardware and software, a BCI can bypass a patient's damaged neural pathways by translating modulations in electrophysiological signals from the CNS into output commands to control external or implanted devices, such as robotic prosthetics or spinal stimulators (Schalk et al., 2004; Birbaumer, 2006; Leuthardt, Miller, et al., 2006; Blakely et al., 2009; Daly et al., 2009; Blankertz et al., 2010; Brouwer and van Erp, 2010; Jarosiewicz et al., 2013). These signals, recorded at the single neuron level or as field potentials across various depths and areas in cortical tissue, are representative of cellular actions that drive normal brain communication (Wolpaw et al., 2002; Buzsaki, 2006; Buzsáki, Anastassiou and Koch, 2012). The neuron level recordings, while allowing for focally and temporally rich information, are, unfortunately, highly surgically invasive (Fetz, 1969; Wolpaw et al., 2000; Buzsáki, Anastassiou and Koch, 2012). Thus, though there is some tradeoff in signal quality, for human patients, field potentials, recorded at various distances from the brain with electroencephalography (EEG) at the scalp and ECoG arrays directly over cortical tissues from within the skull, provide for a more tractable BCI signal. Motor imagery (MI) based BCIs, in which cortical activity changes during imagined motor behavior drive control, dominate the landscape of human BCI control paradigms, though not all patient populations can necessarily utilize this pathway (Palaniappan et al., 2002; Curran and Stokes,

2003; Palaniappan, 2006; Wang et al., 2007; Daly et al., 2009; Faradji, Ward and Birch, 2009; Blankertz et al., 2010; Jensen et al., 2011; Myrden et al., 2011). With recent advances in computing power and mobile hardware, significant strides have been made in the realms of signal processing and device control using increasingly complicated algorithmic strategies to improve system performance.

These strategies, however, dependent as they are on coarse representations of cortical activity and relying primarily on simplistic single source to end state feed forward models, rarely result in intuitive or successful dynamic control schema. To allow for truly biomimetic control, as seen in studies with non-human primates, robust systems with high degrees of freedom must be developed. This necessitates both a better understanding of the cortical dynamics during BCI control as well as an improved resolution in the recorded signals without additional invasiveness. Our **central hypothesis** is that with improved signal resolution and a naturalistic architecture designed around bimanual coordination, users will learn BCI control faster and with better performance, and be able to utilize systems with a higher degree of complexity. Specifically, we:

Aim 1: Develop a bimanual framework to examine the dynamics of hemispheric control

Brain-computer interface (BCI) technologies have traditionally been designed under the assumption that BCI users are patients who no longer exhibit any significant motor control abilities. However, there is a much larger population of patients who retain some residual motor function, who could benefit significantly from BCIs. An important question that has yet to be systematically studied is: can subjects use BCIs simultaneously coordinated with overt motor activity, e.g., for bimanual control? To that extent, we designed a set of bimanual BCI tasks, tested initially with subjects using a noninvasive electroencephalographic (EEG) framework, to determine the logistical implications and constraints of bimanual coordination of motor imagery and overt motor control.

Aim 2: Evaluate changes in cortical dynamics during coordinated bi-manual control of a virtual object

The ability to volitionally control brain activity without modifying overt behavior is very important in BCI applications. However, motor and cortical deficits vary widely across patient populations. In many cases, there remains residual cortical activity related to motor and somatosensory execution. These residual signals are unlikely to be suppressed during BCI use, instead co-activating during control. This would especially occur during any sort of bi-manual task needed

for daily function. Through this aim, we utilize electrocorticography (ECoG) to examine distributed changes in cortical activity related to simultaneous overt and imagined motor behavior during bi-manual control of a virtual object. In addition, we further examine the transient changes during the BCI learning process to evaluate possible markers of cortical adaptation during BCI use related to the coordination of multiple control schema.

Aim 3: Demonstrate the feasibility of coordinated bimanual BCI control for patients with neuromuscular disease

Nominally, almost all BCI research is motivated by particular disease states. However, the preponderance of non-invasive and semi-invasive studies focus primarily on cognitive or behavioral experiments with 'healthy' subjects without truly evaluating the scalability to applications for real use cases. Here we show that a subject with lifelong hemiparesis implanted with ECoG electrodes can learn to perform a 2-D BCI center-out cursor task in which one dimension of control is modulated by motor-imagery related ECoG activity and the other dimension is controlled by overt natural movement. Furthermore, we explore the effects of confounding ipsilateral and contralateral neural activation due to natural movements on BCI control. We also investigate task-related adaptation across cortical areas in the hybrid BCI-manual control task and its relationship with overt motor behavior.

Aim 4: Evaluate cortical representations of human hand dynamics for online control of a robotic hand

Traditional control paradigms transform gross hand movements or imagined hand movements into single-axis cursor control. For dexterous control of an actual robotic hand or prosthetic with up to twenty-one degrees of freedom, a single degree of control is insufficient, especially in consideration of bimanual coordination. However, from a mechanistic control perspective, the brain is also likely utilizing some form of dimensionality reduction to affect its own control of the hand. We hypothesize, this may be represented cortically as differing patterns of activity related to prototypical finger and hand movements. Here we show that clinical ECoG grids, though functional, may not necessarily be sufficient to fully decode these patterns. High-density micro-ECoG arrays may be key in enabling robust control and control of a virtual hand or robotic system.

Providing a framework to train bimanual naturalistic dynamic control during closed-loop control of BCIs will enable our **long-term goal** to develop advanced BCIs for real world applications. Successful implementation of these aims will also lead to an enhanced understanding of the neural dynamics of cortical control during high-dimensional volitional modulation of electrophysiological signals. The proposed work promises to develop better understanding of how improved signal scale and bimanual coordination can influence the way the subjects adapt within an abstract BCI framework as well as how signals from the brain can be used to convey information and used for control in future therapy or rehabilitative applications.

Chapter 2: Neuromuscular Disease and the Rise of the BCI

The philosophy of embodied cognition would hold that an agent's cognition is strongly influenced by aspects of said agent's body beyond the brain itself. Put more simply, an individual's perceptual self and corresponding actions can be defined or shaped by their physicality as juxtaposed with the world around them. Indeed, an individual's ability to physically interact with the world often defines their identity or sense of self. Unfortunately, there exist a host of neuromuscular disorders and physical impairments, with a vast range of etiologies, which can severely impact an individual's somatosensory function and volitional motor abilities. Individuals with these types of impairments are often no longer able to dexterously move within or manipulate their environments or find themselves incapable of physically communicating. In many cases, their impairments result in the loss of both types of behavior. Promisingly, due to many of the ongoing advancements in robotics, machine learning, wearable computing, material fabrication, and neurophysiological bio-sensing, the field of neural engineering has developed to the point of being able to develop brain computer interface (BCI) technologies that may give researchers and clinicians the opportunity to restore these lost functions for affected populations. However, BCI devices are currently quite limited and do not perform well enough to fully replace or advance beyond the current state of the art therapies or treatments. To understand how these systems might be improved or redesigned for better efficacy, we must first examine the nature of impairment and the corresponding development of BCIs.

2.1 The Nature of Impairment

Neuromuscular disorders are a broad class of ailments that can cause loss of function through one or more of the following means: (1) by disrupting the central nervous system's ability to generate an appropriate motor command, (2) by disrupting the transfer of information from the central to the peripheral nervous system, or (3) by disrupting the peripheral nervous system's ability to effectively execute that motor command. Amyotrophic lateral sclerosis is one type of disorder, and likely the most historically cited for BCI development, which in its advanced stages causes the most severe types of broad function loss. However, there are numerous others including traumatic brain injury, stroke and spinal cord injury. These disorders have been seen to already affect nearly two million, and growing, people in the United States, and many more worldwide (Murray et al., 1996). Severity varies from patient to patient, and can range from mild impairment of motor function to complete

loss of voluntary muscular control (i.e., in the case of late stage ALS), an affliction that is referred to as locked-in syndrome (Smith and Delargy, 2005).

Current treatments for neuromuscular disorders vary widely in concordance with the severity of the ailment, but can be separated into two primary groups. In the event that limited muscular function remains (e.g., some cases of ischemic stroke or incomplete spinal cord injury), rehabilitative physical therapy (Pascual-Leone et al., 2005) may be used as a recourse to attempt to restore as much of the lost function as is possible. Experimental enhancement of physical therapy via transcranial magnetic stimulation (TMS) (Plautz et al., 2003; Harvey and Nudo, 2007), transcranial direct-current stimulation (tDCS) (Schlaug, Renga and Nair, 2008), and direct cortical stimulation (DCS) (Adkins-Muir and Jones, 2003; Adkins et al., 2006; Adkins, Hsu and Jones, 2008; Huang et al., 2008; Levy et al., 2008; Plow et al., 2009) has also being explored in the past decades to limited success. In cases where rehabilitative therapies are not an option, such as in the advanced stages of ALS or other degenerative disorders, other means have been explored to replace lost function using eye-tracking and blink interfaces (Doble et al., 2003) or other types of assistant-mediated communication (Wu and Voda, 1985). Though these strategies have been effective at providing some patients with a simulacrum of their original function, they leave much to be desired in terms of complete restoration or replacement.

2.2 The Rise of Neural Interfaces

In response to this clinical need, over the past two decades, many researchers have been investigating directly interfacing with the nervous system as a means to create rehabilitative and assistive devices that would provide patients with a significantly greater portion of their original function than the current standard of care (for more in-depth reviews see Green & Kalaska, 2011(Green and Kalaska, 2011); Moran, 2010; Wander & Rao, 2014; Wolpaw et al., 2002). Researchers have been attempting to build interfaces to the nervous system at a number of different levels, including the cerebral cortex, the spinal cord, and even the neuromuscular junction; the versions of these devices that interface with the cortex are referred to as BCIs or alternatively brain-machine interfaces (the latter primarily in the context of animal studies). In the context of restoring lost motor output, the purported mechanism of action for an assistive BCI is to record neural activity 'upstream' of where an ailment has impacted the nervous system, and then decode that activity to determine the patient's intended action, an external device can be driven to carry out that action.

The current major testbeds for BCI research can be categorized into the following: cursor control and communication in tetraplegic and locked-in patients (Kübler et al., 2001; Hochberg et al., 2006) and neural control of prosthetic arms (Pfurtscheller et al., 2000; Carmena et al., 2003; Velliste et al., 2008). As alluded to before, many researchers have focused on the latter population of patients as appropriate short-term targets since the prospect of restoration of communication to locked-in patients may soon outweigh the risk associated with the current invasiveness of many BCI electrode implantation procedures (Moran, 2010; Gilja et al., 2011).

It is important to note that BCI is, in itself, a non-specific term applied to a variety of system architectures ranging from BCIs for motor control to deep brain stimulators (DBS) for the treatment of clinical depression and beyond. As per the clinical considerations discussed so far, for the duration of this section, the focus will be to provide of brief review of the state of the art for motor control based BCIs. Correspondingly, we consider only BCI schema which leverage volitional modulation of neural activity for the manipulation of some type of end effector, i.e., a computer cursor or robotic limb analog. In the foundational work of this field, Fetz and colleagues demonstrated in non-human primates that, when given feedback, the brain could learn to volitionally modulate the activity of single neurons (Fetz, 1969). In this experiment, the estimates of individual firing rates of a small number of cortical neurons were mapped directly to a simple visual feedback device, and the subject developed the capacity to modulate these firing rates, effectively controlling a simple, one-dimensional (1-D) BCI. A similar feat was accomplished decades later in humans by Wolpaw and colleagues using, in this case, a non-invasive approach, mapping spectral (mu-beta) changes recorded at the scalp to vertical control of a cursor on a computer monitor (Wolpaw et al., 1991). Since these initial studies, the primary investigative and engineering push in the field has been to increase the dexterity, robustness, and clinical viability of these devices across all scales of electrophysiological investigation, with a corresponding disparity in the functional ability of the "state of the art" related to the degree invasiveness. In humans, aggregate activity from a large numbers of neurons (field potentials) has been used to control end effectors in up to three dimensions (McFarland, Sarnacki and Wolpaw, 2010; Wang et al., 2013) with the high-bar currently set by Collinger and colleagues who were able to train a human user in their system to control a seven degree of freedom (DOF) robotic arm using neural signals recorded with a microelectrode implant (Collinger et al., 2013). Unfortunately, direct comparison across these and other experiments is extremely difficult because

of inconsistencies in task paradigms and evaluation metrics (Thomas, Dyson and Clerc, 2013). In addition, in recent years, the convergence of system scale and robotic automaticity, has changed the benchmarks and focus of many of these studies towards more coadaptive bidirectional action-perception frameworks (Gage et al., 2005; Vidaurre et al., 2011; Faller et al., 2013).

There are a number of impediments to the long-term clinical deployment of brain-computer interfaces, including host-response to implanted electrodes, long-term power requirements, and wireless communication of neural signals to remote devices. One of the largest road-blocks in the development of these devices is simply that their performance relative to the current standard of care is not good enough to warrant the risk and cost to the patient (Gilja et al., 2011). As a result, there is a collective push in the field to increase BCI performance in applications that restore a patient's ability to communicate or to control external devices. There are a number of approaches being investigated; the two most common being an increase of coverage density in motor cortex (i.e., higher number of input channels per unit area) and development of more sophisticated decoding algorithms (i.e., extracting more robust signals from the input channels). Recent work by the Schwartz (Wang et al., 2013) and Shenoy (Gilja et al., 2012) groups, respectively, provides examples of developments in these two directions. Other groups are working in a different, but potentially complimentary direction, constructing BCI systems that maximize the performance gains made possible by the tremendous adaptive capability of the brain (Orsborn et al., 2012).

An important point to note, however, is that the vast majority of BCIs harness signals recorded solely from primary motor cortex (M1) or premotor cortex (PMv / PMd) (Wolpaw et al., 1991; Blakely et al., 2009; Simeral et al., 2011; Wang et al., 2013). An exception to this is the line of research being pursued by Andersen and colleagues that utilizes activity patterns in posterior parietal cortex (PPC) (Mulliken, Musallam and Andersen, 2008) though this approach still utilizes firing rate changes in a single cortical area to achieve BCI control. In addition, work out of our group (Wander and Rao, 2014), examining the nature of BCI learning, underscores what we know from a vast body of electrophysiological and imaging motor studies, that the generation of dexterous, goal-directed movement is a coordinated effort on the part of multiple cortical areas, and that the functional roles being carried out in these areas are diverse. Correspondingly, we posit that BCI schema may benefit significantly from the analogous incorporation of multiple streams of task-relevant information across a variety of cortical sources. One example of this type of BCI scheme might be a system which

decodes, from one set of cortical structures, an individual's higher-level goal and, from another area, the low-level BCI motor commands they are utilizing and utilizes both channels of information to improve BCI performance (Shanechi et al., 2013). This notion of hybrid BCI is discussed more in chapter 6 where we employ control signals at multiple levels of abstraction to attempt bimanual control (Cheung et al., 2012), but overall it has yet to reach its full potential. However, to better understand the difference in these approaches, it is important to examine the difference in the underlying electrophysiological scale of the systems.

2.3 Electrophysiological Models for BCI

There are two primary classes of physiologic signals used to drive BCIs: electrophysiologic or hemodynamic. Electrophysiological recordings range in scale and invasiveness from highly-invasive single-unit activity (Carmena et al., 2003; Lebedev et al., 2005; Jackson, Baker and Fetz, 2006; Moritz, Perlmutter and Fetz, 2008) and local field potentials (LFP) (Moran, 2010) to semi-invasive ECoG(Felton et al., 2007; Schalk et al., 2008; Blakely et al., 2009; Krusienski and Shih, 2011; Wander et al., 2013) and finally to non-invasive electroencephalography (EEG) (Moran, 2010; Pfurtscheller, 2010) or magnetoencephalography (MEG) (Mellinger et al., 2007). Hemodynamically driven BCIs typically rely on noninvasive methods such as blood-oxygen level dependent (BOLD) changes as measured by fMRI (Sitaram et al., 2008) or functional near infra-red spectroscopy. Alternative modalities such as optogenetic and ultrasound-based imaging methods also exist, though these are much less common and not necessarily scalable across species to humans. As indicated previously, we will instead focus on electrophysiological recordings and discuss the relative merits and demerits of each 'scale' in the context of real-time BCI for control of an abstract end effector. In addition, further sections below will examine our group's work with ECoG and why it is, perhaps, the most appropriate signal modality for the work described throughout this document. The methods used to acquire these signals range from very invasive (single unit activity and LFP) to minimally or semi-invasive (ECoG) to non-invasive (EEG). In general, there is a formidable tradeoff with spatial resolution, temporal resolution, or both as less invasive signal acquisition methods are used (Moran, 2010; Gilja et al., 2011). The majority of BCI experiments as well as pre-clinical BCI applications (Flor et al., 1995; McFarland, Lefkowicz and Wolpaw, 1997; Birbaumer et al., 2000; Pfurtscheller et al., 2000; Wolpaw and McFarland, 2004) use EEG as a signal source because it is non-invasive, healthy test subjects are readily available, the necessary equipment is comparatively inexpensive, signal

quality typically does not degrade over time, and the use of EEG in humans does not impose the same regulatory burdens as ECoG or microelectrode recordings. Within the EEG modality, BCIs have been constructed that use evoked potentials such as the visual evoked potentials in the P300 speller, volitional changes in slow cortical potentials, and volitional event-related desynchronization and/or synchronization of the sensorimotor rhythms (SMR) mu and beta (Wolpaw et al., 2002). Regrettably, there are a number of factors that currently make EEG poorly suited for clinical deployment and for the purposes of the study described below. First, the dura mater, cerebrospinal fluid (CSF), skull and scalp collectively act to spatially mix and low-pass filter the true cortical potentials, such that the potentials recorded at the surface of the scalp have lost tremendous spatial specificity and typically do not contain frequency content above approximately 60 Hz. Second, EEG is easily contaminated by surface electromyographic (EMG) potentials as well as ambient electromagnetic noise (e.g., 50/60 Hz line noise) resulting in a relatively poor signal to noise ratio (SNR). As a result, EEG-based BCI typically use classification-based decoder architectures (selecting from a discrete set of control parameters) as opposed to regression-based decoder architectures (mapping to a continuous space of control parameters), and require longer time intervals over which to average observations to collect a statistically robust assessment of the underlying neural activity.

At the other end of the spectrum are electrophysiological recordings made using invasive microelectrodes, such as the Utah electrode array (UEA), a microelectrode array consisting of 100, 1-1.5 mm long electrodes configured in a 10x10 grid with an inter-electrode spacing of 300-400 µm. The electrodes themselves are shielded along the shank and conductive only at the tip. It is immediately apparent that there is a tremendous difference in spatial specificity between the UEA and an EEG system. However, it is important to note that the UEA itself records from an area of less than 13 square millimeters, making correct placement over anatomical areas a critical component of experimental design and execution; microelectrode recordings from distributed cortical sites require multiple implants. The UEA and other microelectrode recording devices are designed to record extracellular action potentials and LFPs from nearby cell bodies, thus they are typically placed such that the conductive tip sits as near to the layer V pyramidal neurons as possible. Action potentials recorded from these neurons provide an extremely high-fidelity signal that has been utilized in a BCI for continuous end effector control on numerous occasions (e.g., Fetz, 1969; Simeral et al., 2011). Though these signals provide excellent fidelity and have been demonstrated to be highly capable of

adaptation to task requirements (Fetz, 1969; Fetz and Baker, 1973; Ganguly and Carmena, 2009; Ganguly et al., 2011), the long-term recording of activity from single units is a difficult technical task that has yet to be solved completely. Though there are limited instances of microelectrode implants that can still record sufficient neural activity to control a BCI up to 3 years post-implant (Simeral et al., 2011), in most cases, either due to movement of the array or underlying physiological changes such as those from a foreign body response (Shain et al., 2003), intracortical implants are functionally limited to shorter operating time-frames (Kipke et al., 2008).

A signal modality that strikes a compromise between these two is ECoG. ECoG is referred to as a minimally invasive recording technique as it still requires surgery to implant the necessary electrodes, but the electrodes lie on (instead of penetrating) the pial surface. ECoG has even been demonstrated to allow for successful acquisition of spectral components up to 200 Hz when recorded epidurally (Gomez-Rodriguez, Grosse-Wentrup, et al., 2010), potentially further lessening its invasiveness. ECoG signals are almost exclusively acquired in the context of clinical treatment for intractable epilepsy wherein patients undergo long-term monitoring (approximately seven days) of ECoG activity during ictal events for the identification and eventual resection of a seizure focus. Within the context of motor function and cognitive processing, there are two frequency ranges of the ECoG signal that have been focused on heavily in the literature. They are a band-limited, low frequency feature (12-25 Hz), which is the ECoG correlate of the mu-beta rhythm discussed in EEG literature, and a broadband, high frequency feature (70-200 Hz), referred to as high-gamma (HG). Changes in HG activity have been postulated to reflect changes in the overall firing rate and/or firing synchrony of underlying neural populations (Miller et al., 2007; Ray et al., 2008). Changes in HG activity are more spatially focal than changes in the mu/beta band (Miller et al., 2007), and have subsequently been used more often in research that uses the ECoG signal modality as a temporally and spatially local indicator of underlying cortical processing. This signal has been applied to a number of ECoG BCI paradigms, typically with changes in spectral estimates of HG power being directly mapped to end effector control parameters (Schalk et al., 2008; Blakely et al., 2009).

2.4 Brain-computer Interfaces and Electrocorticography

A little over a decade ago, ECoG cortical potentials were first leveraged as control signals for a BCI application (Leuthardt et al., 2004). Since that time, a number of subsequent studies have demonstrated not only that ECoG BCI users are capable of performing multiple simultaneous types

of motor imagery to achieve multiple dimensions of control (Schalk et al., 2008; Wang et al., 2013), but also that ECoG BCI can be successfully used over multiple days without the need for classifier retraining (Blakely et al., 2009). ECoG BCIs are generally controlled through volitional modulation of HG activity at one or more electrodes; in humans, initial execution of the task is done through the use of a motor (e.g., hand motor imagery) or cognitive (e.g., mental arithmetic) task that modulates activity in the controlling electrodes. Because clinical-scale ECoG grids typically cover approximately 64 cm2 of cortical tissue, and are only controlled by a subset of the electrodes in the grid, ECoG BCIs provide an excellent opportunity to probe the nervous system for additional physiological details relevant to BCI use (Wander & Rao, 2014). One example of this is a recent study demonstrating a spatially focal change in sleep spindle density correlated with training on BCI task, a finding suggestive of offline learning taking place in the brain after having the opportunity to perform the highly novel BCI task (Johnson et al., 2012). Additionally, this study was followed by another which showed that BCI learning closely mimics general motor learning (Wander et al., 2013) in terms of cortical areas affected or involved during the learning process. Both were produced by our research group.

2.4.1 Disadvantages of ECoG BCI

It is important to note that ECoG data are collected in an opportunistic recording model. With few exceptions, ECoG subjects are undergoing long-term monitoring for epileptic focus identification and resection. Depending on the etiology of their epilepsy, these subjects can exhibit a range of neural complications, including but not limited to inter-ictal activity and cortical reorganization (Hill et al., 2012). The full extent of how epilepsy impacts the nervous system is still largely unknown and likely varies across individuals; conclusions drawn from studies based on this patient population must be accompanied by this consideration. In addition to this, the median duration of observation for epileptics undergoing this procedure is 7d. Typically subjects are neither able nor willing to participate in research studies until the third or fourth post-operative day, which limits the amount of training time a given subject can receive on the BCI to at most four days. Extensive studies on cortical adaptation associated with BCI (e.g. responses to perturbation after the user achieves a learned state) use are extremely difficult under these circumstances.

2.4.2 Advantages of ECoG BCI

These caveats to the research use of ECoG recordings notwithstanding, ECoG-based BCIs possess several advantages relative to SUA and EEG-based BCIs that make them the appropriate tool

for the inquiry discussed in this document. First, because the electrodes are not typically moved from day-to-day, and the cortical potentials are fairly stationary, ECoG BCIs allow for robust control over the course of multiple days without retraining of the classifier (Blakely et al., 2009). ECoG recordings easily remain consistent over multiple days, and have been shown to perform well for up to 30 days (Wang et al., 2013) with daily classifier updates. Relative to scalp surface potentials, ECoG presents an excellent opportunity for BCI research because, as of yet, there are no robust computational algorithms for extracting spatially focal HG activity from EEG on a single trial basis. Work is being performed to construct an inverse model that will permit us to back project likely cortical sources of EEG data (Darvas et al., 2004, 2010), thus increasing SNR and potentially providing access to information in the HG range at the scalp. As was mentioned above, ECoG provides an excellent compromise (relative to EEG and microelectrodes) of spatial distribution of coverage and signal fidelity, making it an appropriate tool for the investigation of activity patterns in diverse cortical areas during BCI use as well as enabling schema with multi-site control.

To that extent, however, it becomes important to understand the actual nature of motor control and the dynamics of this control within the abstracted BCI architecture. Though ECoG might be an ideal modality of recording, without an understanding of the areas in consideration, nor the aspects of behavior and control that are relevant to natural volitional movement, our methods may be doomed to misery. The following chapters attempt to examine these issues before describing our raison d'être, incorporating dynamic dexterous bimanual control within the framework of brain-computer interfaces.

Chapter 3: Effecting Control I – The Brain & Motor Control

Motor control can refer to the cognitive or physiologic processes by which humans and animals activate and coordinate the muscles and limbs involved in the performance of a motor skill. Fundamentally, it is the integration of sensory information, both about the world and the current state of the body, to determine the appropriate set of muscle forces and joint activations to generate some desired movement or action. This process requires cooperative interaction between the central nervous system and the musculoskeletal system, and is thus a problem of information processing, coordination, mechanics, physics, and cognition (Mitz and Wise, 1987; Vaid, 2002; Rosenbaum, 2009). Successful motor control is crucial to interacting with the world, not only determining action capabilities, but regulating balance and stability as well. The organization and production of movement is a complex problem and so, accordingly, the study of motor control has been approached from a wide range of disciplines, including psychology, cognitive science, biomechanics, and neuroscience. While the modern study of motor control is an increasingly interdisciplinary field, the corresponding research questions have historically been defined as either physiological or psychological, depending on whether the focus is on physical and biological properties, or organizational and structural rules (Schmidt, 1988). Brain-computer interfaces attempt to bridge various aspects of these properties to restore "lost" function. As such it is important to have some familiarity with both the physiologic and behavioral models of motor control to identify the aspects in which BCIs become relevant in situations of deficit or damage.

3.1 Relevant Motor- and Neuro- Physiology

An extensive review of neurophysiology and motor physiology is beyond the scope of this document. For additional information, the reader is encouraged to review the seminal text by Kandel and Schwartz (Kandel & Schwartz 2012). However, in an effort to provide context for the experimental designs, results, and discussions that follow, we will provide a brief summary of the cortical structures relevant to BCI use, and the underlying neurophysiology that is leveraged in the electrophysiological recording models described below.

3.1.1 Components of the Motor Cortex

Three prominent areas of the motor cortical system are:

1. The *primary motor cortex* (M1) is the main contributor to generating neural impulses that pass down to the spinal cord and control the execution of movement. However, some of the other motor areas in the brain also play a role in this function. M1 is located on the anterior paracentral lobule on the medial surface and is the focus of most BCI motor studies.

2. The *premotor cortex* (PMC) is responsible for some aspects of motor control, possibly including the preparation for movement, the sensory guidance of movement, the spatial guidance of reaching, or the direct control of some movements with an emphasis on control of proximal and trunk muscles of the body. PMC is located anterior to the primary motor cortex

3. The *supplementary motor area* (or SMA), has many proposed functions including the internally generated planning of movement, the planning of sequences of movement, and the coordination of the two sides of the body such as in bi-manual coordination. SMA is located on the midline surface of the hemisphere anterior to the primary motor cortex

The posterior parietal cortex (PPC) is sometimes also considered within the motor cortical areas; however it is best to regard PPC as more of an association cortex rather than motor. It is thought to be responsible for transforming multisensory information into motor commands, in addition to being responsible for some aspects of motor planning, as well as many other functions that may not be motor related.

The primary somatosensory cortex, especially the part called area 3a (as per the Brodmann Area referencing convention, Brodmann 1909), which lies directly against the motor cortex (see Figure 1), is sometimes considered to be functionally part of the motor control circuitry. Other brain regions outside the cerebral cortex are also of great importance to motor function, most notably the cerebellum, the basal ganglia, pedunculopontine nucleus and the red nucleus, as well as other subcortical motor nuclei. These structures are deeper and not readily accessible by most current electrophysiological recording modalities and, as such, are not within the scope of most BCI studies.

3.1.2 Primary Motor Cortex

The cerebral cortex is spatially organized into areas that have been linked with specific functions, initially through post-mortem correlation of behavior with the locations of damage or

lesion (Brinkman, 1981), and now, through *in vivo* functional imaging and electrophysiology. When locating cortical areas associated with motor outputs from the body, one of the most important cortical landmarks to identify is the central sulcus (marked in red in Figure 1), which starts at the lateral fissure and travels superiorly and posteriorly. It separates the frontal lobe and the parietal lobe. Canonically, the gyrus anterior to the central sulcus, called the pre-central gyrus, is referred to as M1, though cytoarchitectonic delineations specify that M1 comprises only the posterior half of the lateral portion of the pre-central gyrus (M1 corresponds to Brodmann Area [BA] 4). The majority of descending afferent motor tracts that carry neural activity that will eventually result in motor output originate in M1.

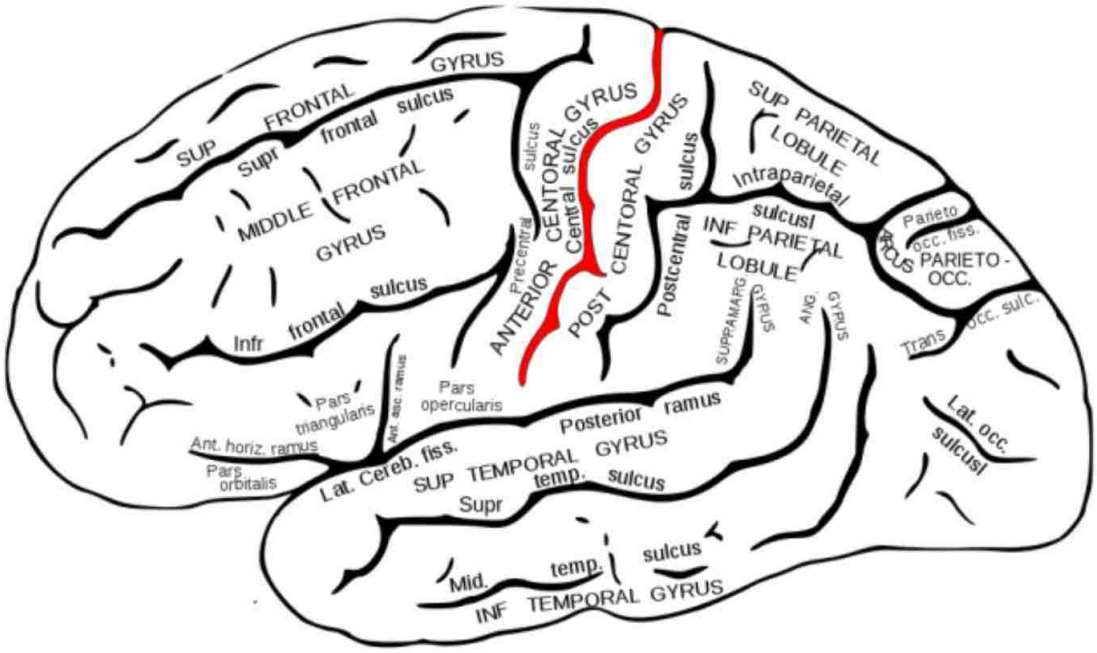

Figure 1 – Drawing of generalized Cortex with anatomical labels. Lateral view of the human brain, the central sulcus is highlighted in red. Image is public domain, source: http://commons.wikimedia.org

As was determined in the 1930s (Penfield & Boldrey, 1937), motor cortex itself is somatotopically organized such that the motor outputs of the body are represented in an orderly fashion across M1. This can be seen in the image of the motor homunculus, below. Another feature of the motor representation on M1 that is important to the use of these neural populations for BCIs is that the amount of cortical area dedicated to a specific part of the body is related to the degree

and precision of motor control executed in that part. Consequently, the motor cortical representation of face and hand movements is very large in humans and non-human primates (NHPs).

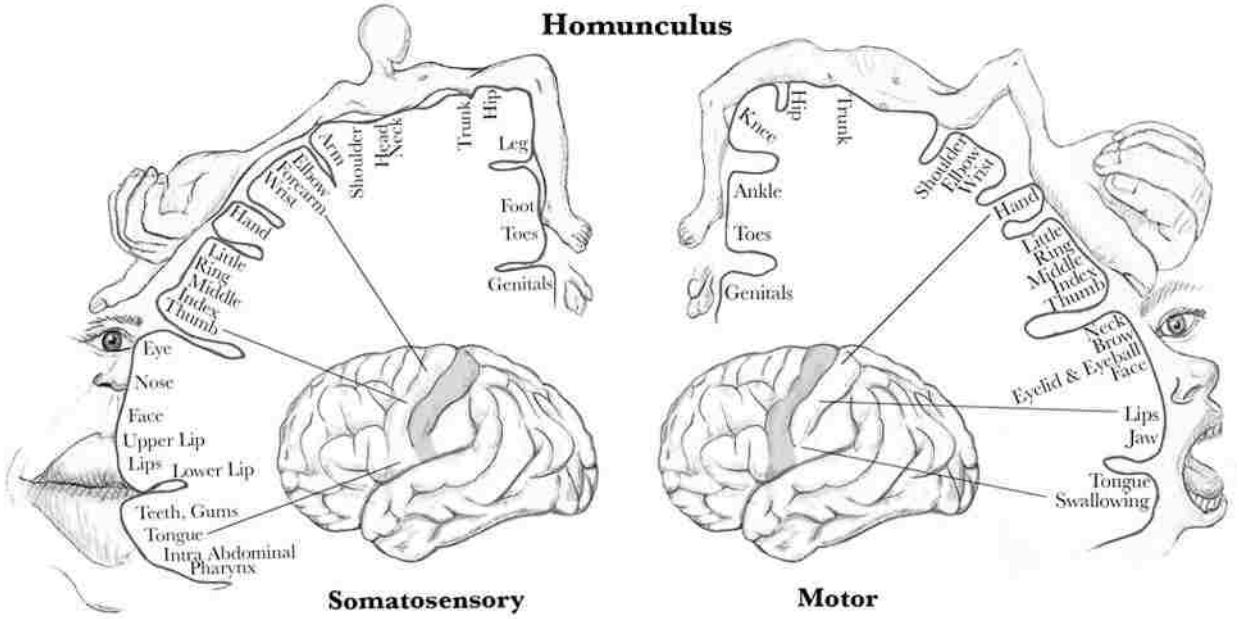

Figure 2 - Cartoon of the Motor and Somatosensory Homunculus. Relative arrangement of M1 and SMA shown in regards to the functional anatomy or function. Hand and Tongue areas are highlighted. Image is public domain, source: http://commons.wikimedia.org

This large representation of hand and face movement, combined with the somatotopic organization of M1 is one of the primary reasons that it is often selected as a target site for BCI, however there are other critical reasons that should also be noted. First, layer V of M1 contains the cell bodies of many large pyramidal neurons, from which extracellular recordings can be readily taken, and which (because of the orientation of their dendritic arbor and their columnar organization) generate relatively discernible cortical and scalp potentials. Second, an extensive foundation of motor electrophysiology studies has demonstrated strong directional tuning between M1 pyramidal neurons and position and velocity of distal limbs, allowing for BCI decoders to be seeded with parameters derived from neural recordings taken during overt motor movement.

3.1.3 Non-M1 Frontal Cortices

Directly anterior to M1 and extending from the lateral sulcus to the superior frontal sulcus is the premotor cortex (BA 6), which is further divided into dorsal and ventral areas (PMd and PMv). Superior to this and wrapping around to the medial aspect of the brain, stopping at the cingulate sulcus is the supplementary motor area (SMA); coverage of this portion of the brain is exceedingly

rare in an ECoG epilepsy model and is thus not discussed extensively in the remainder of this document. Premotor areas, on the other hand, are commonly covered during epilepsy monitoring and thus provide an excellent first candidate region for BCI-relevant extra-M1 neural activity. PMv has been studied extensively in NHPs, and is traditionally held to be involved in preparatory motor activity related to hand motion (Rizzolatti & Luppino, 2001; Weinrich & Wise, 1982) , and during the movement for both reaching and grasping actions (Xiao et al., 2006). Additionally, so-named "mirror neurons" in PMv have been seen to respond to observation of relevant movements (Rizzolatti et al., 1996).

Though also active during preparation (Mauritz & Wise, 1986), PMd has been demonstrated previously to be more associated with trajectory planning and control of the more proximal musculature involved in reach motions (Pesaran et al., 2006). In an NHP model, cells have been found in PMd that respond to changes in characteristics of the target of a reach (Shen & Alexander, 1997), which, when taken with the above, implies a role for PMd in the translation of a reach target to a motor command through the use of internal models. Collectively, the area of brain anterior to the premotor areas is called prefrontal cortex (PFC), further subdivided into a number of regions that vary, to some degree depending on the body of literature in which they are being discussed. In general PFC is considered the cortical center for executive control (Fuster, 2000) and a critical region for orchestrating coordinated complex behaviors to achieve higher- level goals (Miller & Cohen, 2001). Various regions of the PFC have also demonstrated involvement in complex, goal-driven behavior in both human (Rudorf & Hare, 2014) and NHP (Kobayashi et al., 2007) models.

3.1.4 Parietal and Temporal Cortices

Posterior to the central sulcus is primary somatosensory cortex (S1; BAs 1-3). Though it is not discussed extensively in the context of this document, it is one of the sensory processing areas – along with auditory and visual processing areas – that provides sensory information to its more caudal neighbor, the posterior parietal cortex (PPC; BAs 5 and 7). PPC is a group of cortical regions, located, as the name implies, in the posterior portion of the parietal lobe. It is bisected by the intraparietal sulcus (IPS) into the superior and inferior parietal lobules (SPL and IPL, respectively). The PPC on the whole is an associative cortical region implicated in planning and online control of visually guided movements (Buneo & Andersen, 2006a; Mulliken et al., 2008). A significant amount of work has gone into understanding the subregions of PPC and their particular functional roles in the variety of motor

movements carried out by primates (reviewed in Vesia & Crawford, 2012). It is worth noting that the terminology between the two species differs and can be confusing. In NHPs, we commonly discuss three major regions the PPC: the parietal reach region (PRR), the lateral intraparietal area (LIP), and the anterior intraparietal area (AIP). These areas are classically associated with reaching, saccades, and grasping respectively (Rizzolatti et al., 1998). The human homologues are slightly less well defined, but they are the mid-posterior IPS (mIPS), mIPS and the parieto-occipital sulcus (SPOC), and the anterior IPS (aIPS), respectively. Recent imaging studies have begun to demonstrate similar roles for these regions, though the functional separations do not appear to be as strict (Gallivan et al., 2011, 2013).

Inferior to the IPL, surrounding the supramarginal gyrus, where the temporal and parietal lobes meet is a region called the temporoparietal junction (TPJ; BAs 22, 39 and 40). Though not explicitly involved in reach and grasp planning, the TPJ is implicated in a number of cognitive functions. Of particular interest to its potential role during BCI execution is evidence of involvement in bottom-up modulation of sensory inputs relevant for target selection (Geng & Mangun, 2011).

Anterior and inferior to this is another cortical region of interest, namely the posterior portion of the superior temporal gyrus (STG). Classically thought to be involved primarily in emotional, social and language-related processing (Friederici & Rueschemeyer, 2003; Radua et al., 2010), the STG has recently been demonstrated to be involved in multiple cognitive processes that may be highly relevant to neuroprosthetic control. More specifically, the posterior portion of the STG has been demonstrated to be activated during selective processing of visual stimuli (Hopfinger et al., 2000) and during observation of geometric shapes that were following goal-directed trajectories (Schultz et al., 2004). The discovery and understanding cognitive process as per the particular cortical areas are also key aspects of the behavioral models alluded to initially and discussed further below.

3.2 Considerations for Modeling Motor Control with BCI

Beyond understanding the direct function of physiologic areas that could be replaced by specific targeted brain-computer interfaces, it is important to understand the behavioral models in which most BCI schema will generally find themselves couched in consideration of restoring lost function. These models also closely mimic traditional control theory approaches for distributed electronic systems.

3.2.1 Sensorimotor Feedback

The way bodies move in response to external and internal stimuli (perceptive and proprioceptive) is a key component of motor controls and greatly affects the development and execution of motor programs. There are two general schema into which these strategies fall.

3.2.1a Closed Loop Control

The classical definition of a closed loop system for human movement comes from Jack A. Adams:

"A closed loop system has feedback, error detection and error correction as key elements. There is a reference that specifies the desired value for the system, and the output of the system is fed back and compared to the reference for error detection and, if necessary corrected... A closed loop system is self-regulating by compensating for deviating from the reference."(Adams, 1971)

Most movements that are carried out during day-to-day activity are formed using a continual process of accessing sensory information and using it to more accurately continue the motion. This type of motor control is called feedback control, as it relies on sensory feedback to control movements. Feedback control is a situated form of motor control, relying on sensory information about performance and specific sensory input from the environment in which the movement is carried out. This sensory input, while processed, does not necessarily cause conscious awareness of the action. Closed loop control is a feedback based mechanism of motor control, where any act on the environment creates some sort of change that affects future performance through feedback (Schmidt, 1988). Closed loop motor control is best suited to continuously controlled actions, but does not work quickly enough for ballistic actions. Ballistic actions are actions that continue to the end without thinking about it, even when they no longer are appropriate. However, as this type of feedback control relies on sensory information, it is naturally constrained to be as slow as sensory processing. These movements are also subject to a speed/accuracy trade-off, because sensory processing is being used to control the movement, the faster the movement is carried out, the less accurate it becomes.

3.1.1b Open Loop Control

Again as defined by Adams, the classical definition of open-loop control is as follows:

"An open loop system has no feedback or mechanisms for error regulation. The input events for a system exert their influence, the system effects its transformation on the input and the system

has an output..... A traffic light with fixed timing snarls traffic when the load is heavy and impedes the flow when the traffic is light. The system has no compensatory capability."(Adams, 1971)

Some movements, however, occur too quickly to integrate sensory information, and instead must rely on feed forward control. Open loop control is a feed forward form of motor control, and is used to control rapid, ballistic movements that end before any sensory information can be processed. To best study this type of control, most research focuses on deafferentation studies, often involving cats or monkeys whose sensory nerves have been disconnected from their spinal cords. Monkeys who lost all sensory information from their arms resumed normal behavior after recovering from the deafferentation procedure. Most skills were relearned, but fine motor control became very difficult (Taub, Ellman and Berman, 1966).

3.2.2 Coordination

A core motor control issue is coordinating the various components of the motor system to act in unison to produce movement. The motor system is highly complex, composed of many interacting parts at many different organizational levels. Peripheral neurons receive input from the central nervous system and innervate the muscles. In turn, muscles generate forces which actuate joints. Getting the pieces to work together is a challenging problem for the motor system and how this problem is resolved is an active area of study in motor control research.

3.2.2a Reflexes

In some cases the coordination of motor components is hard-wired, consisting of fixed neuromuscular pathways that are called reflexes. Reflexes are typically characterized as automatic and fixed motor responses, and they occur on a much faster time scale than what is possible for reactions that depend on perceptual processing (Dewhurst, 1967). Reflexes play a fundamental role in stabilizing the motor system, providing almost immediate compensation for small perturbations and maintaining fixed execution patterns. Some reflex loops are routed solely through the spinal cord without receiving input from the brain, and thus do not require attention or conscious control. Others involve lower brain areas and can be influenced by prior instructions or intentions, but they remain independent of perceptual processing and online control.

The simplest reflex is the monosynaptic reflex or short-loop reflex, such as the monosynaptic stretch response. In this example, Ia afferent neurons are activated by muscle spindles when they deform due to the stretching of the muscle. In the spinal cord, these afferent neurons synapse directly

onto alpha motor neurons that regulate the contraction of the same muscle (Tobergte and Curtis, 2013). Thus, any stretching of a muscle automatically signals a reflexive contraction of that muscle, without any central control. As the name and the description implies, monosynaptic reflexes depend on a single synaptic connection between an afferent sensory neuron and efferent motor neuron. In general the actions of monosynaptic reflexes are fixed and cannot be controlled or influenced by intention or instruction. However, there is some evidence to suggest that the gain or magnitude of these reflexes can be adjusted by context and experience (Matthews, 1986).

Polysynaptic reflexes or long-loop reflexes are reflex arcs which involve more than a single synaptic connection in the spinal cord. These loops may include cortical regions of the brain as well, and are thus slower than their monosynaptic counterparts due to the greater travel time. However, actions controlled by polysynaptic reflex loops are still faster than actions which require perceptual processing (Kandel, 2012). While the actions of short-loop reflexes are fixed, polysynaptic reflexes can often be regulated by instruction or prior experience (Evarts, 1973).

3.2.2b Synergies

A motor synergy is a neural organization of a multi-element system that (1) organizes sharing of a task among a set of elemental variables; and (2) ensures co-variation among elemental variables with the purpose to stabilize performance variables (Latash and Anson, 2006; Alnajjar et al., 2013). The components of a synergy need not be physically connected, but instead are connected by their response to perceptual information about the particular motor task being executed. Synergies are learned, rather than being hardwired like reflexes, and are organized in a task-dependent manner; a synergy is structured for a particular action and not determined generally for the components themselves. A notable early example comes from the work of Nikolai Bernstein, in which he demonstrated synergies at work in the hammering actions of professional blacksmiths. The muscles of the arm controlling the movement of the hammer are informationally linked in such a way that errors and variability in one muscle are automatically compensated for by the actions of the other muscles. These compensatory actions are reflex-like in that they occur faster than perceptual processing would seem to allow, yet they are only present in expert performance, not in novices. In the case of blacksmiths, the synergy in question is organized specifically for hammering actions and is not a general purpose organization of the muscles of the arm. Synergies have two defining characteristics in addition to being task dependent; sharing and flexibility/stability (Latash, 2008).

"Sharing" requires that the execution of a particular motor task depends on the combined actions of all the components that make up the synergy. Often, there are more components involved than are strictly needed for the particular task (see "Redundancy" below), but the control of that motor task is distributed across all components nonetheless. A simple demonstration comes from a two-finger force production task, where participants are required to generate a fixed amount of force by pushing down on two force plates with two different fingers (Scholz et al., 2002). In this task, participants generated a particular force output by combining the contributions of independent fingers. While the force produced by any single finger can vary, this variation is constrained by the action of the other such that the desired force is always generated.

Co-variation also provides "flexibility and stability" to motor tasks. Considering again the force production task, if one finger did not produce enough force, it could be compensated for by the other (Scholz et al., 2002; Latash, Scholz and Schöner, 2007). The components of a motor synergy are expected to change their action to compensate for the errors and variability in other components that could affect the outcome of the motor task. This provides flexibility because it allows for multiple motor solutions to particular tasks, and it provides motor stability by preventing errors in individual motor components from affecting the task itself.

Synergies simplify the computational difficulty of motor control. Coordinating the numerous degrees of freedom in the body is a challenging problem, both because of the tremendous complexity of the motor system, as well as the different levels at which this organization can occur (neural, muscular, kinematic, spatial, etc.). Because the components of a synergy are functionally coupled for a specific task, execution of motor tasks can be accomplished by activating the relevant synergy with a single neural signal (Bernstein, 1967). The need to control all of the relevant components independently is removed because organization emerges automatically as a consequence of the systematic covariation of components. Similar to how reflexes are physically connected and thus do not require control of individual components by the central nervous system, actions can be executed through synergies with minimal executive control because they are functionally connected. Beside motor synergies, the term of sensory synergies has recently been introduced (Alnajjar et al., 2015). Sensory synergy are believed to play an important role in integrating the mixture of environmental inputs to provide low-dimensional information to the CNS thus guiding the recruitment of motor synergies.

3.2.2c Motor Programs

While synergies represent coordination derived from peripheral interactions of motor components, motor programs are specific, pre-structured motor activation patterns that are generated and executed by a central controller (in the case of a biological organism, the brain) (Schmidt, 1975). They represent at top-down approach to motor coordination, rather than the bottom-up approach offered by synergies. Motor programs are thought to be executed in an open-loop manner, although sensory information is most likely used to sense the current state of the organism and determine the appropriate goals. However, once the program has been executed, it cannot be altered online by additional sensory information.

Evidence for the existence of motor programs comes from studies of rapid movement execution and the difficulty associated with changing those movements once they have been initiated. For example, people who are asked to make fast arm swings have extreme difficulty in halting that movement when provided with a "STOP" signal after the movement has been initiated (Henry and Harrison, 1961). Interestingly, this reversal difficulty persists even if the stop signal is presented after the initial "GO" signal but before the movement actually begins. This research suggests that once selection and execution of a motor program begins, it must run to completion before another action can be taken. This effect has been found even when the movement that is being executed by a particular motor program is prevented from occurring at all. People who attempt to execute particular movements (such as pushing with the arm), but unknowingly have the action of their body arrested before any movement can actually take place, show the same muscle activation patterns (including stabilizing and support activation that does not actually generate the movement) as when they are allowed to complete their intended action (Wadman et al., 1979).

Although the evidence for motor programs seems persuasive, there have been several important criticisms of the theory. The first is the problem of storage. If each movement an organism could generate requires its own motor program, it would seem necessary for that organism to possess an unlimited repository of such programs and where these would be kept is not clear. Aside from the enormous memory requirements such a facility would take, no motor program storage area in the brain has yet been identified. The second problem is concerned with novelty in movement. If a specific motor program is required for any particular movement, it is not clear how one would ever produce a novel movement. At best, an individual would have to practice any new movement before

executing it with any success, and at worst, would be incapable of new movements because no motor program would exist for new movements. These difficulties have led to a more nuanced notion of motor programs known as generalized motor programs (Schmidt, 1988). A generalized motor program is a program for a particular class of action, rather than a specific movement. This program is parameterized by the context of the environment and the current state of the organism.

3.2.2d Redundancy

An important issue for coordinating the motor system is the problem of the redundancy of motor degrees of freedom. As detailed in the "Synergies" section, many actions and movements can be executed in multiple ways because functional synergies controlling those actions are able to co-vary without changing the outcome of the action. This is possible because there are more motor components involved in the production of actions than are generally required by the physical constraints on that action. For example, the human arm has seven joints which determine the position of the hand in the world. However, only three spatial dimensions are needed to specify any location the hand could be placed in. This excess of kinematic degrees of freedom means that there are multiple arm configurations that correspond to any particular location of the hand.

Some of the earliest and most influential work on the study of motor redundancy came from the Russian physiologist Nikolai Bernstein. Bernstein's research was primarily concerned with understanding how coordination was developed for skilled actions. He observed that the redundancy of the motor system made it possible to execute actions and movements in a multitude of different ways while achieving equivalent outcomes (Bernstein, 1967). This equivalency in motor action means that there is no one-to-one correspondence between the desired movements and the coordination of the motor system needed to execute those movements. Any desired movement or action does not have a particular coordination of neurons, muscles, and kinematics that make it possible. This motor equivalency problem became known as the degrees of freedom problem because it is a product of having redundant degrees of freedom available in the motor system.

3.3 Perception in Motor Control

Related, yet distinct from the issue of how the processing of sensory information affects the control of movements and actions is the question of how the perception of the world structures action. Perception is extremely important in motor control because it carries the relevant information about objects, environments and bodies which is used in organizing and executing

actions and movements. What is perceived and how the subsequent information is used to organize the motor system is a current and ongoing area of research. This is especially important to BCI systems in which, often, the only form of feedback is visual information.

3.2.1 Model Based Control Strategies

Most model based strategies of motor control rely on perceptual information, but assume that this information is not always useful, veridical or constant. Optical information is interrupted by eye blinks, motion is obstructed by objects in the environment, and distortions can change the appearance of object shape. Model based and representational control strategies are those that rely on accurate internal models of the environment, constructed from a combination of perceptual information and prior knowledge, as the primary source information for planning and executing actions, even in the absence of perceptual information (Kawato, 1999).

3.2.1a Inference and Indirect Perception

Many models of the perceptual system assume indirect perception, or the notion that the world that gets perceived is not identical to the actual environment. Environmental information must go through several stages before being perceived, and the transitions between these stages introduce ambiguity. What actually gets perceived is the mind's best guess about what is occurring in the environment based on previous experience. Support for this idea comes from the Ames room illusion, where a distorted room causes the viewer to see objects known to be a constant size as growing or shrinking as they move around the room. The room itself is seen as being square, or at least consisting of right angles, as all previous rooms the perceiver has encountered have had those properties. Another example of this ambiguity comes from the doctrine of specific nerve energies. The doctrine presents the finding that there are distinct nerve types for different types of sensory input, and these nerves respond in a characteristic way regardless of the method of stimulation. That is to say, the color red causes optical nerves to fire in a specific pattern that is processed by the brain as experiencing the color red. (To be exactly accurate, the color red does not actual cause optical nerves to fire; rather the specific wavelength of light activates photoreceptors in the eye. “Red” is a property of the brain to which humans have given context and meaning). However, if that same nerve is electrically stimulated in an identical pattern, the brain could perceive the color red when no corresponding stimuli is present.

3.2.1b Forward Models

Forward models are a predictive internal model of motor control that takes the available perceptual information, combined with a particular motor program, and tries to predict the outcome of the planned motor movement. Forward models structure action by determining how the forces, velocities, and positions of motor components affect changes in the environment and in the individual. It is proposed that forward models help with the neural control of limb stiffness when individuals interact with their environment. Forward models are thought to use motor programs as input to predict the outcome of an action. An error signal is generated when the predictions made by a forward model do not match the actual outcome of the movement, prompting an update of an existing model and providing a mechanism for learning. These models explain why it is impossible to tickle yourself. A sensation is experienced as ticklish when it is unpredictable. However, forward models predict the outcome of your motor movements, meaning the motion is predictable, and therefore not ticklish (Blakemore, Wolpert and Frith, 2000).

Evidence for forward models comes from studies of motor adaptation. When a person's goal-directed reaching movements are perturbed by a force field, they gradually, but steadily, adapt the movement of their arm to allow them to again reach their goal. However, they do so in such a way that preserves some high level movement characteristics; bell-shaped velocity profiles, straight line translation of the hand, and smooth, continuous movements (Shadmehr and Mussa-Ivaldi, 1994). These movement features are recovered, despite the fact that they require startlingly different arm dynamics (i.e., torques and forces). This recovery provides evidence that what is motivating movement is a particular motor plan, and the individual is using a forward model to predict how arm dynamics change the movement of the arm to achieve particular task level characteristics. Differences between the expected arm movement and the observed arm movement produces an error signal which is used as the basis for learning. Additional evidence for forward models comes from experiments which require subjects to determine the location of an effector following an unseen movement (Wolpert, Ghahramani and Jordan, 1995).

3.2.1c Inverse Models

Inverse models predict the necessary movements of motor components to achieve a desired perceptual outcome. They can also take the outcome of a motion and attempt to determine the sequence of motor commands that resulted in that state. These types of models are particularly

useful for open loop control, and allow for specific types of movements, such as fixating on a stationary object while the head is moving. Complimentary to forward models, inverse models attempt to estimate how to achieve a particular perceptual outcome in order to generate the appropriate motor plan. Because inverse models and forward model are so closely associated, studies of internal models are often used as evidence for the roles of both model types in action.

Motor adaptation studies, therefore, also make a case for inverse models. Motor movements seem to follow predefined "plans" that preserve certain invariant features of the movement. In the reaching task mentioned above, the persistence of bell-shaped velocity profiles and smooth, straight hand trajectories provides evidence for the existence of such plans (Shadmehr and Mussa-Ivaldi, 1994). Movements that achieve these desired task-level outcomes are estimated by an inverse model. Adaptation therefore proceeds as a process of estimating the necessary movements with an inverse model, simulating with a forward model the outcome of those movement plans, observing the difference between the desired outcome and the actual outcome, and updating the models for a future attempt.

3.2.2 Information Based Control

An alternative to model based control is information based control. Informational control strategies organize movements and actions based on perceptual information about the environment, rather than on cognitive models or representations of the world. The actions of the motor system are organized by information about the environment and information about the current state of the agent (Warren, 2006). Information based control strategies often treat the environment and the organism as a single system, with action proceeding as a natural consequence of the interactions of this system. A core assumption of information based control strategies is that perceptions of the environment are rich in information and veridical for the purposes of producing actions. This runs counter to the assumptions of indirect perception made by model based control strategies.

3.2.2a Direct Perception

Direct perception in the cognitive sense is related to the philosophical notion of naïve or direct realism in that it is predicated on the assumption that what we perceive is what is actually in the world. James J. Gibson is credited with recasting direct perception as ecological perception (Gibson, 1979). While the problem of indirect perception proposes that physical information about object in our environment is not available due to the ambiguity of sensory information, proponents

of direct perception (like Gibson) suggest that the relevant information encoded in sensory signals is not the physical properties of objects, but rather the action opportunities the environment affords. These affordances are directly perceivable without ambiguity, and thus preclude the need for internal models or representations of the world. Affordances exist only as a byproduct of the interactions between an agent and its environment, and thus perception is an "ecological" endeavor, depending on the whole agent/environment system rather than on the agent in isolation.

Because affordances are action possibilities, perception is directly connected to the production of actions and movements. The role of perception is to provide information that specifies how actions should be organized and controlled (Michaels and Carello, 1981); the motor system is "tuned" to respond to specific type of information in particular ways. Through this relationship, control of the motor system and the execution of actions are dictated by the information of the environment. As an example, a doorway "affords" passing through, but a wall does not. How a one might pass through a doorway is specified by the visual information received from the environment, as well as the information perceived about one's own body. Together, this information determines the pass-ability of a doorway, but not a wall. In addition, the act of moving towards and passing through the doorway generates more information and this in turn specifies further action. The conclusion of direct perception is that actions and perceptions are critically linked and one cannot be fully understood without the other.

3.2.2b Behavioral Dynamics

Building on the assumptions of direct perception behavioral dynamics is a behavioral control theory that treats perceptual organisms as dynamic systems that respond to informational variables with actions, in a functional manner (Warren, 2006). Under this understanding of behavior, actions unfold as the natural consequence of the interaction between the organisms and the available information about the environment, which specified in body-relevant variables. Much of the research in behavioral dynamics has focused on locomotion, where visually specified information (such as optic flow, time-to-contact, optical expansion, etc.) is used to determine how to navigate the environment (Fajen and Warren, 2003; Fajen and Matthis, 2011). Interaction forces between the human and the environment also affect behavioral dynamics as seen in by the neural control of limb stiffness.

3.4 Bayesian Theory & Motor Control

A more modern perspective on motor control pushes past traditional sensor/controller based issues and applies Bayesian approaches to brain function to investigate the capacity of the nervous system to operate in situations of uncertainty in a fashion that is close to the optimal prescribed by Bayesian statistics (Clark, 2013; Sanders, 2016). Studies associated with this term often strive to explain the brain's cognitive abilities based on statistical principles. It is frequently assumed that the nervous system maintains internal probabilistic models that are updated by neural processing of sensory information using methods approximating those of Bayesian probability (Knill and Pouget, 2004; Doya et al., 2007).

3.4.1 Psychophysics

A wide range of studies interpret the results of psychophysical experiments in light of Bayesian perceptual models. Many aspects of human perceptual and motor behavior can be modeled with Bayesian statistics. This approach, with its emphasis on behavioral outcomes as the ultimate expressions of neural information processing, is also known for modeling sensory and motor decisions using Bayesian decision theory. Examples are the work of Landy (2006, 2008), Jacobs (1999, 2003) Jordan, Knill (2005, 2007), Kording and Wolpert (2004), and Goldreich (1975, 2007, 2013).

3.4.2 Neural Coding

Many theoretical studies ask how the nervous system could implement Bayesian algorithms. Examples are the work of Pouget, Zemel, Deneve, Latham, Hinton and Dayan. Of particular note, George and Hawkins published a paper that establishes a model of cortical information processing called hierarchical temporal memory that is based on Bayesian network of Markov chains. They further map this mathematical model to the existing knowledge about the architecture of cortex and show how neurons could recognize patterns by hierarchical Bayesian inference (George and Hawkins, 2009).

3.4.3 Predictive Coding

Rao and colleagues have also shown predictive coding as a neurobiologically plausible scheme for inferring the causes of sensory input based on minimizing prediction error (Rao and Ballard, 1999). These schemes are related formally to Kalman filtering and other Bayesian update schemes (Mulliken, Musallam and Andersen, 2008; Blakely, 2013). In the predictive coding framework, each level of a hierarchy employs a generative model to predict representations in the level below. This

generative model uses backward connections to convey the prediction to the lower level where it is compared to the representation in this subordinate level to produce a prediction error. This prediction error is then sent back to the higher level, via forward connections, to adjust the neuronal representation of sensory causes, which in turn change the prediction. This self-organizing, reciprocal exchange of signals continues until prediction error is minimized and the most likely cause of the input has been generated. It can be shown that this scheme is formally equivalent to empirical Bayesian inference, in which prior expectations emerge naturally from the hierarchal models employed (Friston 2002, 2003, 2005). It should be noted that the prediction addressed in predictive coding is predicting the sensory effects from their cause. In other words it is about the mapping between the cause (motor commands to grasp) and the sensory (i.e., visual or proprioceptive) expression or effect of that cause. It is not about forecasting (i.e., predicting the sensory states in the future, given the sensory state now), otherwise known as prospective coding (Schultz-Bosbach and Wolfgang Prinz 2007).

3.4.4 Free Energy & Active Inference

During the 1990s some researchers such as Geoffrey Hinton and Karl Friston began examining the concept of free energy as a calculably tractable measure of the discrepancy between actual features of the world and representations of those features captured by neural network models (Tschudi, 2010). A synthesis has been attempted recently by Karl Friston, in which the Bayesian brain emerges from a general principle of free energy minimization (Friston, 2010). In this framework, both action and perception are seen as a consequence of suppressing free-energy, leading to perceptual (Friston, 2005) and active inference (Young et al., 2016) and a more embodied (enactive) view of the Bayesian brain. Using variational Bayesian methods, it can be shown how internal models of the world are updated by sensory information to minimize free energy or the discrepancy between sensory input and predictions of that input. This can also be cast (in neurobiologically plausible terms) as and expansion on predictive coding or, more generally, Bayesian filtering and applied to motor control as seen in Figure 3.

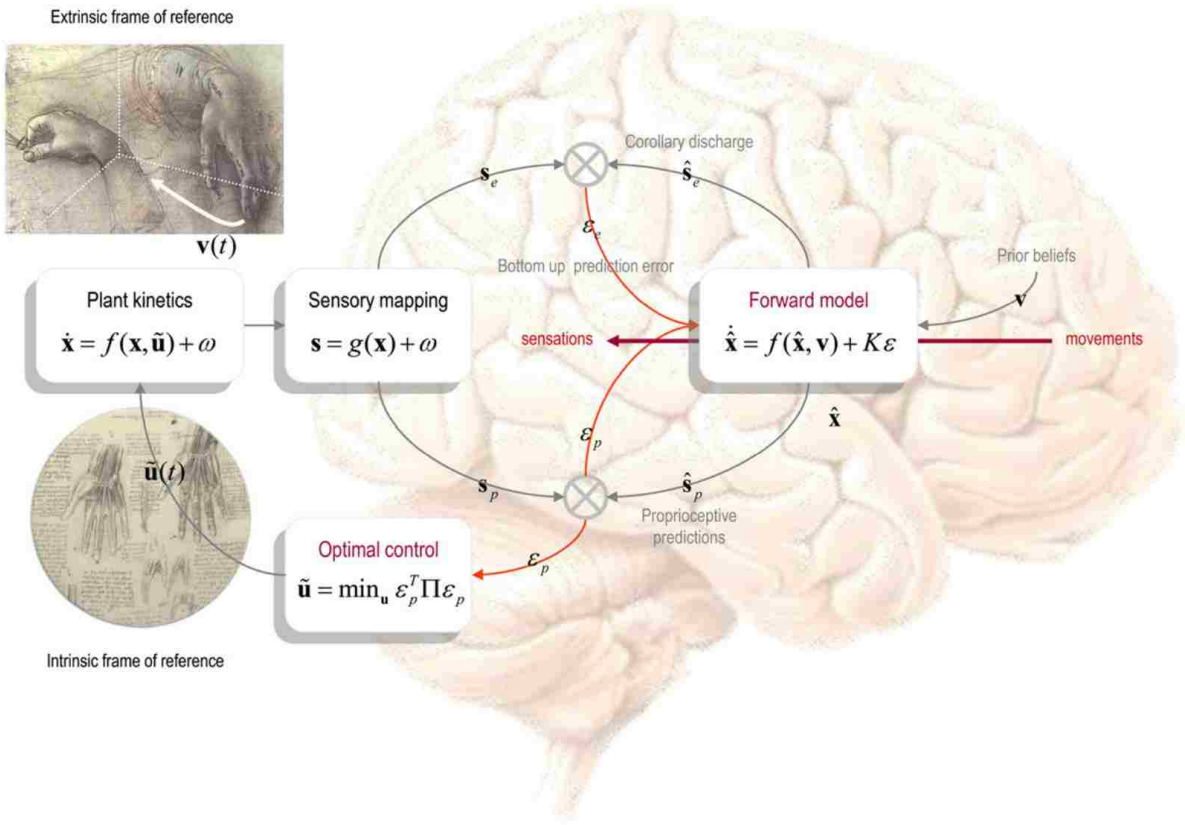

Figure 3 - Active Inference & Motor Control. This figure represents the final simplification of the predictive coding scheme as described in Friston, 2011. Going beyond traditional optimal control models of human motor control, Friston proposes a framework in which the cost functions have been replaced by prior beliefs about (desired) trajectories in an extrinsic frame of reference. These beliefs enter the Bayesian filter to guide predictions of sensory inputs. Proprioceptive predictions are fulfilled in the periphery through classical motor reflex arcs, while predictions of exteroceptive inputs correspond to corollary discharge and are an integral part of perceptual inference. Note that optimal control now reduces to simply suppressing proprioceptive prediction errors, i.e., active inference.

These considerations, while not the primary focus of this work, are important when assessing the role BCIs play in restoring or testing various aspects of motor control. In addition, the existing models in the field can help us understand situations in which BCI control does not line up with standard motor control expectations. While abstracted control of virtual objects (i.e., a cursor or robotic hand) may be considered to be similar to general hand or limb effector control, the actual dynamics may greatly vary as many of the structural components (e.g. efference copy mechanism as seen in Figure 3) simply do not exist intrinsically and may be emergent features that arise with experience or learning (i.e., a Bayesian developmental process). An important example for bimanual coordination is discussed further in Chapter 3.

Chapter 4: Effecting Control II – Motor Dissociation with BCI

During closed-loop control of a brain–computer interface, neurons in the primary motor cortex can be intensely active even though the subject may be making no detectable movement or muscle contraction. How can neural activity in the primary motor cortex become dissociated from the movements and muscles of the native limb that it normally controls?

Here we examine circumstances in which motor cortex activity is known to dissociate from movement – including mental imagery, visuo-motor dissociation and instructed delay. Many such motor cortex neurons may be related to muscle activity only indirectly. Furthermore, the integration of thousands of synaptic inputs by individual α-motoneurons means that under certain circumstances even cortico-motoneuronal cells, which make monosynaptic connections to α-motoneurons, can become dissociated from muscle activity. The natural ability of motor cortex neurons under voluntarily control to become dissociated from bodily movement may underlie the utility of this cortical area for controlling brain–computer interfaces.

The past decades have witnessed rapid technological advances in brain–computer interfaces (BCIs), devices in which activity recorded from the neuromuscular system of a waking subject is processed by a computer, and the computational output then used to accomplish a task and/or drive a physical machine (Donoghue et al. 2004, 2007a; Schwartz, 2004; Fagg et al. 2007; Nicolelis & Lebedev, 2009). For input, many of these BCIs have used neural signals – single- and multi-unit spikes, local field potentials and electrocorticographic potentials – recorded from the primary motor cortex (M1). Under voluntary control, this area of the cerebral cortex normally provides the most direct cortical output to the spinal cord and to the α-motoneurons there that drive muscles to move the subject's native limbs. In many of these studies, the experimental subjects have been monkeys, particularly macaques, both because these animals can be trained to perform complex behaviors, and because their nervous system and muscles are comparatively close to those of humans.

A common daily paradigm for BCI studies goes as follows. At first, the subject performs a behavioral task that requires a variety of movements of the native limb, a 'hand-control' mode. For example, the subject may hold a joystick while reaching to a variety of different target locations. The subject typically does not watch its hand directly, but rather this motion is displayed to the subject

as a cursor moving on a computer screen, just as the motion of a computer mouse is displayed on a screen to someone using a personal computer. As the subject performs these movements, neural data are recorded from M1. These neural data are then decoded to extract detailed information about motion of the hand (here equivalent to motion of the cursor) in time. Impressively accurate descriptions of the motion can be decoded from the collective neural activity. The mathematical algorithms used to decode movements from neural activity then are used to provide a prediction of the movement that would occur given any particular pattern of neural activity. Thereafter, the output predicted by the decoding algorithm is used to control the motion of the cursor, substituting for the actual motion of the hand holding the joystick (or computer mouse). Now in this second 'brain control' mode, the decoded output of the subject's recorded neural activity drives the motion of the cursor, not the native limb or joystick. Using brain control, the subject again moves the cursor to various indicated target locations on the screen.

One of the most striking observations to come from such studies is the dissociation of neural activity in M1 from movement of the subject's native limb. During hand control, the firing rate of many M1 neurons varies systematically in relation to the direction of the native limb's movement, and this direction-dependent variation can be used to define a preferred direction for each neuron (Georgopoulos et al. 1982, 1986). The preferred directions of M1 neurons typically span the entire range of movements studied, and a population vector can be computed from their concurrent firing rates that predicts the direction and speed (velocity) of hand motion in space (Moran & Schwartz, 1999a, b; Schwartz & Moran, 1999). During brain control, however, the directional tuning of many M1 neurons changes substantially, with the preferred directions of various neurons changing in different directions (Taylor et al. 2002; Ganguly & Carmena, 2009). Furthermore, although the monkey initially may continue to move its native limb during brain control, movements of the native limb often diminish and may cease entirely. Recording electromyographic (EMG) activity may show that the muscles which normally move the limb are completely silent (Carmena et al. 2003). M1 neurons then continue to discharge, driving motion of the cursor through the decoding algorithm, in the absence of limb movement or any contraction of limb muscles. How can the activity of M1 neurons that are so intimately involved in controlling movement of the subject's native limb be so readily dissociated from limb movement? Below we explore this paradox by examining instances in which the M1 activity that otherwise might be thought obligatorily related to the production of native

limb movement becomes dissociated from the movement per se. As we proceed, it may be helpful to keep in mind two fundamental facts. First, although commonly thought of as 'upper motor neurons' (Phillips & Landau, 1990), different neurons in M1 have various input and output connectivity. M1 neurons in cortical layers II and III exchange information with other cortical areas, largely the premotor, supplementary motor, cingulate motor and somatosensory cortical areas. Different neurons in corticofugal output layer V project to the basal ganglia, red nucleus, cerebellum (via pontine nuclei), pontomedullary reticular formation, and/or to the spinal cord. Of those that do project to the spinal cord, only a fraction (~55%) have detectable synaptic effects directly onα-motoneurons (Lemon et al. 1986). Hence it should come as no surprise that many M1 neurons can be active in dissociation from movement of the native limb (Fetz & Cheney, 1987).

Second, even those M1 neurons that do make monosynaptic connections to spinal α-motoneurons do not control those motoneurons to the extent implied by the term 'upper motor neurons'. The axon of each spinal α-motoneuron branches within its target muscle making such a strong synaptic contact (end-plate) on each muscle fiber it innervates that discharge of the α-motoneuron always is followed by contraction of all of its muscle fibers. Whereas each muscle fiber receives input from only one α-motoneuron, each α-motoneuron receives thousands of synaptic inputs from a wide variety of neurons – including I-a afferents, inhibitory and excitatory spinal interneurons, propriospinal neurons, vestibulospinal neurons, reticulospinal neurons (Baker, 2011), rubrospinal neurons and corticospinal neurons. None of these input neurons makes such a strong synaptic connection on an α-motoneuron as to be able to drive it consistently. Because each α-motoneuron integrates thousands of synaptic inputs from a wide variety of sources, no CNS neurons other than α-motoneurons have a direct, obligatory coupling to muscle fibers, and hence to movement. Even the cortico-motoneuronal (CM) cells of the primary motor cortex, which are commonly viewed as directly driving spinal α-motoneurons, can have a variable relationship to the activity of the muscles they 'control'.

4.1 Motor Imagery and Mirror Neurons

Humans often imagine themselves performing a particular action or sequence of actions, a process termed motor imagery. A dancer, for example, might imagine him or herself making the movements required for a particular dance. By repeatedly imagining a particular motor performance, termed mental rehearsal, human subjects like the dancer can improve their eventual performance of

the actual movements (Avanzino et al. 2009; Munzert et al. 2009). Several fMRI studies have shown that during motor imagery and mental rehearsal the normal human M1 is activated in a location similar to that activated during actual movement, though the activation is less intense (Munzert et al. 2009). Similarly, when human amputees imagine moving their missing limb, fMRI activation appears in the somatotopically appropriate region of M1. Hence motor imagery and mental rehearsal provide a circumstance in which the human M1 is activated as part of a normal process, but in the absence of actual movement. Even observing someone else perform a movement may provoke some degree of motor imagery in the observer. When you watch a dancer dance, for example, to some extent you may imagine yourself performing the dance. Rizzolatti and colleagues originally described neurons in the ventral premotor cortex (PMv) of monkeys that discharge not only when the monkey makes a specific grasp with its hand, but also when the monkey watches another primate – monkey or human – use the same type of grasp (di Pellegrino et al. 1992; Gallese et al. 1996; Rizzolatti & Craighero, 2004). The investigators termed these 'mirror' neurons. Had the discharge of these neurons not been recorded while the subject watched another primate making the same grasp, these mirror neurons would instead have been considered as closely linked to the monkey's own movement as other grasp-related neurons in PMv. Lemon and colleagues (Bennett and Lemon, 1994; Vigneswaran et al., 2013; Eisen et al., 2015) also note two additional important points. First, during grasp observation, mirror neurons are active with no detectable EMG activity in the subject's muscles. Hence the subject is not mirroring the observed grasp per se, despite the activity of these cortical neurons. And second, some PMv mirror neurons have pyramidal tract axons, indicating that during grasp observation such mirror neurons are transmitting information to the spinal cord, even though there is no muscle activation (Kraskov et al. 2009). Although most studies of mirror neurons have focused on PMv, preliminary observations from Lemon's group suggest that there also may be mirror neurons in M1, and that some of these M1 mirror neurons also have axons in the pyramidal tract. Again, if discharge during grasp observation had not been examined, these M1 mirror neurons would appear to discharge during specific grasps performed by the monkey, like any other M1 neuron. Although the role of mirror neuron discharge during grasp observation is not yet fully understood, we might speculate that while observing the movement of another primate, the monkey is imagining itself performing the same movement.

4.2 Visuomotor Dissociation

When you reach out to pick up your coffee cup, the place to which you reach is identical to your visual perception of the coffee cup's location. But the location to which a movement is made also can be dissociated from the location of the visual cue. When using a computer mouse, for example, pushing your hand horizontally away from you moves the cursor, not horizontally away, but vertically up on the screen. Three studies in which the locations of visual targets were dissociated from the required voluntary motion of the limb have revealed that many M1 neurons represent the visually perceived location of the target in external space rather than the motion of the limb per se. In a seminal study, dissociation of the visual cue location from limb movement was produced by training monkeys to perform a mental rotation (Georgopoulos et al. 1989). In this case, the monkeys made reaching movements from a central home position to one of eight targets arranged at 45 degree intervals on a peripheral circle. The monkeys were trained, however, to move their hand to the target location 90 degree counter-clockwise from the target cued visually. Under these circumstances, the initial, short-latency responses in M1 encoded the direction to the visual cue, albeit at low amplitude. Through the remainder of the monkey's reaction time, the overall activity of M1 neurons increased, and the direction encoded by the active population of M1 neurons gradually rotated to point in the direction of actual limb movement just before the onset of that movement. Though ultimately indicating the direction of actual movement, the initial response of the M1 population had indicated the location of the visual cue.

In a second visuomotor dissociation study, monkeys made flexion–extension elbow movements with the right arm held out to the side, such that elbow extension moved the hand to the right and elbow flexion moved the hand to the left (Alexander & Crutcher, 1990a). The angular position of the elbow controlled the right/left motion of a cursor viewed by the monkey on a computer screen. In different blocks of trials, the coupling between the motion of the elbow and the cursor could be either direct (elbow extension that moved the hand to the right also moved the cursor to the right) or inverted (elbow extension that moved the hand to the right instead moved the cursor to the left), dissociating the direction of cursor movement from the direction of elbow movement. In individual trials the monkey positioned the cursor in a central starting position, a target appeared on the left or right, and after an instructed delay the monkey was required to move the cursor to the target. Under these conditions, 15% of M1 neurons discharged in relation to the direction of actual

elbow movement during the preparatory instructed delay period and 71% during the movement itself. But 40% of M1 neurons during the preparatory period and 14% during the movement remained coupled to direction of cursor motion on the screen rather than the movement of the elbow.

In a third study, monkeys used wrist movements to control a cursor, moving the cursor from a center position to eight peripheral targets, again arranged in a circle at 45 degree intervals. (Kakei et al. 1999). Here, different blocks of trials were performed with the forearm in three different pronation/supination postures: fully pronated, intermediate, and fully supinated. In different forearm postures, moving the hand in a given direction required activation of different combinations of wrist muscles. For example, with the forearm fully pronated, moving the hand toward the upward target involved contraction of wrist extensor muscles extending the wrist, but with the forearm fully supinated, wrist flexor muscles contracted to flex the wrist and thereby move the hand toward the upward target. With the forearm in the intermediate position, the radial wrist flexor and extensor muscles co-contracted to lift the hand upward. In this paradigm, which used different forearm postures to dissociate the direction of both motion at the wrist and contraction of wrist muscles from the target direction, only 28 of 88 M1 neurons (32%) showed discharge patterns most closely associated with patterns of muscle contraction. In contrast, 44 of the 88 M1 neurons (50%) discharged in relation to the location of the target, whichever wrist muscles and wrist motion were used to move the hand toward the target. In all three of these studies, had the activity of M1 neurons not been examined under conditions that dissociated visual target location from limb movement direction, all these M1 neurons would have been considered directly related to the limb movement per se. Yet when observed under the right conditions, these M1 neurons became substantively dissociated from motion of the limb per se.

4.3 Temporal Dissociation during Instructed Delays

We often think about movements and prepare to make them well before we actually perform them. Upon hearing, 'On your mark, get set. . .', for example, sprinters prepare themselves to 'Go!' During the time interval between receiving a specific instruction and the subsequent Go signal, the brain can plan the movement to make, but must withhold actually starting the movement. We now know that during such an instructed delay period neural activity related to the specific upcoming movement appears in a wide variety of cortical and subcortical structures (Prut & Fetz, 1999; Buford & Davidson, 2004), including a substantial proportion of M1 neurons (Tanji & Evarts, 1976; Thach,

1978; Alexander & Crutcher, 1990b). During instructed delays, neurons in M1 (including CM cells; Fetz & Cheney, 1987) and elsewhere thus may be active for hundreds of milliseconds in the absence of EMG activity or limb movement.

4.4 Dissociating Cortico-motoneuronal Cells from Their Target Muscles

The cortico-motoneuronal (CM) cells that send their axons from M1 down the corticospinal tract to synapse directly on spinal α-motoneurons constitute the most important descending pathway for control of fine movements. The presence of such CM cells in certain monkey species has been demonstrated using a variety of techniques. Intracellular recordings from monkey α-motoneurons have demonstrated monosynaptic EPSPs following electrical stimulation of M1 (Clough et al. 1968; Porter & Hore, 1969). Corticospinal axons filled with tracer have been shown to have synaptic boutons on α-motoneuron dendrites (Lawrence et al. 1985). And injection of rabies virus into muscles to produce retrograde trans-neuronal labelling has shown first-order labelling in α-motoneurons and second-order labelling in M1 layer V neurons (Rathelot & Strick, 2006, 2009). These CM cells provide the most direct pathway through which the cerebral cortex influences movement of the body (Kandel, 2012).

Although CM synapses exert powerful excitatory effects on α-motoneurons, the same motoneurons also receive many other inputs (Fuglevand, 2011), including those from Ia afferents, spinal interneurons, propriospinal neurons, reticulospinal neurons and rubrospinal neurons (Mewes & Cheney, 1991; Flament et al. 1992; Porter & Lemon, 1993; Perlmutter et al. 1998; Riddle et al. 2009). Any individual α-motoneuron receives thousands of synaptic contacts. The handful of synaptic contacts from a given CM cell therefore does not consistently drive the discharge of any particular α-motoneuron. How then can an M1 neuron recorded in an awake, behaving monkey be identified as a CM cell? If an M1 neuron could be stimulated intracellularly so as to stimulate only that neuron, and if intracellular recordings could be made simultaneously from numerous α-motoneurons so as to observe EPSPs, individual CM cells could be identified unambiguously.

Although pioneering studies have achieved intracellular recording from M1 neurons in awake animals (Matsumura et al. 1988, 1996; Chen & Fetz, 2005), the technical difficulty of obtaining such intracellular recordings in M1 neurons with concurrent intracellular recording in spinal α-motoneurons to date has precluded absolute identification of CM cells in awake behaving animals. Peaks in the cross-correlation histogram formed between the spikes of an extracellularly recorded

M1 neuron and those of a single intramuscularly recorded motor unit can provide correlational evidence that the M1 neuron is a CM cell (Mantel & Lemon, 1987), but maintaining isolation of single motor units in behaving animals is difficult as well. Likewise, although cross-correlation histograms between pairs of motor units in human hand muscles have provided information about the divergence of supraspinal and potentially corticospinal inputs (Fuglevand, 2011), the activity of CM cells remains unrecorded when applying this technique. The technique of spike-triggered averaging of EMG activity, while also correlational, therefore has been used to detect monosynaptic input from a recorded CM cell onto a pool of α-motoneurons. Because of the numerous other synaptic inputs, the individual spikes recorded from a CM cell produce no consistent observable effect in the EMG activity of any target muscle. Nevertheless, the arrival of a CM EPSP in the motoneuron pool can elicit the next action potential from those few motoneurons that happen to be close to threshold. If the motoneuron pool already is active to some extent, then the spike of a CM cell in the cortex is followed at a short, fixed latency by an increased likelihood that some α-motoneurons within that pool will discharge. By averaging rectified EMG activity aligned (triggered) at the times of hundreds to thousands of spikes from a CM cell, statistically significant increases in the discharge probability of motoneurons in a muscle's pool can be identified, reflecting the influence of the synaptic input from the triggering CM cell. The spike-triggered average of rectified EMG activity then shows a peak relative to the average EMG baseline, referred to as a post-spike facilitation (PSF) of muscle activity. If the onset latency of the peak is consistent with the time needed for conduction from the cortical neuron to the motoneuron pool, monosynaptic excitation of α-motoneurons, conduction from the motoneuron pool to the muscle fibers, and excitation of the muscle fibers, then the PSF can be taken as evidence that the M1 neuron is a CM cell (Fetz & Cheney, 1980; Buys et al. 1986; Lemon et al. 1986; Smith & Fetz, 2009b). The amplitude of the PSF peak can be quantified relative to the averaged EMG baseline as the percentage increase of the maximum value of the peak (peak percentage increase, PPI) or the mean amplitude of the peak from its onset to offset (mean percentage increase, MPI). Although all corticospinal neurons are thought to be excitatory, not uncommonly troughs are found in spike-triggered averages. Such post-spike suppression (PSS) of EMG activity is thought to represent the presence of inhibitory interneurons that receive EPSPs from the CM cell and then deliver IPSPs to the α-motoneurons.

While the PSF produced by a CM cell in a given muscle's EMG generally has been regarded as relatively fixed, a more flexible relationship between the level of activity in the CM cell and the level of activity in the target muscle has been observed in a variety of situations (Fetz & Cheney, 1987). CM cells are among those M1 neurons that may begin to discharge well before their target muscles become active. They may be active during static holds at low force levels when target motor units are inactive; and conversely CM cells may be relatively inactive during ballistic, forceful movements when their target muscles are vigorously active. During individuated finger movements, a CM cell may be coactive with a target muscle during instructed movement of one finger, active without the target muscle during instructed movement of another finger, and/or inactive while the target muscle is active during yet another finger movement (Schieber & Rivlis, 2007). And recently, monkeys also have been operantly conditioned specifically to discharge a CM cell without activating its target muscles, and conversely, to contract target muscles without discharging the CM cell (Eaton et al. 2010). The post-spike facilitation produced by a CM cell in a given target muscle is not entirely fixed, however. Occasional studies have reported anecdotal observations in which the effect produced by a CM cell in a given muscle varied in amplitude during different phases of a behavior. In monkeys performing a precision pinch task, for example, the PSF observed in triggered averages compiled from spikes discharged during the movement phase of the task was larger than the PSF in averages compiled with spikes discharge during the static hold (Buys et al. 1986).

In another series of foundational studies, Fetz and colleagues had shown that monkeys could be operantly conditioned to voluntarily control the firing rates of individual M1 neurons (Fetz, 1969), to coactivate M1 neurons with particular muscles, and to dissociate the activity of M1 neurons and the muscles with which they normally were coactivated (Fetz & Finocchio, 1971, 1972, 1975). Schieber and colleagues (Schieber, 2011) built off of this and developed a paradigm in which, after first performing a simple hand squeeze task, a monkey was rewarded for discharging a certain number of spikes simultaneously (±6 ms) with large motor unit action potentials (MUAPs) discriminated from the EMG activity of a given muscle. Because the monkey could not intentionally generate such synchronous spikes in the M1 neuron and MUAPs in the muscle, the monkey achieved rewards by finding a motor behavior that coactivated the M1 neuron and the muscle. To do so, the monkey typically explored various movements and postures of the arm and hand, and within a few minutes performed a motor behavior that produced rewards. After collecting data while the monkey

produced this motor behavior, they could switch to using the EMG from a different muscle, asking the monkey to find a motor behavior that coactivated this muscle with the same M1 neuron. They termed this behavioral paradigm 'reinforcement of physiological discharge' (Schieber, 2011).

4.5 Considerations for bimanual control.

Many M1 neurons thus have a natural ability to discharge in dissociation from the limb movements to which they normally contribute control. Some M1 neurons are active when no movement is being made by the body, either as we watch someone else move, or as we imagine ourselves performing movements. The activity of other M1 neurons is coupled more to motion of the external target than to that of the native limb per se. As discussed in the previous chapter on motor control and the brain, such activity in M1 can be viewed as cognitive (Georgopoulos et al. 1993). Yet even the activity of CM cells that do make monosynaptic connections on α-motoneurons does not always effectively drive those motoneurons. Referring to any of these M1 neurons as 'upper motor neurons' is so misleading that the term should no longer be used. In large part, such dissociability may underlie the ability of M1 neurons to control a BCI. Upon switching to closed-loop BCI control of an output effector, i.e., control in which the subject must use the effector to accomplish a task, the brain recognizes that the native limb no longer is being controlled. Because the decoding algorithm output driving the effector is not an exact replica of signals driving the native limb, the visually observed motion of the BCI effector is not exactly the motion expected by the brain.

In addition to visual feedback, proprioceptive and tactile feedback from the native limb cues the brain that the native limb is no longer controlling the visually observed effector. The brain then may organize neural activity to control the BCI effector per se, instead of working to control the native limb (Wolpaw, 2010). During such behavior, the CNS may reduce wasted effort by reducing or eliminating concurrent muscle contractions that would move the native limb for no purpose. This may also hold for any corresponding ipsilateral representative motor or related signals (Scherer et al., 2009; Bundy et al., 2012). Furthermore, the fact that a substantial fraction of M1 neurons normally are active in relation to external targets, more than to native limb movements, may play a role in implementation of BCIs for subjects who are unable to make native limb movements due to amputation, spinal cord injury or stroke. The discharge of such M1 neurons as the subject watches movement of a BCI effector – from a cursor on a screen to a sophisticated mechanical arm – may be sufficient to develop a decoding algorithm through which the subject can begin to learn to control

the BCI effector voluntarily (Donoghue et al. 2007b; Velliste et al. 2008). The ability of M1 neurons to dissociate from movement of the native limb, and even from activation of muscles, also raises the possibility that such neurons might be assigned arbitrarily to control a particular degree of freedom (Schmidt et al. 1978; Kennedy et al. 2000). For example, monkeys were able to use M1 neurons to drive functional electrical stimulation of temporarily dennervated wrist muscles, even when there had been no observable relationship to wrist movement prior to the denervation (Moritz et al. 2008). Ensembles of neurons then might simply be assigned to control particular degrees of freedom. If the subject could learn to control such arbitrary ensembles, different ensembles might be used to control desirable degrees of freedom over which a population of decoded neurons has inadequate control. Furthermore, a BCI controlling the hand, for example, would not necessarily be constrained by any of the lower level biomechanical or neuromuscular properties of the native hand (van Duinen and Gandevia, 2011). But can any M1 neurons be trained to perform any arbitrary function; to what extent is the function of which M1 neurons hardwired or developmentally intrinsic versus flexible? More importantly, for our purposes, how might these disparate ensembles scale at the local field level or beyond and what can that tell us about designing BCIs for our target populations?

4.6 Takeaways for ECoG-based BCIs

It is clear that BCIs show great promise for changing how we interact with the world. The field of brain-computer interfacing has demonstrated the tremendous adaptive potential of brain and machine by showing BCIs can be based on activity from one to millions of neurons (Moran, 2010), with response latencies from tens to thousands of milliseconds. However, the performance of these devices is not currently sufficient to warrant the risk and expense to their target patient population. We posit that the relative single-mindedness of current architectures is one significant obstacle to the performance improvements necessary to make these devices clinically viable. We propose the utilization of BCI architectures that recognize and leverage the spatially and temporally heterogeneous patterns of activity observable across the brain to overcome this obstacle. Though we have, as a field, demonstrated the capability of the brain to develop control over these novel interfaces, we have done so with little attention to the adaptive processes taking place in neural populations that are not directly linked to control of the BCI. An important first step is to develop an understanding of which cortical structures are involved in BCI skill acquisition and task execution and to characterize the relationships between these regions. From there, specific relationships between

neural activity and task demands can be extracted and provided to computational systems as additional channels of highly task-relevant information.

In the studies described in the remainder of this document, we demonstrate two important points that advance our understanding of the way brain and machine interact during BCI use. First, we demonstrate that execution of neuroprosthetic control in a 2-D bimanual ECoG BCI is accompanied by changes in neural activity in a variety of functionally heterogeneous cortical structures, and that these distributed regions interact with M1 in meaningful ways that are indicative of underlying patterns of structural and functional connectivity. Second, we provide a framework to expand beyond simple cursor control BCIs to build on bimanual interactions and design systems for dexterous hand control. By understanding the nature of coordination and dissociation for BCI motor control as well as the functional utility of recording scale we hope to push ECoG based BCIs towards the gains that have been seen with SUA and MUA based systems. First, however, there is one last aspect of 'control' that has be examined: the human interaction with and perception of BCI control.

Chapter 5: Effecting Control III – The Ghost in the Machine.

In parallel with understanding the relationship between brain-computer interfaces (BCIs) and motor control, it may be important to attempt for a better specification of the concept of "control" in BCIs and neurofeedback (NF) research. To that extent we aim to distinguish "self-control of brain activity" from the broader concept of "BCI control," since the first describes a neurocognitive phenomenon, as discussed previously in part I and II, and is only one of the many components of "BCI control." As per this distinction, we posit a conceptual framework based on dual-processes theory that describes the cognitive determinants of self-control of brain activity as the interplay of automatic vs. controlled information processing. Further, we attempt to distinguish between cognitive processes that are necessary and sufficient to achieve a given level of self-control of brain activity and those which may not. Those cognitive processes which are not necessary for the learning process can hamper self-control because they cannot be completely turned-off at any time, i.e., ipsilateral or efferent copy representation of motor behavior. This framework aims at a comprehensive description of the cognitive determinants of the acquisition of self-control of brain activity underlying BCI schema such as those discussed herein which require the user to achieve regulation of brain activity as well as some form of neurofeedback learning. This will hopefully help provide a modicum of perspective as per the experience subjects have in interacting with these systems.

5.1 The Challenge of "Specifying Control"

In the process of using BCIs, individuals learn how to induce certain patterns of brain activity, which can be detected and transcoded into some form of action or feedback in the external device. One special case of BCI is neurofeedback (NF), in which the aim is not purely to control an external device but rather to use external feedback to modulate specific aspects of physiological signal intrinsic to the brain, i.e., alpha or gamma waves. As already discussed in some detail and shown repeatedly over the past 40 years, human and nonhuman animals are able to learn to use BCI/NF with a short amount of training (Sterman, 1977; Nicolelis and Lebedev, 2009; Phillippens and Vanwersch, 2010). Generally, the term "BCI control" has been used interchangeably to refer to two different processes. On the one side, "BCI control" refers to the ability to control an external device and can be seen mainly as a complex problem of neuroengineering (Donoghue, 2008). This definition simultaneously involves neuro-bio-psychological, data analytical and ergonomical aspects (see Kübler

et al., 2011). On the other side, “BCI control” may refer to the much more specific ability of an individual to control some aspects of his/her own brain activity (Hinterberger et al., 2003; Halder et al., 2011), which is clearly a neurocognitive topic that is central but not restricted to BCI/NF. Broadly speaking, not only BCI/NF but many other processes such as meditation techniques (Tang et al., 2014), emotion regulation (Thayer and Lane, 2000) and even psychotherapy (Beauregard, 2007) also induce some form of self-control of brain activity. This is becoming especially important as BCI stray from motor to more communication or emotional regulation (DBS for depression). (Blankertz et al., 2010; Broccard et al., 2014) Since the definition of “BCI control” from either a neuroengineering perspective or from a neurocognitive perspective seems to differ, it is necessary to disentangle both views. For the sake of transparency, “BCI control” as self-regulation of neuronal activity will be called hereafter “self-control of brain activity.” With the aim of better understanding BCI/NF learning, the first step to characterize “self-control of brain activity” is to specify the cognitive mechanisms responsible for learning control. The more popular models of BCI/NF discuss “operant conditioning” and a “motor skill learning” as these mechanisms (Hammer et al., 2012 & Wander et al, 2013). In fact, our group has previously shown how similar “BCI learning” is to general “motor learning”, at least in regards to regions of cortical activation. However, many studies indicate that other cognitive mechanisms such as locus of control towards technology (Burde and Blankertz, 2006; Ninaus et al., 2013; Witte et al., 2013), aptitude towards BCI (Hammer et al., 2012; Halder et al., 2013), motivation (Kleih et al., 2010) and spontaneous strategies (Kober et al., 2013) also influence BCI or NF learning. As a consequence, these predictors may either constitute a secondary correlate of self-control of brain activity or may represent key cognitive processes in addition to conditioning and skill learning, aka the “ghost in the shell.”

Given the high variety of cognitive and emotional processes apparently associated with self-control of brain activity and BCI learning, it is particularly useful to define a simple but comprehensible framework to evaluate the common and unique contributions of each one of these processes. Who or what is in control during BCI/neurofeedback? Some researchers have related a dual-processes theory to BCI/NF learning (Lacroix, 1986; Hammer et al., 2012). In the following, we briefly elucidate how this theory can be employed to better understand how the processes mentioned above might determine self-control of brain activity and why this might be important for bimanual coordination within the abstracted BCI system.

5.2 Two Types of Mental Activity

The dual-processes theory categorizes the whole mental activity into two main types of processing: more automatic and capacity-free processes (i.e., type I processes) vs. more controlled and capacity-limited processes (i.e., type II processes) (Wood et al., 2014). Type I processes reflect the automatic, capacity-free, effortless and context-specific information processing such as for instance trying to open the office door with the home key because one has been thinking about dinner. Moreover, type I processes are usually unconscious and difficult to control through self-instruction. Type II processes reflect the activity of a supervisory attention system, specialized in monitoring and regulating the activity in other cognitive systems (Shallice and Cooper, 2011). Type II processes are usually in the center of our focus of attention and may be regulated mainly by self-instruction. They are also fundamental for executive functions and metacognitive abilities (Bewick et al., 1995). Accordingly, control beliefs are much more related to the function of the type II processes while the heuristics regulating most of our cognitive activity and behavior are type I processes.

A central aspect of the dual-processes theory is that both automatic and controlled processes have control of behavior as well as of different aspects of cognition (Ferrer et al, 2013) but both learn from and react to different aspects of the task at hand. Automatic systems learn only through cumulative reward while controlled systems are more flexible, context-oriented and learn fast from instructions. The latter most closely mimics that of a motivated BCI user. However, motivation itself may consist of a more controlled intrinsic motivation, highly sensitive to self-instruction and self-efficacy beliefs, and a more automatic extrinsic motivation, which is more sensitive to the current amount of reward received (Ryan and Deci, 2000). Accordingly, as long as some reward can be obtained during BCI/NF learning, automatic processing may predominate. Controlled processing are then engaged when negative feedback predominates over longer periods of time and will have a larger impact, if the participant shows high levels of intrinsic motivation. In summary, dual-process models such as Lacroix (1986) make clear that self-regulation is not a unitary process but rather the result of the conjoint action of type I and type II processes. Also, while not an explicit corollary, these are analogous to the Bayesian descriptions of information processing and decision making in motor programs briefly mentioned previously. In our BCI studies, it can be important to note what type of process we are actually studying.

5.3 A Framework of Self-control of Brain Activity

Automatic and controlled processes can determine self-control of brain activity in very different ways. Even more, not every cognitive process is necessary and sufficient to perform a specific BCI/NF task; only a small subset may play a key role. The remaining mental activity – that is neither necessary nor sufficient for a specific BCI/NF task – will act on BCI/NF learning in one of two ways: firstly, this activity can interfere with the learning process, if it hampers self-control of the specific aspect of brain activity being targeted in a specific BCI/NF task. Secondly, activations can promote the learning process indirectly, if they do not interfere with the activity in that small subset of both automatic and controlled processes necessary and sufficient to perform the BCI/NF task at hand. Although, while for some BCI classes, such as those employing certain kinds of stable and specific brain signals (e.g. SSVEP), the influence of unspecific processes signal is barely important, cognitive BCIs (Astrand et al., 2014) or BCI classes based on cognitive tasks such as mental calculation and motor imagery (Halder et al., 2011; Hammer et al., 2012) should be more subject to the effects of different forms of self-control over brain activity. Based on the differentiation between automatic vs. controlled processing as well as necessary vs. unnecessary processes, a framework of self-control of brain activity can start to be defined.

The optimal level of self-control of brain activity in a local control network is achieved under two main conditions: (i) avoidance of irrelevant associations between internal states and external reward; and (ii) staying engaged and focused on the task at hand without distractions. Condition (i) can be achieved when activity in the organismic control network is reduced to a minimum and condition (ii), when the central control network frees the most of its limited resources for the local control network.

Inspired by the work of Neuper and colleagues (Wood et al., 2014), we can adopt a framework of three concentric circles (Figure 4) representing the three sources of self-control. First, the outmost and thus most unspecific level of response to feedback reflects basically automatic processes. Second, the middle circle depicts central control networks performing controlled processing. Finally, in the innermost level, we describe networks responding specifically to the BCI/NF learning protocol. This local control relies on both automatic and controlled processes. We define those automatic processes unnecessary to perform a given BCI/NF task as the organismic control network. We call them organismic control because it reflects the activity of the thousands of automatic and

unconscious mental processes regulating the largest part of cognitive activity (Dijksterhuis and Nordgren, 2006). The interference of these processes is high when unnecessary automatic reactions to feedback are triggered, which compete with the learning process taking place in the local control network. Rumination, for instance, describes the intrusion of negative feelings about past experiences in the stream of thoughts and emerges primarily during relaxation (Nolen-Hoeksema et al., 2008).

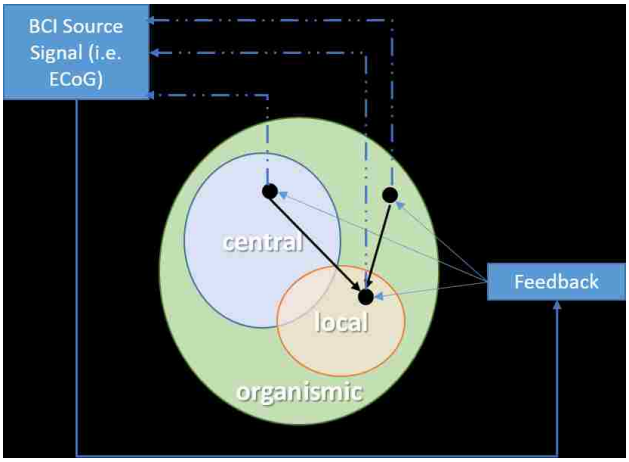

Figure 4 - A schema of different types of self-control of the brain activity. A schema of different types of self-control of the brain activity. Specific cognitive processes such as for instance motivation, mood, attention and executive functions are represented by black dots. Black arrows connecting the dots represent the interactions between the different cognitive functions. Two dots are depicted over the domain of organismic control network to illustrate that these processes are largely independent from one another. The contribution of the three types of self-control to physiological signals is represented by the dashed lines linking the specific cognitive processes to the physiological signals being recorded for BCI/NF learning. (Adapted from Wood et al, 2014)

The intrusion of ruminative thoughts is an example of the negative impact of the organismic control network on self-control of brain activity during BCI/NF learning. Cognitive processes subsumed under organismic control network are not easily influenced by direct instructions and mostly not even conscious to the participant. Therefore, it may be very important to monitor any signs of negative influences originating in organismic control networks. This unwanted activity should be fed back in a timely manner during training. As a consequence, processes like increased anxiety or intrusive thoughts are accessible to BCI/NF users and can trigger appropriate learning mechanisms capable to control or suppress these processes. Finally, we define the central control network as those controlled processes not strictly necessary to perform a given BCI/NF task. Controlled processes have limited capacity, so that every bit of irrelevant information being employed in the central control

network will be missed by the local control network. The negative impact of central control network is high when improper strategies, self-instruction, over-instruction or excessive attention to the self (Leary et al., 2006) withdraw resources from the local control network and hamper the regulation of the learning process in a similar way as a dual-task (Logan and Gordon, 2001) drains resources. In contrast to the organismic control network, controlled processing is largely under conscious control and can be modulated directly by instructions (Dijksterhuis and Nordgren, 2006). In summary, the aim of any BCI/NF learning is to magnify the signal produced by local control networks and suppress as much as possible the activity elsewhere. To do that, it may be necessary to take into consideration the specificities of two types of cognitive activity subsumed under organismic control networks and central control networks, since they imply very different learning mechanisms sensitive to different types of cues and reward. On the one side, participants could learn to decouple irrelevant from those relevant automatic processes. One way to achieve this is to monitor the automatic processes regulating for instance negative emotional reactions and anxiety as well as with a more selective schedule of reward and punishment. On the other side, participants may learn to use the central control networks to suppress irrelevant cognitive activity operating under conscious control such as excessive attention to the self (Leary et al., 2006). This could be achieved by direct instruction or self-instruction, i.e., motivated effort. Once achieved, this balance should improve the outcome of BCI/NF learning. Indeed, as demonstrated in the following chapters, incorporating this way of thinking within the design and execution of our BCI studies can lead to marked improvement in subject interaction and experience with our BCIs systems. While learnable, in the particular experimental conditions of the clinical wards, ECoG based BCI can be extremely difficult to implement and master, despite the apparent SNR advantages and ease of use. Therefore, keeping this type of framework in mind may be extremely valuable for continuing studies beyond the scope of this particular work.

Chapter 6: ECoG BCI @ the University of Washington.

Whether intended as a therapeutic device or as an experimental tool for fundamental research, many of the constituent components of a BCI are the same. Additionally, many of the neuroscientific methods associated with processing of the data that drive a BCI are common across our different analyses. Accordingly, this section outlines the standard BCI architecture and a number of the experimental techniques and analytical tools that are used throughout the remainder of this document. Though the implementation of the individual subunits vary widely from research group to research group, and are generally focused on engineering efforts to improve BCI performance, the typical architecture for all BCIs is the same. Systems include the following: a means of recording neural signals, a computational algorithm to extract features of interest from those signals, a decoder to transform those features into one or more control signals, and a device, virtual or realized, that carries out the actions dictated by the control signals and provides feedback to the user via one or more sensory modalities.

6.1 Components of a BCI

6.1.1 Data acquisition hardware.

Research in the area of fully implantable data acquisition hardware is moving quickly and will be critical in the development of viable and dependable BCIs. For the time being, however, the majority of human BCI studies use general purpose biosignal amplification systems. Most common electrophysiological data acquisition systems record between 16 and 256 channels simultaneously, at sampling rates specific to the signal being recorded. ECoG signals are typically sampled at > 1000 Hz using either AC or DC coupled instrumentation amplifiers, depending on the intended use of the signals being recorded.

6.1.2 Feature selection algorithm.

There exists a wide variety of methods to extract features of interest from neural signals. Many of these are highly specific to the type of signal being recorded, such as the isolation of action potentials from individual neurons using a window discriminator-based spike sorter, or the spatial unmixing of EEG signals using independent components analysis. Often, feature selection algorithms are chosen to effectively leverage the strengths of the decoder that will be fed the output of the feature selection algorithm, with specific attention to reducing or increasing the dimensionality of

the feature set as appropriate. Typically feature selection also attempts transform the neural data in such a way that the neural signals being discriminated become linearly separable. Typically, real-time feature extraction in an ECoG BCI involves re-referencing one or more previously selected channels to reduce common mode signal, and using a spectral estimator to determine a time variant estimate of power in the HG range recorded from the electrodes of interest.

6.1.3 Decoding

Decoding architecture options are as numerous as feature selection algorithms if not more so. Decoders are also typically highly application specific, based not only on the dimensionality and nature of the decoder outputs, but also on engineering tolerances specific to the application for which the BCI will be used. One trend in the field of BCI research has been toward building more intelligent decoders that are capable of robustly mapping motor-based neural features to BCI control, however the work discussed initially in this document provides an alternative view of decoder enhancement. We posit that decoders will benefit from additional channels of information that are more cognitive in nature. Understanding activity across a broad range of areas may help add context to highly dynamic signals that change as subjects gain proficiency and "self-control of the brain." This, coupled with improved resolution could fundamentally change how ECoG decoders, at least, are built in the future.

6.1.4 Applications

BCI applications are highly specific to their intended use. They range from EEG-based consumer-grade fashion devices to deep brain stimulators and neurally-controlled robotic limbs to communication devices or point-and-click digital cursor analogs. The content of this document focuses specifically on the cursor analogs for robotic reach and grasp style systems due to clinical relevance to the target population of patients with neuromuscular motor disorders.

6.2 Data collection and signal processing

6.2.1 ECoG Grids.

In all studies described below, subjects were implanted with platinum sub-dural ECoG electrodes for the purpose of seizure focus localization at Harborview Medical Center and Children's Hospital in Seattle, Washington. The physical design (number and arrangement of electrodes) and implant location of all grids were based on clinical indication. Arrays were either 8x8, 6x8, 4x8, or

2x8 grids or 1x8, 1x6, or 1x4 strips with 2.4mm diameter exposed recording surface and a 1cm inter-electrode distance.

6.2.2 Institutional Approval.

Subjects provided informed consent in accordance with the Institutional Review Board's direction and patient data were anonymized in accordance with HIPAA mandate. All procedures were carried out within the University of Washington Regional Epilepsy Center, either at Harborview Medical Center or Seattle Children's Hospital after informed consent was obtained. For children under age 18, parental consent was obtained along with consent from the child (age 14 or above) or assent of the child (age 7-13). The protocol was approved by the Institutional Review Board at both institutes.

6.2.3 Recordings.

Experimental recordings were performed at the patient's bedside without interrupting the clinical recording systems. Either g.USBamps (GugerTec, Graz, Austria) or TDT (Tucker Davis, Florida) sampled 1200 Hz were used for recording. Cortical potentials referenced against a scalp electrode were digitized and processed using the BCI2000 software suite (Schalk et al., 2004) which provided real-time feedback to the user.

6.2.4 Motor Screening

Prior to online control, subjects performed overt motor screening to determine candidate electrodes for BCI use. Depending on each subject's coverage, they performed gross hand motor movements (of the hand contralateral to the implant site), mouth motor movements, or both. Visual cues were presented for 3 sec followed by a 3 sec inter-trial interval. This process was repeated 10-30 times for each of the two motions. Subjects were then asked to repeat this screening process but with imagined movement. Electrodes that demonstrated statistically significant change in HG power during activity as compared to rest in either or both of these tasks were chosen as candidate controlling electrodes. In cases where there was more than one candidate controlling electrode, the electrode used for online control was chosen based on the magnitude of change between activity and rest and/or neuroanatomical relevance.

6.2.5 BCI Tasks

Both ECoG BCI paradigms were driven by spectral power changes in a portion of the HG frequency band of a single electrode determined to be modulated by motor imagery. Only a subset

of the HG range was used during online control (approx. 75-100 Hz) for computational tractability and to eliminate the need for real-time notch filtering to reduce line noise harmonics. HG activity was chosen as the control feature as it has been previously postulated that HG activity is a correlate of underlying population level firing rates or coherence in firing (Ray et al., 2008).

6.2.6 Initial training: the right-justified box task

The standard right justified box task (RJB) (Wolpaw et al., 2003) is depicted in Figure 5. During execution of this BCI task, a subject is presented with one of two targets, each either occupying the top half or the bottom half of the right-most edge of the screen. After a cue interval of two sec, the cursor appears on the left edge of the monitor and travels to the right at a constant horizontal velocity, such that the duration of the feedback period is fixed (typically 3 sec). The subject controls the vertical velocity of the cursor by modulating HG activity at the previously selected controlling electrode (CTL); performance of motor imagery causes the cursor to travel up and remaining at rest causes the cursor to travel down. Their objective is to complete each trial with the cursor in the specified target area for that trial. HG activity recorded at CTL is mapped to vertical cursor velocity using a simple linear decoder that was trained in the first set of trials. The task consists of four phases: rest, cue, feedback, and reward. In relation to the RJB task or other 1-D tasks – targets occupying the top half and bottom half of the screen are referred to as "up-targets" and "down-targets," respectively. The cursor's vertical velocity was updated every 40ms and controlled by changes in HG activity at the controlling electrode as calculated by an auto-regressive filter using the previous 500ms of data. This time-variant estimate of HG activity was z-normalized against 12 seconds of stored data (6 for each target type) and then mapped to cursor velocity. The normalizer was typically adapting (collecting reference data and updating normalization parameters) only during the first run (18 trials), however in cases where non-stationarity of the signals showed obvious bias, the normalizer was allowed to recalibrate. After initial training, subjects participated in further experiments with additional tasks (see Chapter 6-8) over the course of multiple days; duration of the recording sessions was dictated by the subjects' willingness and capability to participate.

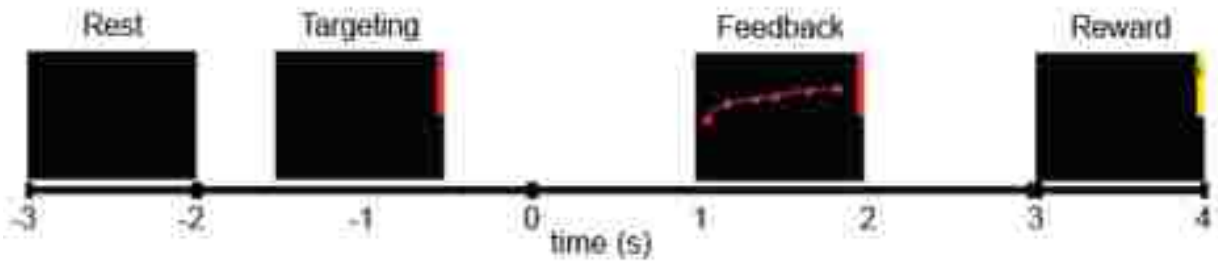

Figure 5 - Overview of the 1-D RJB task. Subjects were presented with a target occupying either the upper (up target; shown) or lower half (down target; not shown) of the right-most edge of the screen and had 3 sec to control the vertical position of the cursor. Horizontal movement towards the target was preset as a function of task time.

6.2.7 Cortical reconstructions and anatomical labeling.

Pre-operative magnetic resonance images (MRI) were co-registered with post-operative Computed Tomography (CT) scans using the Statistical Parametric Mapping software package (Penny et al., 2006). Three-dimensional reconstructions of the pial surface were generated using Freesurfer (freely available for download at http://surfer.nmr.mgh.harvard.edu/) and custom code implemented in Matlab (The MathWorks, Natick, MA). Electrode positions estimated from post-operative CT were projected to the reconstructed pial surface using the method outlined by Hermes and colleagues (Hermes et al., 2010). MRI images and projected electrode locations were normalized to Talairach coordinates using Freesurfer. Anatomical labels were estimated using the Human Motor Area Template (HMAT) (Mayka et al., 2006), and the Talairach Daemon (Lancaster et al., 1997, 2000).

Chapter 7: Designing a Bimanual BCI Platform.

As indicated previously in detail, much of the research on BCI has focused on developing assistive devices for patients with severe neuromuscular disorders, such as amyotrophic lateral sclerosis (ALS), brainstem stroke, and spinal cord injury, all of which result in degradation of volitional motor abilities (Wolpaw et al., 2002). Thus, typically, conventional wisdom applies BCI technologies to cases in which there is no motor ability remaining at all. However, there is a much larger population of patients that retain some residual motor function, even with degradation, who could benefit significantly from BCIs. In addition, looking further into the future, how could BCIs be augmented into a healthy-function motor system? An important question that had yet to be systematically studied is: can subjects use BCIs simultaneously coordinated with overt motor activity? More importantly, how do the cortical networks involved in the learning of this type of complex motor task change and what transient adaptation occurs in the targeted cortical areas that allow for control even in the presence of a highly mixed signal with highly simplistic decoding systems. For BCIs to be functional in the real world, even for simple tasks like opening a jar with two hands let alone something complicated like playing piano, patients would have to be able to utilize a BCI in coordination with other motor behavior. Our group has previously shown that the overall learning process involves motor-like learning networks, but there is a significant amount of cortical adaptation occurring during BCI control that is still not fully understood. This first study provides steps towards identifying these changes in the framework of a dexterous bi-manual hand coordination task in which individuals must learn to coordinate opposing BCI and overt motor behaviors.

7.1 A Non-invasive First Step for SimulBCI

A successful combination of BCI and manual control could push development of new user interfaces. One particularly challenging case involves using sensorimotor rhythm BCIs such as motor imagery and manual hand control, as there is significant overlap in the brain regions used. There is anecdotal evidence from BCI-based gaming studies supporting the possibility, but the question of overlap between BCI and overt motor activity has not yet been systematically studied. In this chapter we report the first steps in this direction by reporting results from our initial study combining motor imagery BCI with joystick control.

Though we have so far been discussing invasive methods like ECoG, for this initial design step we focused on EEG BCI. EEG non-invasively records brain signals from the scalp, and has advantages such as portability and cost effectiveness and accessibility to test subjects, though it suffers from a poor signal-to-noise ratio (Buzsáki, Anastassiou and Koch, 2012). EEG is also, unfortunately, susceptible to muscle artifacts when users produce eye movements or other types of overt movements (Wolpaw et al., 2000). Because our study explicitly aims to combine manual control with BCI, muscle artifacts become an important issue in contaminating EEG. We used electromyography (EMG) to ensure that muscle artifacts were not a major factor in the brain-control component of our experiments. We report results from three subjects who learned to use right-hand motor imagery to control the vertical movement of a cursor while simultaneously using a joystick with their left hand to control the horizontal movement of the cursor. All three subjects exhibited the ability to hit one of four possible corner targets on the screen.

7.2 Methods

7.2.1 Study Subjects

Three male graduate students who were right-handed and had prior experience in motor-imagery BCI volunteered to participate in our study. All subjects gave informed consent using study protocols approved by the University of Washington IRB.

7.2.2 Data Collection

Data were collected using g.USBamp (Guger Technologies) at a sampling rate of 1200Hz. A 13-electrode montage was chosen such that a Laplacian derivation could be obtained over motor areas centered at C3, Cz, and C4 electrode positions based on the international 10-20 system for EEG (distance between electrodes center was ~3.5cm). One additional electrode was used for ground and reference, placed at location AFz. All electrode impedances were measured and monitored to be within an acceptable range throughout the data collection sessions. We also placed three EMG electrodes on the right hand and forearm along the wrist extensor to monitor whether any right hand movement was being performed (as measured by EMG) during right hand imagery. EEG data were notch filtered between 58-62 Hz to eliminate line noise artifacts. Online right-hand imagery control was based on EEG data from the Laplacian derived C3 channel in our experiments, though other locations could also potentially have been used based upon the standard 10-20 montage.

7.2.3 Subject Training and System Configuration

Prior to the actual experiment, subjects underwent a training phase to verify that they were capable of performing motor imagery and to configure the BCI system's parameters. The training phase used a visual cue-based paradigm with no feedback. For each subject, data were collected for 20 trials of right-hand motor imagery (herein referred to as imagery or MI) and 20 trials of rest (i.e., no MI). Subjects were instructed to sit comfortably and to refrain from overt movement. For imagery trials, subjects were instructed to imagine moving their right hand, with imagery of fist clenching given as an example. For rest trials, subjects were instructed to relax and pay special care to refrain from blinking or making jaw/body movements.

These data were analyzed using the BCI2000 r2 and frequency spectrum (Schalk et al., 2004) functions to select two or three candidate frequency bands that correlate the best with the imagery task. The classification feature used was estimated band power, obtained with a band-pass filter and moving average of 0.5 seconds. Using the estimated power for imagery and rest classes for each of the candidate frequency bands, we selected the frequency band with the best discriminability (based on mean and variance), and set a threshold function for classification. This relatively simple system configuration was chosen to avoid the effects of changing and re-training the classification system, and was sufficient for binary classification of imagery/rest classes for all three subjects.

In the final step of the training phase, users performed online motor imagery with feedback. A right-justified box (RJB) paradigm was used (see **Error! Reference source not found.**); the cursor started at the left edge, moving rightward at a constant rate over the trial length until it reached the right edge. There were two targets, a bottom (rest) target and a top (imagery) target, that completely spanned the right edge such that on any given trial the random chance level of a hit was 50%. This online feedback paradigm is similar to the two-target task in [6]. The subject controlled the up and down motion of the cursor in the following manner: every 50 ms, the binary threshold-based classifier decided whether the recorded EEG signal was in the imagery class or the rest class. The cursor moved up by a fixed amount when imagery was detected, and moved down by the same amount when the rest class was detected.

One online feedback block contained five imagery and five rest trials (randomly interleaved). Each trial consisted of the following sequence of events. First, an auditory cue (a beep) is presented to the subject along with the visual target. Two seconds later, the trial begins, giving the subject six

seconds to control the up/down motion of the cursor to the designated target region. The rightward movement was set such that it took six seconds for the cursor to reach the right edge. At the end of six seconds, the trial ended, followed by a three second break before the next trial. Subject continued to perform online feedback blocks until they could hit 18/20 targets consecutively.

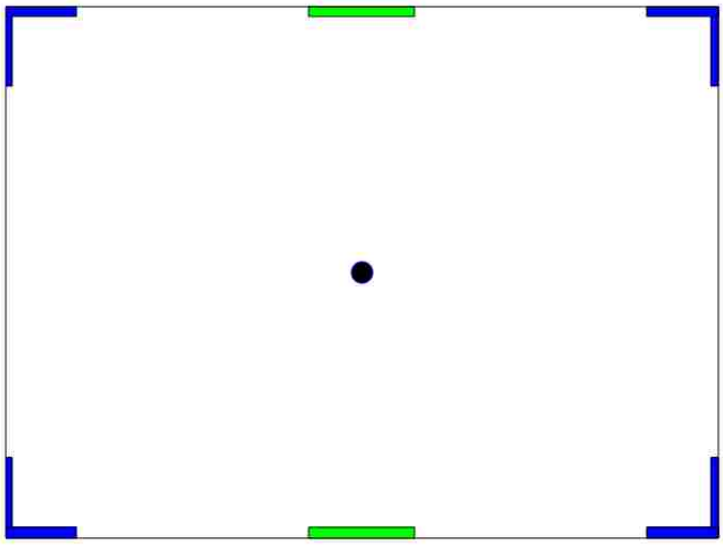

Figure 6 - Simultaneous Brain- and Manual-Control Task. The cursor (black ball) is shown in the center (the starting location) along with all possible targets. During BCI-only blocks, only the top and bottom (green) targets were shown. During the simultaneous BCI + manual control blocks, only the corner (blue) targets were shown. For any given trial, only one target is active. Activating motor imagery moves the cursor up, resting (no motor imagery) moves the cursor down. Left and right cursor movement is controlled using a joystick.

7.2.4 Experiments and Simultaneous BCI-Manual Task

Our experimental procedure consisted of two sessions over two days, each session lasting 1.5 hours (including electrode setup). For all experiments, the parameters from the online feedback training phase (threshold classifier and mapping to cursor movement) were maintained for each subject. On each day, subjects ran six blocks of BCI-only (motor imagery/rest) and nine blocks of simultaneous BCI + manual control (using a joystick). The task setup seen in Figure 6 was used for both types of blocks, but different targets were shown (top/down for BCI-only, corners for simultaneous task). The sequence of events was the same as the online feedback training, except that the target could be hit before the 6-second trial duration ended. In this case, cursor movement stopped until the 6-second duration expired, and subjects were instructed to continue with imagery or rest depending on the condition.

In the BCI-only blocks, movement of the cursor was constrained to be along the vertical axis. Each block contained five imagery trials and five rest trials, resulting in 30 trials per class. For the

simultaneous BCI + manual control blocks, the horizontal movement of the cursor was mapped to the left and right movement of a joystick, controlled by the subject's left hand. Horizontal movement was again by a constant amount (no acceleration). Each block contained three trials each of the following different cases: right motor imagery + joystick left, right motor imagery + joystick right, rest + joystick left, rest + joystick right. For data analysis, we pooled the joystick left and right such that there were two conditions: right motor imagery + joystick and rest + joystick. The nine blocks yielded six trials for each condition, resulting in 60 trials per class over one day.

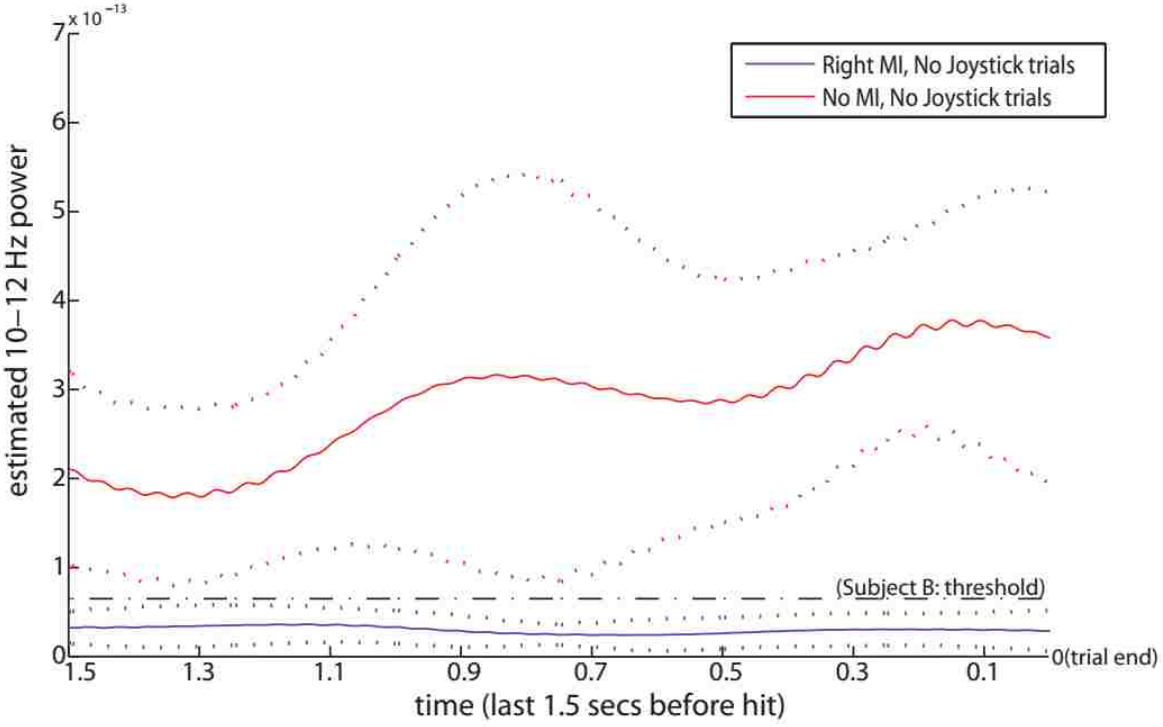

Figure 7 - Comparison of EEG Band Power for MI versus no MI. The red and blue solid lines indicate trial averaged power in 10-12 Hz; dotted lines indicates one standard deviation. The black dash-dot line shows the threshold chosen for classification.

7.2.5 Results

The feature selected for all three subjects was the 10-12 Hz band, since all subjects showed robust and consistent difference between imagery and rest classes in this band. This feature is validated by previous BCI work from the Wadsworth group (Wolpaw et al., 1991; Wolpaw, McFarland and Vaughan, 2000; Daly and Wolpaw, 2008). Though the band is maintained, the threshold function for each subject was different and individually determined during the initial training phase. An example of the threshold is shown for Subject B in Figure 7.

Table 1 shows the performance of the three subjects in the two-day experiment. Most notable is the difference in the simultaneous motor imagery BCI (MI) + joystick condition from the first day to the second. For subjects B and C, their first day was heavily biased toward the top targets ("MI + joystick" in Table 1), indicating active interference from ipsilateral motor control of the joystick. However, on the second day, subjects appear to have learned to overcome this interference from joystick control, balancing the top versus bottom target hits and exhibiting a much higher degree of purposeful control.

Subject Performance

Subject/Day	MI Only		MI + Joystick	
	Top Hits	Bottom Hits	Top Hits	Bottom Hits
A (day 1)	9/30 (30%)	23/30 (76%)	36/54 (67%)	21/54 (39%)
A (day 2)	12/30 (40%)	16/30 (53%)	33/54 (61%)	28/54 (51%)
B (day 1)	24/30 (80%)	18/30 (60%)	50/54 (92%)	2/54 (3%)
B (day 2)	18/40 (45%)	32/40 (80%)	37/60 (61%)	42/60 (70%)
C (day 1)	15/30 (50%)	16/30 (53%)	49/54 (90%)	1/54 (2%)
C (day 2)	17/30 (57%)	27/30 (90%)	27/54 (50%)	23/54 (42%)

Table 1 - EEG-SimulBCI Subject Performance

It is important to note that although performance appears to be low, especially compared to the initial RJB screening task, the limited successes do demonstrate subject-specific control. Neither the up/down nor four corners task is a selection task, in which the chance outcome of a trial would follow the uniform probability distribution of 50% for up/down or 25% for corners. In our cursor movement task, a subject had a possible 140 movement steps (including along diagonals), with 62 consecutive steps from the origin necessary to hit either the up or down target. Assuming arbitrary random walk, the likelihood of hitting either the up or down target in the time allotted (6 secs) is low. To ensure consistent movement and a successful hit, a subject must maintain their signal for at least three seconds (62*50ms). Since the chance of hit in this case is less than 0.005%, any hit requires concentrated effort on the part of the subject.

Histograms of the 10-12 Hz band power show interesting differences in alpha desynchronization activity (assessed with estimated band power from 10-12 Hz band-pass filter and

moving average of 0.5 seconds, units of V2) between the imagery and rest classes for BCI-only and simultaneous BCI + manual control. Figure 8 shows 10-12 Hz ("alpha") band power over C3 channel in the last 1.5 seconds before either a successful hit or timeout of a trial for subjects A & C (we show more in-depth histograms for subject B in Figure 9). Note that for subject C, who had the lowest performance, there is significant overlap in 10-12 Hz power between the imagery and rest classes during BCI + manual control. We postulate that this overlap may have been a factor in the low performance. Figure 9 shows similar histograms with channels Cz and C4 included for Subject B, who had the highest target hit percentage on day 2. As expected from previous work (Wolpaw et al., 2002; Ang et al., 2010; Prasad et al., 2010; Friedrich, Scherer and Neuper, 2012), right hand MI-only resulted in a power decrease in the 10-12 Hz ("alpha") band over the contra-lateral hemisphere (C3), while central (Cz) and ipsi-lateral (C4) areas show similar band power distributions (Figure 9, right column). Simultaneous MI + joystick resulted in more widespread alpha desynchronization (Figure 9, left column) and an overall decrease in power. However, there is still specificity in the C3 region when compared to Cz and C4. (Figure 9, top left).

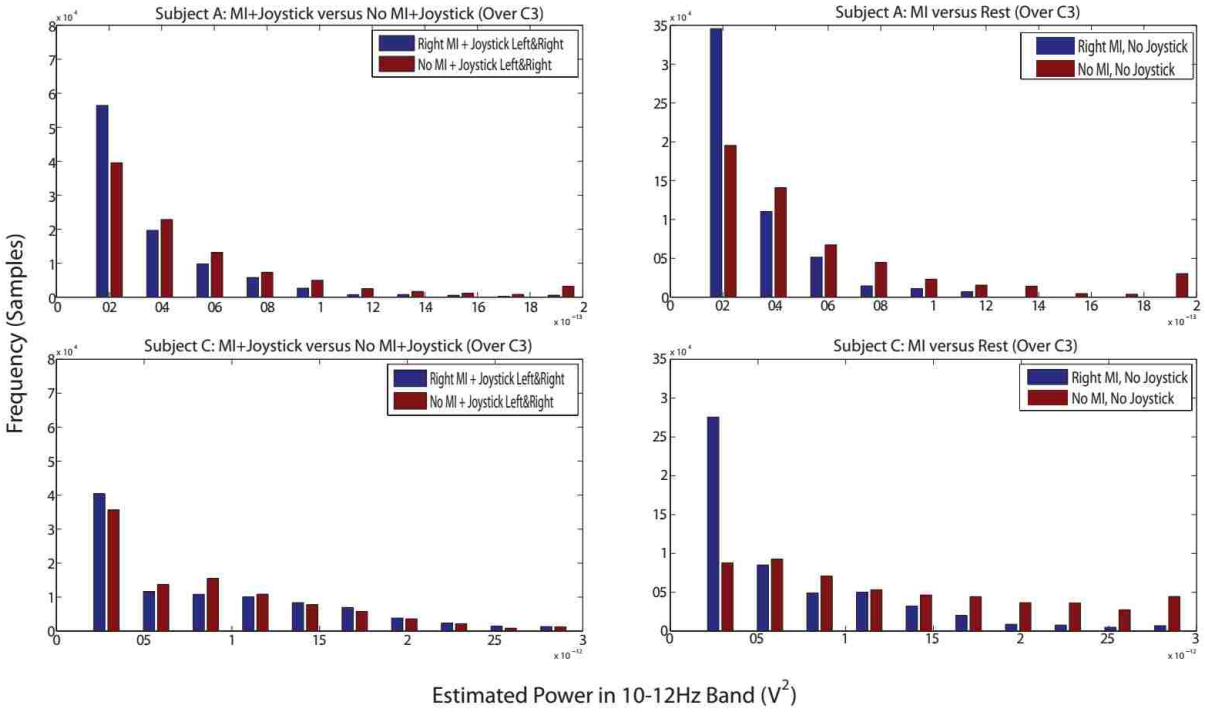

Figure 8 - Distribution of EEG Power for Simultaneous BCI+Manual and BCI-only Tasks. Histograms of 10-12 Hz power estimates for subjects A & C over location C3 on day 2 during the last 1.5 seconds prior to target hit or miss. Top row: Subject A, Bottom row: Subject C. Left column: Simultaneous BCI + manual control, Right column: BCI-only.

Bins are the same within each subject. To help visualize the representative range of the data, outlier values (largest 2% of values) are collapsed into the last bin.

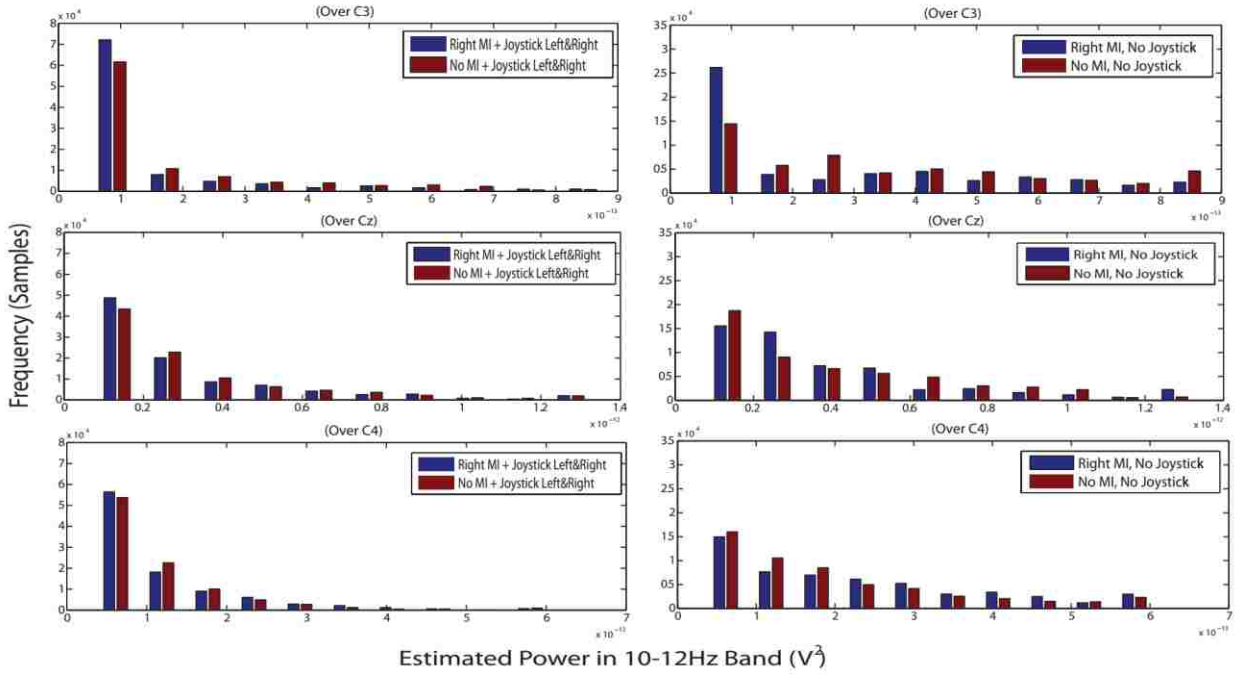

Figure 9 - Distribution of EEG Power (cont.) for a Single Subject. Histograms of 10-12 Hz power estimates for subject B on day 2 during the last 1.5 seconds before a target was hit or end of trial (no hit). The data distribution shows that the subject was able to reduce power specifically over the control electrode location (C3) using right hand imagery, even during simultaneous BCI + manual control condition (left column), although to a lesser extent than BCI-only conditions (right column). Bins are the same within each channel (not the same across channels). To help visualize the representative range of the data, outlier values (largest 2% of values) are collapsed into the last bin.

7.3 Considerations for next steps

Our results suggest that subjects can learn to exert direct brain control over a device while simultaneously engaging in overt motor control over another aspect of the same device. In particular, two of the three subjects in our preliminary study showed marked improvement in performance from the first day of experiments to the second in the simultaneous BCI + manual control task. A possible concern with the present study is whether the subjects used some form of muscle activity to control the cursor instead of imagery-based BCI control. Two types of evidence suggest otherwise. First, EMG activity recorded on the right hand does not appear to be correlated with the EEG signals used for right hand imagery-based control: the r2 correlation of the EMG signals between imagery and rest classes were 0.04, 0.13, and 0.05 respectively for subjects A, B, and C. Second, the histograms for power estimates in Laplacian-derived C3, Cz, and C4 channels show that C3 exhibited clear

differences between imagery and rest conditions, while C4 and Cz did not; this would not be expected in the event of widespread artifact contamination.

It is well-known that muscle artifacts associated with facial movements such as jaw and eyebrow movements can have significant effects on EEG signals (see, for example,). However, the current study suggests that muscle movements that are distant from the scalp, such as the overt left arm movements used in the study, may not have such a strong effect on the EEG signal. Instead, activation of overlapping motor areas for imagery and movement may be a major factor affecting EEG BCI in these cases (Miller et al., 2010). Evidence for this suggestion can be seen in the histograms in Fig. 9 for C3 and C4, where overt movement of the joystick during rest trials also caused the power distribution to shift into the lower power range, similar to imagery trials.

The study reported here was the first in a series of studies aimed at systematically investigating the extent to which BCI use can overlap with normal physical activity. Further studies, as elucidated in the rest of this document, evaluate effects of long-term training, and include a larger subject pool utilizing electrocorticographic arrays for more focused control and nuanced examination of cortical changes during task performance. It is our hope that these efforts will help broaden the reach of BCIs by expanding their realm of applicability to the larger populations of individuals.

Chapter 8: Bimanual Coordination with Electrocorticography.

Building off the overall design in Aim 1, in this study, we attempt to answer the important question of whether individuals can use BCIs in their current state in simultaneous or concurrent coordination with overt motor activity akin to that which occurs during normal bimanual natural movement. Of importance, as well, is how the cortical networks involved in the learning and mediation of this type of complex motor control might adapt and affect the already challenged BCI decoding and translating systems. In the previous chapter, we have shown that for a noninvasive bimanual BCI control paradigm that even with the interfering activations from the overt behavior ipsilateral to BCI-control, users are able to develop a remarkable level control with enough training (Cheung et al., 2012). However, the initial task developed was not sufficient as users developed staggered, switching strategies which reduced the periods of concurrent bimanual activation. In addition, the basic task was extremely difficult, with subjects reaching fatigue points before full success could be attained. Nevertheless, the limited control is promising, though the modality of EEG prevents the deep examination of the byplay between overt and BCI bimanual control. For that, we need to scale to more invasive methods, in this case ECoG, with a newly designed task.

Some potential insight for what to expect when moving beyond EEG comes from the non-human primate literature in which complex hand grasp and limb behavior has been studied in infinitesimal detail. In these models, it has been shown that cortical networks are, in fact, optimized for bimanual limb control, and thus, for neural populations in a cortical hemisphere tuned towards control or movements of the contralateral hand or arm, there is a limited representation of the ipsilateral limb kinematics as well (Ganguly and Carmena, 2009; Ganguly et al., 2009). In a similar vein, at the level of local field potentials in humans, this type of mixed signal has been seen as a detectable but less pronounced 70-200Hz high gamma (HG) frequency response with a boosted beta frequency (12-30Hz) profile for finger movements ipsilateral to the recording site (Zanos, Miller and Ojemann, 2008; Scherer et al., 2009). Therefore, much for the same reasons that many BCI paradigms see this neural activity as signal noise (Prasad et al., 2010) and require 'healthy' test subjects to minimize overt movements during testing, we hypothesize that residual movement abilities not directly associated with the BCI control could affect the accuracy of the BCI performance. However, in one non-human primate study, for the case of simultaneous execution of BCI and overt movement,

a force hold behavior during a cursor task, monkeys were able to gain proficiency with their paradigm without completely disrupting their learned neuroprosthetic control skills (Orsborn et al., 2014). This is, then, promising for expansion of similar studies in humans.

It is clear, that for real bimanual coordination, though challenging, the chaotic cortical networks manage to enable learning and development of these complex motor behaviors (Kadivar et al., 2011). As our group has previously determined, the overall learning process for BCI tasks involves motor-like learning networks and, as such, dexterous bimanual BCI coordination is not so unfathomable despite the difficulties (Wander et al., 2013). We believe leveraging a more focal methodology such as electrocorticography (ECoG) (Leuthardt et al., 2004; Blakely et al., 2009; Moran, 2010) which also allows for examining distributed cortical activity(Darvas, Ojemann and Sorensen, 2009; Gomez-Rodriguez, Grosse-Wentrup, et al., 2010; Miller et al., 2010; Wander et al., 2013), should allow for the development and use of a BCI despite these complex cortical interactions. Rather than consider any opposing movement execution activity as a hindrance to BCI performance, we examine to what extent they can coexist when the activity is distributed cortically. For five subjects, we train and evaluate their performance and cortical response for a bimanual 2-D center-out cursor task in which they are required to coordinate key presses with one hand with motor imagery of the other, opposite hand. Though challenging, subjects show gains in proficiency and ability, especially in the situations requiring concurrent output of both motor behaviors for success.

8.1 Materials and Methods

All subjects were patients with intractable epilepsy undergoing monitoring with implanted subdural ECoG electrodes for seizure focus localization at either the University of Washington's Harborview Medical Center or Seattle Children's Hospital. Electrodes were platinum-iridium electrodes (Adtech Inc., Racine, WI or Integrahealth, Plainsboro, NJ) suspended in silastic with a 1cm inter-electrode distance for all arrays and 2.3mm diameter of exposed surface for each electrode. Electrodes were placed by medical staff over the cortical areas as per the clinical indications. Patients provided informed consent to participate as subjects for research activities during clinical monitoring under Institutional Review Board guidelines for University of Washington and Seattle Children. For any patient under 18 years of age, parent(s) or legal guardian(s) provided consent. For inclusion in this study, patients had to present with intact hand motor function, with implant coverage such that at least one ECoG electrode would be over the traditional M1 hand motor knob and show a

corresponding signal response to hand movement (further discussed below). In addition, as epilepsy can often result in various cognitive impairments, after consent subjects had to be able to satisfactorily comprehend and attend to behavioral tasks before interacting with the BCI task. Though additional subjects were recorded from for parallel studies, all subjects discussed herein meet the stated criteria.

8.1.1 Subjects

Subject demographics and research involvement for this study can be seen in Table 2. This study includes 5 subjects ranging from thirteen to fifty with three females and two males. Relative implant locations can be seen in Figure 10-a. Due to available experimental time and unexpected clinical interventions during experimentation, subjects performed different lengths of tasks, though all went through the same basic protocols. Subjects completed as many task runs as possible; the number of recording sessions was highly dependent on subject's rate of fatigue and interruption from clinical staff. At the least, 24 trials were attempted per run up to as many as 64. To prevent subject fatigue and reduce the risk of interruption and improper task completion, each task run was limited a max of 10minutes, though both still occurred as noted.

Subject ID	Age	Gender	Implant Hemi.	'Simul'-BCI Task Information and Notes			
				BCI Electrode	Overall Acc.	Session Notes	Previous BCI
3f6772 (S1)	26	M	B (L)	21	52.1%	Single Session, day 6 after implant. 2 long Runs.	none
6b68ef (S2)	50	F	R	5	63.9%	Single Session, day 6 after implant. 4 short Runs; often interrupted by clinical staff	1-D BCI, d5/d6
6cc87c (S3)	11	F	L	26	81.8%	Single Session, day 4 after implant. Few medium Runs; several aborted runs (removed).	1-D BCI, d4
a9952e (S4)	13	F	L	7	46.0%	Single session, day 10 after implant. Few short Runs; one long run. Many clinical interruptions	1-D BCI, d9
ada1ab (S5)	16	M	R	29	58.1%	Single Session, day 6 after implant. Few medium Runs; some aborted runs (removed); clinical interruptions.	1-D BCI, d5

Table 2 - Demographics and task information for implanted subjects. Included are subjects' HIPAA/IRB compliant experimental ID, age and gender at time of experiment, the general implant location, the electrode used for BCI interaction, their overall performance, as well details regarding their experimental process. Further details are provided in the following sections. For S1, Bilateral strips were implanted with only the Left hemisphere recorded during experimentation.

8.1.2 Data Recording and Stimulus Presentation

Experimental recordings were taken at the subjects' bedsides without interrupting the primary clinical recordings. Data were acquired at 1200Hz using four synchronized sixteen-channel g.USBamps (GugerTec) (Kapeller et al., 2014) connected to a high-performance Sager laptop computer. Data were anonymized in accordance with Health Insurance Portability and Accountability Act mandate. For some subjects, 1x8 strips of electrodes were implanted in lieu or in addition to the standard 8x8 electrode grid. Recordings were hardware limited to 64 channels; only the electrodes used during experimentation are shown in Figure 10-a. Cortical potentials were referenced against a scalp electrode and digitized and processed in the BCI2000 software suite(Schalk et al., 2004). Task data were also synchronized with ECoG within the same software setup.

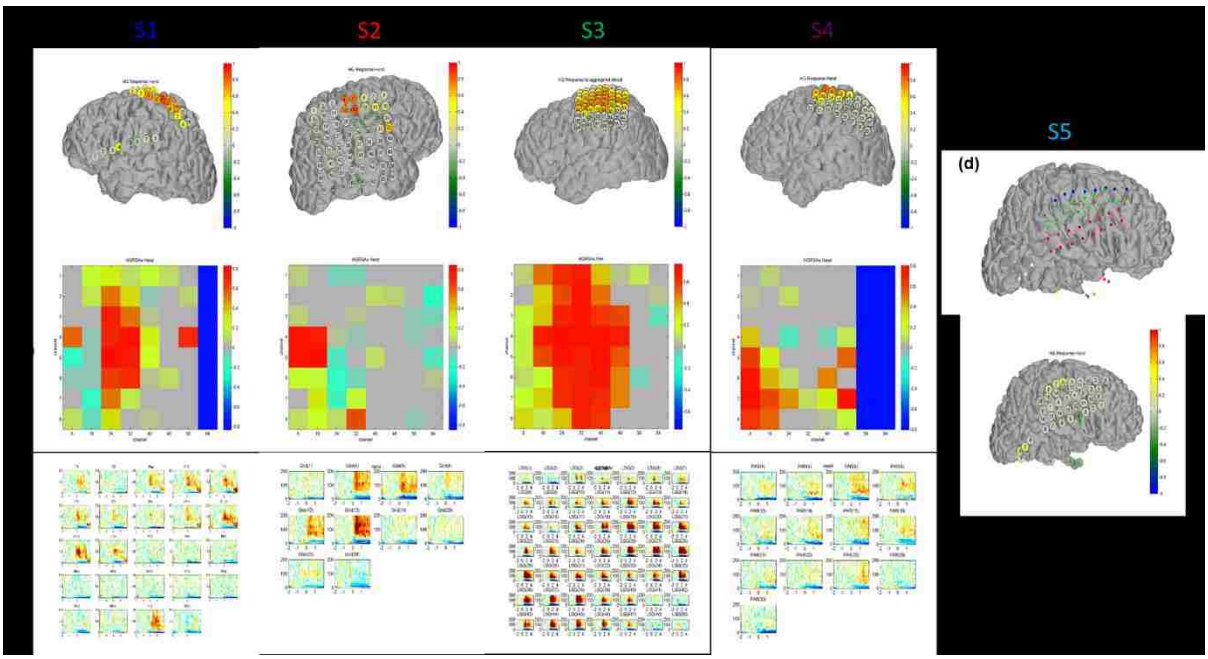

Figure 10 - Relevant Implant Locations and Behavioral Screening Results. a) Implant location for grid arrays recorded from during experiments shown for each subject. Some subjects had multiple arrays and grids; unused arrays not shown for simplicity. Heat map shown for HG response to hand movement as part of behavioral screening, described further in Methods. Patient MR and CT scans were used to create 3D head model reconstructions showing the spatial arrangement of the implanted array in relation to the cortical tissue below. b) Heatmap is self-scaled by subject RSA values to show the degree of activity versus rest for each subject. Blue columns, seen for S1 and S4, represent channels not used for those subjects in the standard 8x8 grid array. c) Time-frequency representations of frequency band-power from 0-200 HZ over the hand movement period for RSA-significant electrodes for each subject. This helps valid statistical selection and shows in-time development of the task-relevant frequency response. d) Due to clinical interventions during the screening session, behavioral response for S5 was much muted. Hand-related electrode was validated for this case based upon separate clinical mapping and testing.

8.1.3 Data Processing and Signal Analysis

All channels recorded from the electrocorticographic grid were common average re-referenced by subtracting the average signal recorded at all electrodes. This was done in an attempt to remove any common noise introduced by activity recorded at the scalp reference electrode in the electrically noisy hospital environment. As per previous ECoG studies from our group, the re-referenced signals were band pass filtered for the high-gamma (HG) range (70-200 Hz) using a fourth-order Butterworth filter (Darvas et al., 2010). The square of the magnitude of the Hilbert Transform was then used to calculate a time-variant estimate of band-power (Wander et al., 2013). Data were then log transformed in order to become approximately normally distributed for proper statistical analyses (Blakely et al., 2009). To account for differences between recording sessions, this log-power estimate was further z-normalized with respect to the rest (behaviorally quiescent) periods for each channel and session. This signal is heretofore discussed as the HG signal or HG activation. Similar extrapolation was done for the lower frequency beta range (8-32 Hz) as well, though not used for primary analyses.

In the screening motor behavior tasks, for every electrode and movement type, we calculated a high and low activation weight by comparing the distributions of HG and beta for each movement type with the corresponding rest distributions. This provided an activity metric based upon the signed, squared cross-correlation value, a measure of how much of the variance in power across both movement and rest epochs was accounted for by the difference in the mean power between movement and rest epochs (Miller et al., 2007). For convenience, this is referred to as the RSA values (HG or β RSA) and can be thought of as analog of the r^2 metric, without the regression. (Miller et al., 2007)

8.2 Experiment Protocol

Though duration was quite different, each subject went through the same basic protocol: a screening task, a training task, and the BCI task. Subjects were given verbal instructions at each stage with information on what they would be presented and what was expected of them for each task. Instructions were repeated at the beginning of each run. The screening task was run with a battery of other traditional cognitive psychology and behavioral tasks the day before BCI training. Due to available experimental time and competing parallel experiments, no subjects performed this BCI task for more than one contiguous session, though some patients performed a prior 1-D center out cursor

task in a previous session. The decision to perform both the 1D and concurrent BCI task was based on time available with the subject.

8.2.1 Screening Process

Before attempting online control, subjects performed an overt motor screening exercise, in addition to clinical motor evaluation. Subjects were visually prompted to move their hand or tongue for 3s with a 3s rest period in between each movement. This is repeated about 20 times. Subjects then repeat the task, imagining the prompted movement without executing an overt motion. As described previously, the signed, squared cross-correlation measure (RSA) can show how many electrodes are active during task compliance. For each subject and task type, the HG and β RSAs were calculated for all electrodes (Figure 10-b). For each electrode with significant task-relevant activity (non-zero HG or β RSA), an aggregate time-frequency representation from 0-200 Hz for each task class was built to examine the frequency power change and distribution over time (Figure 10-c). Electrodes were also plotted in relative spatial orientation (Figure 10-a) as per their cortical location, to validate activity with anatomical landmarks. The electrode with the highest significance in the narrower 70-90Hz band over a putative hand motor region was then chosen as a candidate for use in BCI control. Due to their physical condition and possible drug interactions during screening, Subject 5 (ada1ab) did not show any robust HG activation during screening (Figure 10-d). However, clinical mapping and localization performed by medical staff showed viable electrode candidates for hand motor coverage which was confirmed during training.

8.2.2 Training

The task experienced by some subjects was a one-dimensional variant of the center-out task that has been used in numerous invasive and non-invasive BCI studies (e.g., (Simeral et al., 2011)). Subjects are presented with the target for 2-3s (the 'cue' period), then the cursor appears and the subject must modulate neural activity of the controlling electrode to move the cursor into the space defined by the target (the 'feedback' period). To succeed in any given trial, the subject must move the cursor into the space defined by the target and maintain it within that region for a specified dwell time (1s). If the cursor leaves the target before this dwell duration has completed, any subsequent entry into the target area will still be required to dwell for the entire duration of the dwell time. Movement of the cursor was restricted to vertical dimension and targets were placed along the vertical line that passes through the cursor origin. Unlike the standard center-out task, in this case

targets had properties other than location that varied on each trial. Targets were placed either above or below the origin at one of two distances from the origin (20% or 35% of the total screen height). They were also be one of two diameters (8% or 16% of total screen height). Overall this was a very difficult task, with hit rates being 14.5%, 45.5%, 45.3%, and 16.7% for Subjects 2-5, respectively, with chance around 25%. As the Motor Imagery control scheme between this task and the Concurrent BCI task was the same, signal gain and offset parameters were ported between the two tasks. For Subject 1, who did not perform this task, these parameters were derived from an brief 1-D BCI version (vertical targets only) of the primary 2-D task running the Normalizer/Adaptation pipeline, described further below, before directly engaging with the full task.

8.2.3 Bimanual Concurrent BCI Cursor-Out Dwell Task

Following screening and training, subjects performed a 2-D center-out cursor dwell BCI task using hand motor imagery (contralateral to hemisphere of implant) to control the vertical movement of the cursor and arrow key presses (Key) with the opposite hand (ipsilateral to implant) to control horizontal movement (Figure 11). 'Brain control' of the cursor was driven by spectral power changes in the 70-90Hz band of a single electrode during modulation of motor imagery.

8.2.3a BCI Control Scheme

The cursor's vertical velocity was updated at 40ms driven by changes in HG activity at the controlling electrode as calculated by an autoregressive filter using the previous 500ms of data. Horizontal movement of the cursor was mapped to overt presses of the right or left arrows keys by the opposing hand. Consistent motor activation was insured with a center-facing gravity on the cursor in the horizontal axis, requiring the subject to continuously press a key to keep the cursor moving in the desired. In the horizontal direction, the cursor x-position is updated at 30Hz; with each update the cursor position moved (|right - left key presses| * key press distance) – gravity distance, where key press distance is 1.39% and gravity reversal distance is 0.0005% of the total workspace 0-1(AU). To reach diagonal targets, a subject would need to exhibit and maintain concurrent control. To aid with engagement and motivation, a running score was provided based upon target hit and cursor distance from the center of the target. Task difficulty could be adjusted by changing the diameter of each target based on a difficulty slider (5 to 1, 1 being smallest diameter and highest difficulty). Eight targets distributed radially were presented at random as shown in Figure 11-a.

8.2.3b BCI Trials

We utilized a block-randomized trial design, to present the user with an approximately equal number of occurrences of each target type, even in runs that were aborted before completion, while controlling for potential order effects between trial types. Each block consisted of a single presentation of each of the eight potential targets. Each standard run consisted of three consecutive blocks. Each trial started with the target being cued in one of the 8 locations. Two seconds later the feedback period began with cursor at the center of the screen. Subject was given control for six seconds, followed by a blanking of the screen, with the score still shown. The inter-trial interval was one second with some jitter. Figure 11-c shows the schematic of a single trial. Subjects were instructed to imagine moving their hand (contralateral with respect to hemispheric coverage) when presented with targets in the upper half of the screen (up or +y targets). When presented with targets in the bottom half of the screen (down or –y targets), they were instructed to 'rest' or not engage with motor imagery. Due to the use of a single finger for right & left arrow key presses, targets were consolidated and re-categorized by activity type (target category) where TC1 requires only motor imagery ((+)MI) to be reached, TC2 requires concurrent control of motor imagery and key presses ((+)MI + Key), TC3 utilizes only arrow key control (Key), TC4 requires a quiescence of motor imagery coupled with key presses ((-)MI + Key), and TC5 needing purely downwards motor imagery ((-)MI) activation. A cartoon of this is presented in Figure 11-b for visual reference. Duration of each recording session and the number of runs was dictated by the subjects' willingness and capability to participate at the time of experimentation and as per clinical constraints.

8.2.3c Quantification of Behavioral Outcomes.

Though success on a trial is formally defined as moving the cursor to the target edge (a hit), the task was designed such that there were other behavioral metrics that can be extracted to facilitate statistical comparisons of performance. The dwell time and rate provides for a score metric as an analog of precision. Additionally, we assessed integrated squared error (ISE) of cursor position relative to the nearest edge of the target on each trial.

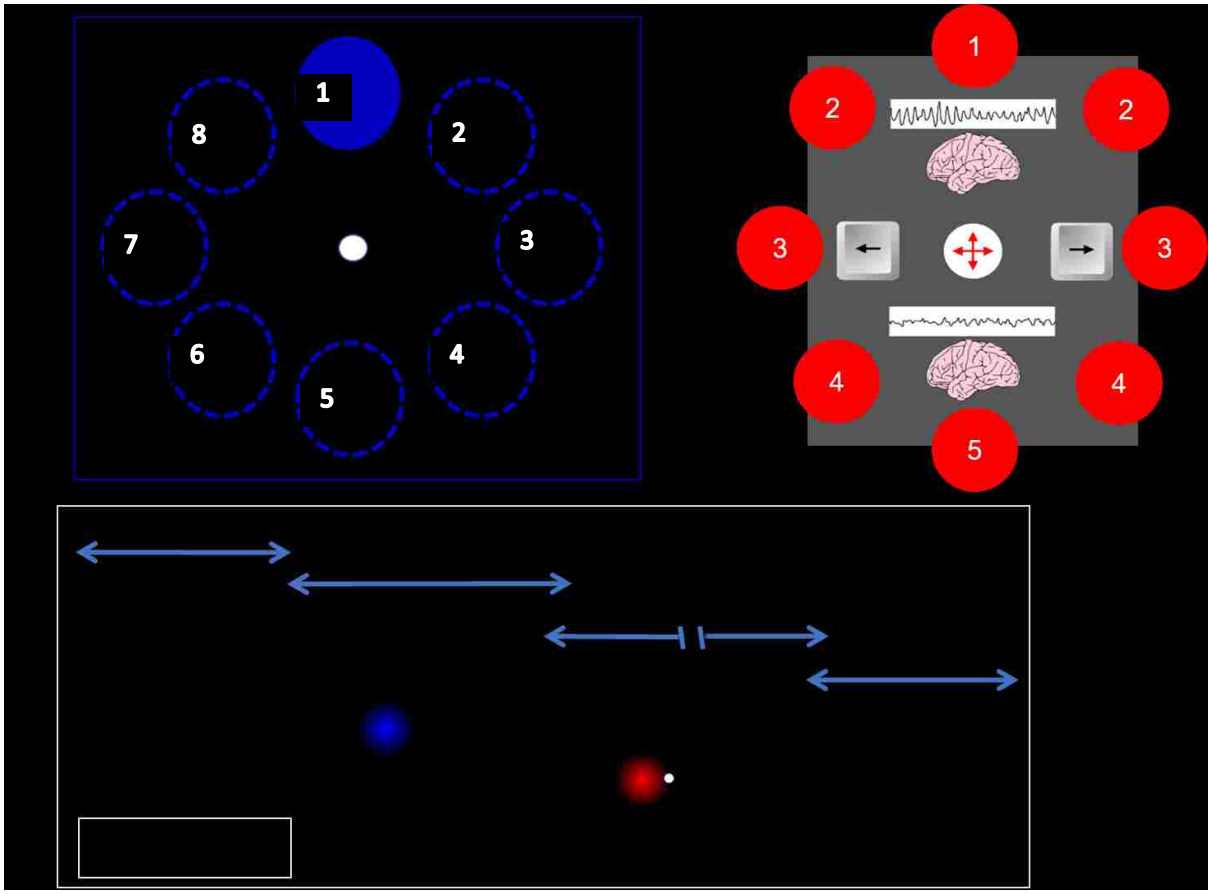

Figure 11 – Two dimensional, Center-Out, Cursor Dwell BCI task. a) Eight targets distributed radially were presented at random. Subjects performed a 2-D center-out cursor dwell BCI task using 'contralateral' hand motor imagery (MI) to control the vertical movement of the cursor and keyboard presses with the 'ipsilateral' hand (Key) to control horizontal movement of the cursor to reach target center. The task window was rectangular justified to a 4:3 aspect ratio with vertical edges and a black background. A running score was provided in the top right corner based upon cursor distance from the center of the target after contact. b) 'Brain control' of the cursor for vertical velocity was driven by spectral power changes in HG of a single electrode during modulation of motor imagery. Targets can be categorized by level (1-5) based on the output behavior required from the subject to achieve success. The BCI control scheme is further described in text. (c) Each trial started with the target being cued in one of the 8 locations. Two seconds later the feedback period began with cursor at the center of the screen. Subject was given control for six seconds, followed by a blanking of the screen, with the score still shown. The inter-trial interval was one second with some jitter. Score was calculated through each run to provide subject with a running, motivating, analog of performance.

8.3 Results

Subjects performed between 64 to 160 total trials, with a reduced number of viable trials based upon clinical or user interruption. These aborted trials as well some early trials in which subjects talked with researchers to clarify instructions or were otherwise distracted were discarded from analysis to ensure proper comparisons between all control behaviors.

8.3.1 BCI Performance

Due to the gravity element in the x-direction and the velocity maximums defined by the 6 second window, chance levels were not 12.5% for all targets as with a traditional 8 target center out task. Rather, chance was defined by the necessary output behavior. For right and left targets along the x-axis requiring only key presses (TC3), the gravity element reduces chance to 0%. Only with a continuous regular output of arrow key presses could a user hit one of these targets. An accidental tap or hold down of the key would only move the cursor one frame in the '+/-' x direction, which would be returned back one increment the following frame. For targets requiring motor imagery, individual chance performance levels varied from subject to subject based on the number of trials performed and differences in cursor kinematics due to variability in the BCI decoder. To characterize chance task performance under the null hypothesis that subjects did not have volitional cursor control, we replayed all recorded cursor trajectories with a randomized target location and recalculated hit rate and ISE. This process was repeated 1000 times per subject to characterize the distributions for hit rate and ISE under the null hypothesis. Assuming proper keyboard output, average chance for all targets with |y>0| coordinates were 26.7%, 19.3%, 22.8%, 25.8%, and 20.5% for each subject, respectively. As reported in Table 2, all subjects perform above chance with overall accuracies of 52.1%, 63.9%, 81.8%, 46%, and 58.1%, respectively.

However, as Figure 12, demonstrates, this alone does not provide an adequate representation of performance. Figure 12-a, compares subjects' accuracy and precision (score). Ideally, subjects would both gain accuracy and precision with more training. This is, in fact the case, for subjects 1 and 4. For Subjects 2 and 3, however, though their overall hit-rate does improve initially with better precision, both slightly lose accuracy over time, though subject two's overall precision or ability to dwell improves dramatically. Subject 5, on the other hand, seems to become worse overall with training, with their final run hit-rate barely being over chance. Further examination of these trends, shows that the loss in ability is primarily driven by gross misses in specific target categories (Figure 12-b). For example, subject 5's poor performance is clearly driven by an inability to hit TC1 or TC2 targets, both types requiring (+)MI output. Similarly, Subject 3's loss in accuracy is driven by misses of TC5 ((-)MI only), despite a 100% hit rate for TC4 ((-)MI + Key).

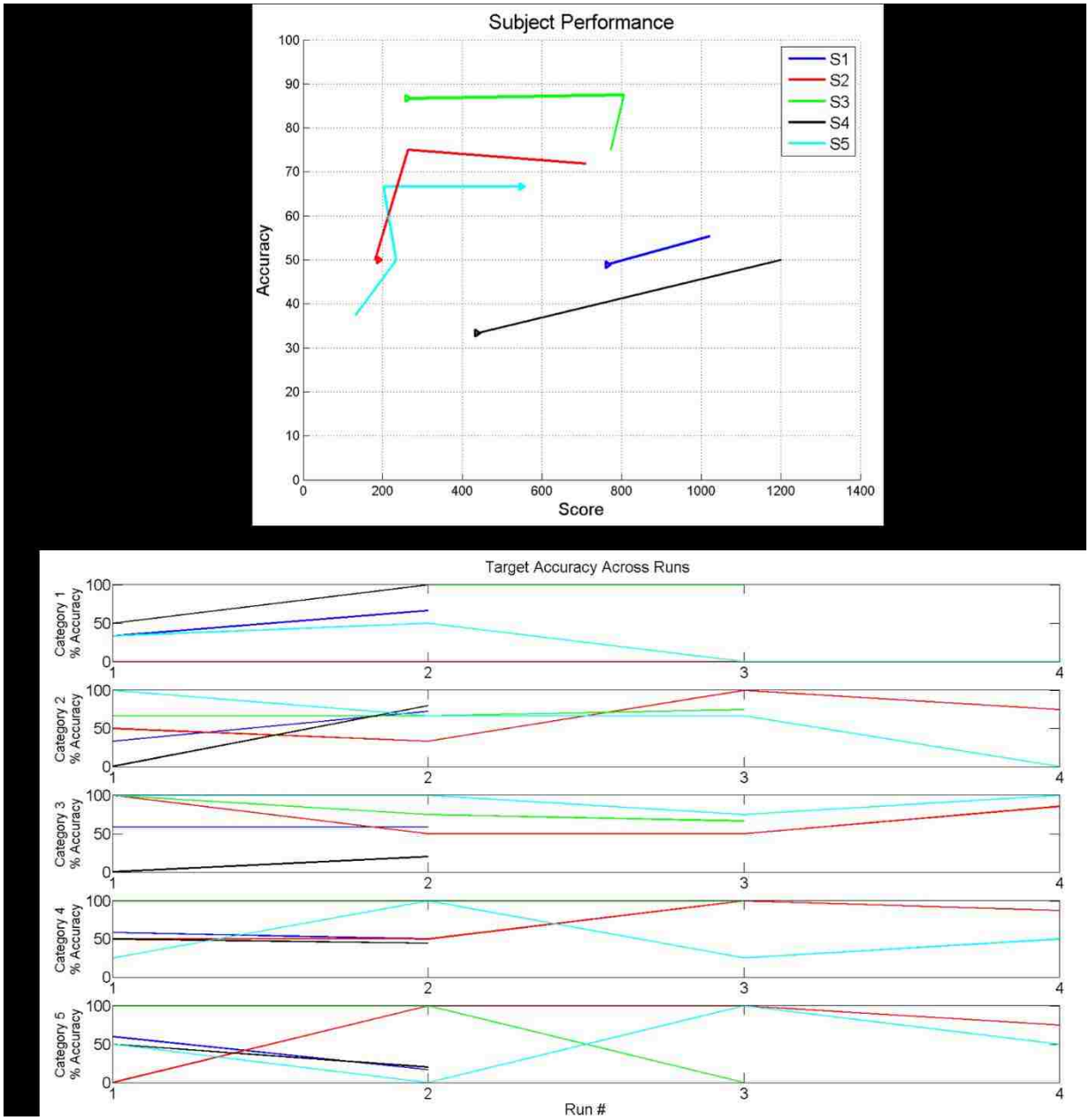

Figure 12 - Subject BCI Performance. a) Accuracy vs. Precision (Score) shown for each subject. Accuracy is the overall hit rate, while score reflected the degree of precise dwell and center reaching ability. The first trial for each subject is shown as a small triangle in the subject's color. S5 does indeed reduce in both accuracy and score over time, while the other subjects show modest relative gains from start. (b) Accuracy is shown for each target category (collapsed from 8 to 1-5) across all runs. Subject legend same as in (a). The strangeness in S5's overall performance can be seen here as a result of their primary difficulty with (+)MI trials over time.

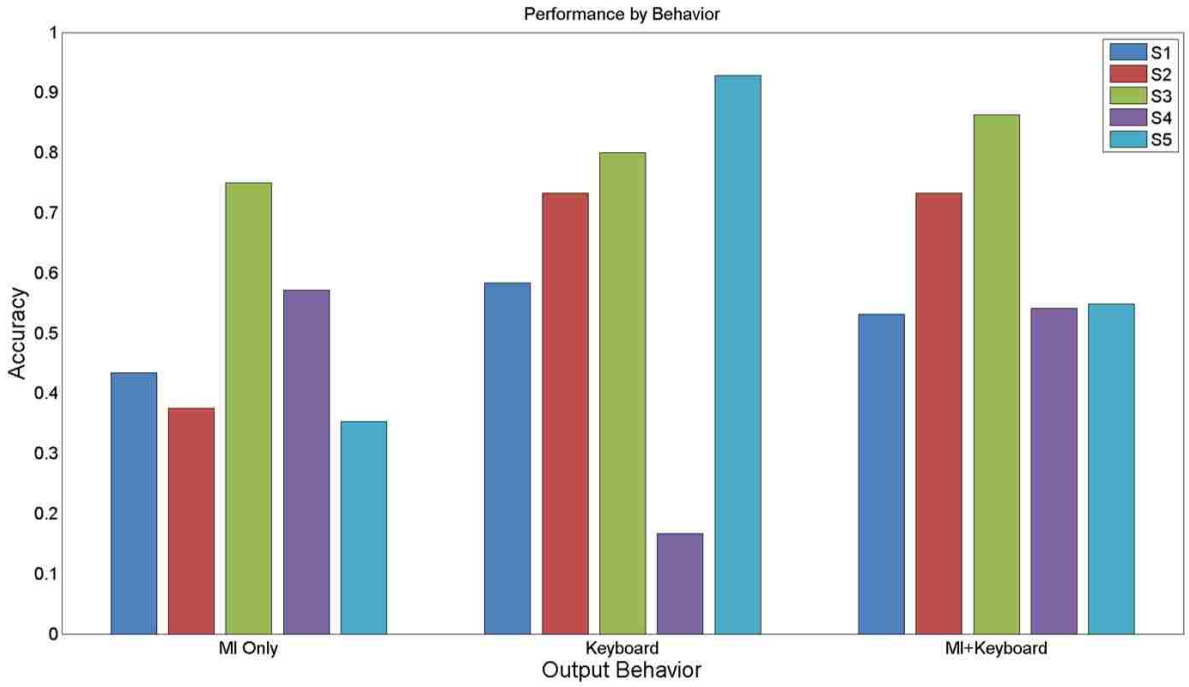

Figure 13 - Subject Accuracy by BCI Output Behavior. Trials separated and tabulated for each behavioral class, as per Target Categories (TC 1-5) and described in text. For each subject, the accuracy is shown for each behavioral type: Motor Imagery Only (+)/(-), Keyboard only (Right/Left), and, the mixed case, Motor Imagery + Keyboard (corner targets, TC2/TC4). As seen in Figure 3, overall subjects had difficulty with consistent hit of keyboard R/L targets, possibly due to unconstrained y-axis movement of cursor during targets. Overall, all subject were best at Keyboard only targets, as would be expected, and surprisingly better at the combined output than with motor imagery alone.

Thus, it seems important to further separate performance based on the output behavior type. In Figure 13, each subjects' accuracy is separated into the BCI control or output behaviors required for control. It is immediately apparent, that subject 4 did extremely poorly for simple Key (R/L) only trials, barely hitting 20% of these trials. Whether this might be due to the cursor being unconstrained along the y-axis or a lack of motor output, is further examined below. Overall, this focus on behavioral output indicates that on average, subjects were better able to output MI and Key presses concurrently than modulate MI alone.

8.3.2 High Gamma Activation at the Control Electrode

To better understand the variance in behavioral performance and examine the nature of each subject's control during concurrent manipulation, it is important to examine the HG behavior in the controller electrode. The electrode selected for control for each subject can be found in Table 2 and identified spatially in Figure 10-a. Ideally, performance changes over time would be reflected to some extent in the HG activation patterns at the control electrode. The trial by trial HG activation for each control electrode is plotted for each target and subject and shown in relative spatial orientation in

Figure 14. Additionally, a radial plot reflecting each subject's target or 'directional' accuracy is shown. As described before, recordings from all channels were common-average re-referenced over the whole grid. Channel data were then band pass filtered for the high-gamma (HG) range (70-200 Hz) using a fourth-order Butterworth filter. A time variant estimate of the HG-band power was calculated from the square of the magnitude of the Hilbert Transform. Data were then log normalized and further z-normalized with respect to the rest (behaviorally quiescent) periods. For each target type, this HG activity is visualized over time and stacked vertically downwards for each trial from beginning to end. Task states from cue, to feedback, and quiescence (inter-trial intervals) are marked. Corresponding BCI control/output behaviors are marked for each set accordingly. Additionally, in Figure 15, the mean z-scored high gamma (zHG) activation at the control electrode over time is plotted for hits vs misses for each behavior type (MI only, Key only, MI+Key) with variance in the signals shown with the standard error of the mean in relief.

(+)MI only: For TC1, Subject 1's performance is initially less than 50%. However, with practice the subject learns to modulate their high gamma signal, seen as increase in zHG intensity post feedback start in the (+) MI-only plot. This behavior is also seen with Subject 3 and 4, both of whom go from roughly 50% accuracy to near 100% in this category. For all three subjects the peak +zHG activation is shortly after feedback starts. This quick increase, as seen in the mean activation plots allow for a high velocity in vertical cursor movement followed by a tapering of the zHG to baseline allowing for dwell behavior with additional peaks of zHG to course correct and diminish aberrant cursor movement. For Subjects 2 and 4, however, their Trial by Trial HG activation pattern shows no discernable modulations initially, though the upwards slope in the mean activation for S5's miss trials as well as the brief peaking HG during run 2 indicates that control may have been developing as performance correspondingly improved, though these gains were lost by the last run. Subject 2, however, may have never figured out an ideal MI strategy.

(-)MI only: The improvements Subject 1 showed in (+)MI control are not reflected for the (-)MI only case, as activation is chaotic overtime and in fact, the HG activation for TC5 is the inverse of TC1, with the end performance dropping from above 50% to around 20%. Conversely, subject 2, who demonstrated poor (+) MI control show significant improvement overtime, going from 0% in the initial run to near 100% before settling at around 80%. The trial by trial raster again reflects this, with HG suppression or quiescence seen as deep blue around 3-4 seconds post cue that is consistent across

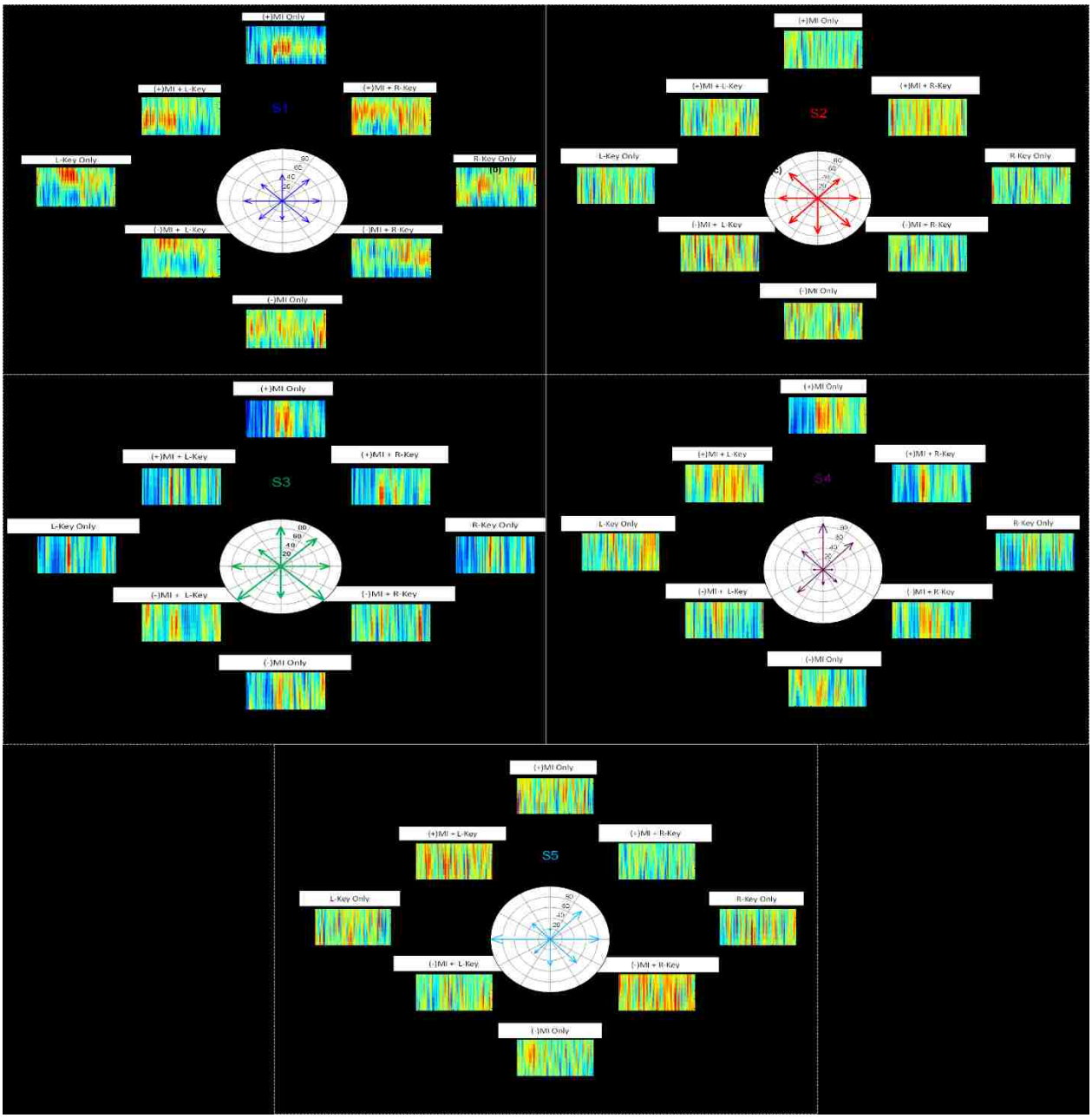

Figure 14 - Trial by Trial raster of HG response at Control Electrode. As described, ECoG recordings were common-average re-referenced over the whole grid. Channel data were band pass filtered for the control high-gamma (HG) range (70-90Hz) using a fourth-order Butterworth filter. A time variant estimate of the HG-band power was calculated from the square of the magnitude of the Hilbert Transform. Data were then log normalized and further z-normalized with respect to the rest (behaviorally quiescent) periods. Heat scale for z-scored, log(HG) activity is -1.5 to 1.5 z-scores. This HG activation for each BCI trial, concatenated top to bottom, is plotted as an image for each target Type, arranged in task-relative spatial orientation. Time axis starts with target presentation at '-2' followed by cursor feedback starting at '0' and ending at '6'. Each target trial raster is labelled with the relevant output behavior (e.g. (+)MI + R-Key for up-right or +x|+y targets). At the center of each set, the 'directional' accuracy, an analog of target accuracy is shown for comparison with performance. Specific discussion of each subject's HG response over time and trials is further elaborated upon in Results and Discussion.

trials after the initial few, ending with peaking zHG in late trials interspersed with this reduction. Note, to affect velocity control, HG need not be maintained for long durations, rather the change in activation should be large enough to counter baseline activity in the previous 500ms. Activation patterns for subject 3, are the reverse of S2, with ideal behavior and stark lower peak zHG around 4 seconds initially, which eventually becomes more similar to the activation matters for (+)MI. Examining the traces and ISE, however, suggest that there were many near misses in later trials, with the possible reversing +HG bump making it difficult for the subject to maintain velocity control in this direction. For subjects 4 and 5, however, both seem to have peaks of increased high gamma activity preceding the feedback cue (seen also in mean activation plots) with subject 5 apparently eventually figuring out a strategy for (-)MI control reflected also in periodic –zHG activity for later trials.

Key only: While Subject 4 had clearly the worst performance for TC3 targets along the x axis, it is not immediately clear why this might be the case. The mean activation shows very little activity change from rest for the zHG for either hit or miss trials. Accordingly, the trial by trial HG activation shows very little change from early to late trials with very different, almost mirror image, patterns for right and left key presses with a peak HG increase toward the end of the trials for leftward targets and quiescence in zHG near feedback end in rightward trials. Comparatively, the response for subject 3 was markedly consistent across trials for right and left with a huge (>0.5 score) +zHG peak after feedback, corresponding in time to the beginning of the continuous key press behavior, with limited additional spiking later in the trials. Subject 5's activation shows a similar kickoff peak post feedback, though with minor attenuations throughout feedback period that seem to increase for later trials especially in the miss cases.

(+)MI+Key: Though, the initial testing suggested any directional preferences for key presses should be negligible, the directional accuracy suggests that each subject had at the least a performance bias within TC2 for these trials, though the trial numbers are not enough to determine real significance. While S1 and S3 had very similar activation patterns for the (+)MI (TC1) case, here they show quite different patterns. Activation response for S1 shows a series of peaking +zHG periods, increasing with later trials. For S3, however, there are two bolus of +zHG activation much like for TC1 that distinctly coalesce around feedback cue for later trials. This behavior is also seen in S4 for the right key, TC2 trials and in later trials across TC2 for S2 and S4 as well. These changes in

activation pattern are reflected in the performance increases for these subjects as well as well as the peak behavior in the mean activation plots.

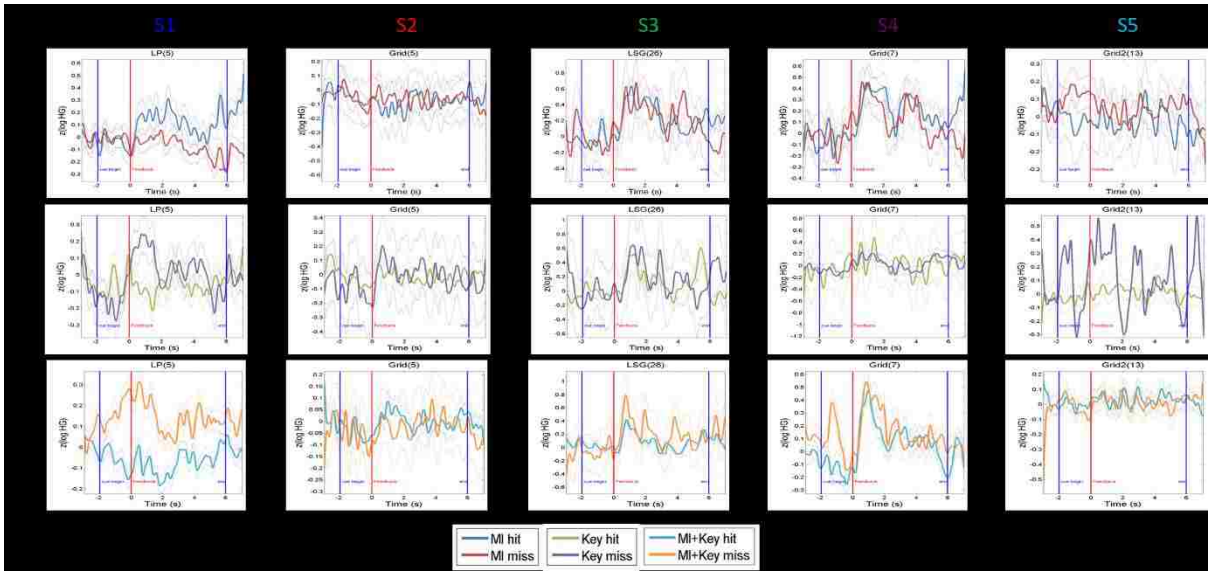

Figure 15 - Mean HG Activation at Control Electrode. Mean HG activity at the controller electrode is shown for each trial across all output behaviors. Relevant task cues are marked in time on each plot. For each meaned HG signal, the standard error of the mean is also plot in dotted relief. Subject specific trends are further discussed in text. a) For each subject, the mean HG activity at the controller electrode during BCI output is plotted for all MI-only trials, separated into hits vs. misses. b) For each subject, the mean HG activity at the controller electrode during BCI output is plotted for all Key-only trials, separated into hits vs. misses. c) For each subject, the mean HG activity at the controller electrode during BCI output is plotted for all Concurrent (MI+Key) trials, separated into hits vs. misses.

(-)MI+Key: The kickoff peak +zHG post feedback cue seen previously for key presses in the solo and combined states for Subject 3 are again seen for TC4 targets, however, with a deep quiescence in the following second. Overall, subject 3 maintains almost 100% hit rate for these targets, throughout with a high consistency in activation patterns throughout later trials. Interestingly, while subject 4's performance would indicate little control for this combined output behavior, the HG activation patterns closely match those of S3, with the mean z-scored HG activation over time matching in progression (Figure 15), but being a fraction of the intensity. Conversely, for Subjects 2 and 5, whose performance for TC4 targets are similar, the mean activation patterns show no significant difference and very little variance between hit or miss when combined with the overall concurrent behavior though the trial by trial activation shows distinct periodic +zHG peaks over time showing very little modulation with training. Finally, subject one, has the most marked difference in HG activation over time, with marked +zHG periods during early trials with marked –zHG for late trials

as would have been expected, though not seen, for TC5 trials of this subject. The mean HG activation over time is also of note, with miss trials showing a wide variance compared to hit for the concurrent control behavior.

8.3.3 Task-Relevant Distributed Cortical Activity

The benefit of using ECoG as the BCI modality, is that task-relevant focal changes (as per the correlated HG response) across distributed cortical areas can be examined in addition to just the activation patterns over time for the control electrode. Though anatomical landmarks in the cortical reconstructions provide one avenue for identifying thematically relevant electrodes, we decided to be more rigorous and test all electrodes for significant differences between all the BCI behavioral classes: MI only versus Key only, Key versus the concurrent MI+Key, and MI only versus MI+Key. Additionally, electrodes were compared for the hit and miss conditions for each output behavior. As all the data had been previously band-passed, z-scored, and then meaned with an assumed normal distribution across all channels, we chose to do a simple paired two-tailed Student's t-test for significance testing, with degrees of freedom corresponding to the channel observation space. (A Mann-Whitney U test (Wilcoxon rank-sum) was also considered for comparison across the processed log(HG) values). To increase selectivity and rigor, we initially chose a cutoff value of $\alpha = 0.05/df$ (where df is the number of channels recorded for that subject). Only three electrodes passed this level across all five subjects and are seen in Table 3 below along with the specific α values for each subject. All electrodes show up for MI related class comparisons.

A second pass significance testing was also done for all cases, but with a lower statistical threshold with an overall $\alpha = 0.01$. As expected, with the more relaxed limit, quite a number more electrodes were identified as behavior significant. This was especially true in the case of hits versus misses for targets requiring concurrent MI+Key output. A sampling of these can be seen plotted in regards to the respective cortical implants in Figure 16. The calculated t-test statistic for each electrode is plotted, with those larger statistical differences indicated with a larger electrode radius. The heat-map scale for these plots is derived from the respective calculated statistical bounds of each class. The mean-HG activation (z-scored as before) is then plotted as before for each behavior type. The electrodes passing the initial screening are shown in Figure 17. A sampling of electrodes that showed significance across multiples classes for each subject, highlighted in italics in Table 3, are additionally plotted in Figure 18. Like before, mean HG activation is plotted for each behavioral class.

I. Electrodes of Interest as per Significance Testing by Behavior (α = 0.05/df)

Subject (α)	MI vs Key	MI vs MI+Key	Key vs. MI+Key	MI: hit vs. miss	Key: hit vs. miss	MI+Key: hit vs. miss
S1 (α = 0.000781)	--	--	--	--	--	--
S2 (α = 0.000781)	--	--	--	**51**	--	--
S3 (α = 0.000781)	--	**54**	--	--	--	--
S4 (α = 0.001042)	--	--	--	--	--	**28**
S5 (α = 0.000806)	--	--	--	--	--	--

II. Electrodes of Interest as per Significance Testing by Behavior (α = 0.01)

Subject (α)	MI vs Key	MI vs MI+Key	Key vs. MI+Key	MI: hit vs. miss	Key: hit vs. miss	MI+Key: hit vs. miss
S1 (α = 0.01)	--	47	--	10	--	12, 15, 48, 55, 64
S2 (α = 0.01)	*5*, 27, 36, 56	*5*, 7, 22, 41, 55	--	31, 32, *39*, 40, 49, 50, **51**	--	2, 16, *39*
S3 (α = 0.01)	**54**	9, 46, **54**	--	--	--	--
S4 (α = 0.01)	*31*	9, *21*, **28**, 46	*31*, 47	--	*31*	6, 8, 12, 14, 20, *21*, 23, 27, **28**, 29, 30, 36
S5 (α = 0.01)	--	--	40	--	--	8, 19

Table 3 - Non-controller, task-relevant electrodes of interest. Tabulated herein, for each subject, are all electrodes deemed significant based on two-tailed Student's t-test comparisons of output behaviors and classes designated in table header. I) To limit extraneously active electrodes, the initial first pass analysis used a stringent α cutoff value of 0.05/df where df was the observational degrees of freedom or, for this purpose, the utilized channel space of each recording. At this level, only 3 electrodes were deemed significant, in bold. II) A second pass was performed with a more relaxed α of 0.01, still under the theoretical 0.05 limit, but orders of magnitude higher than before. To underscore task-relevant electrodes, analysis was focused on any that appeared in multiple class comparisons, shown in italics (e.g. S4 e21).

For subject two, channel 51 showed significance for hits versus miss in the MI case. This channel, as seen in Figure 16-a, is located along a superior parietal electrode on a secondary 2x8 grid array. Despite being indicated as related to motor imagery success, for all behaviors, there are two

HG peaks of note of equivalent z-score across all classes (see Figure 17-a). The first comes immediately after the presentation of target, marked in Figure 18. The second is with cursor onset, rising from cue to peak. It is hard to say whether this is correlated to target location or simply visual cue, but for this activation is more than halved for unsuccessful MI trials.

The significant effect for electrode 54 for subject 3, appears to be driven largely by pretrial or inter-trial interval HG activity, shown in Figure 17-b. For missed trials in the concurrent case, this electrode, lying roughly along central sulcus and possibly in a pre-motor area, shows an almost standard deviation of activity difference in the supposedly quiescent period prior to trial start, and possibly could be an indicator of other underlying behavior leading to the errors to come.

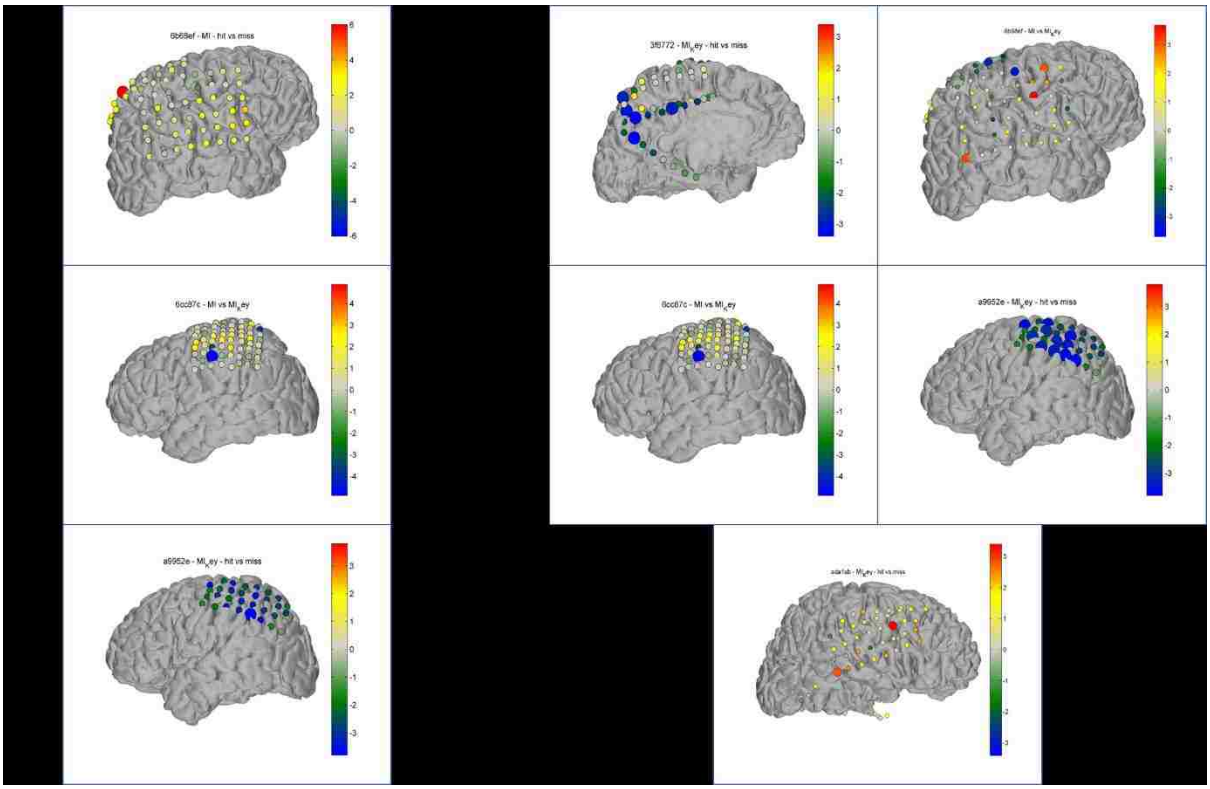

Figure 16 - Example Cortical plots for Significant Electrodes. As outlined in the Results, significant electrodes in each BCI behavior class were vizualized on the cortical surfaces for each subject. For each electrode, the test-statistic is plotted as per the corresponding class analysis. Heatmap color limits are merely the bounds of this measure across the grid. Electrodes meeting the parameter constraint are plotted with an exaggerated electrode radius. This allows for a general cortical region comparison with the spatial layout of the active electrodes. While this is a limited view of all cortical activity, it provides a focused window in which to examine distributed cortical changes during BCI interaction for each subject. a) Plots are shown for the classes with electrodes of interest as per I-α in Table 2. a) Example plots are shown for a sample of classes for each subject with electrodes of interest as per II-α in Table 2.

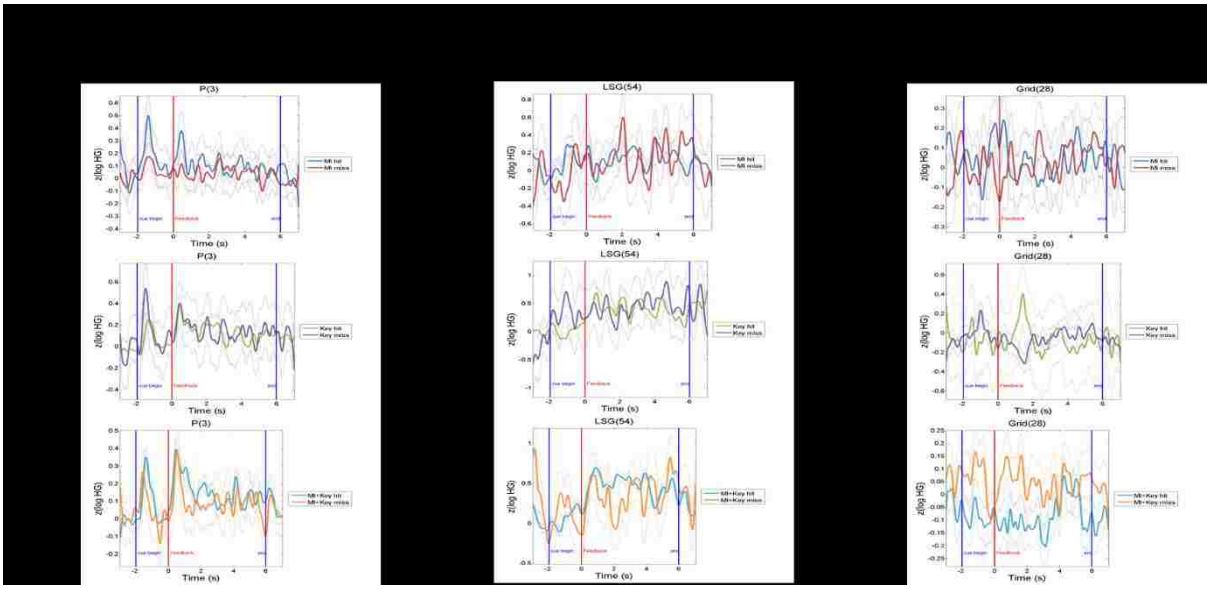

Figure 17 - Mean HG Activation for First Pass Electrodes of Interest. Mean HG activity at the three electrodes selected from Table 2-I are shown for each trial across all output behaviors. Relevant task cues are marked in time on each plot. For each mean HG signal, the standard error of the mean is also plot in dotted relief. Subject specific trends are further discussed in text. a) S2 Electrode 51, located along the parietal array as seen in Figure 16, shows marked activity changes in relation to cue triggers, though it was selected during the MI: hit vs. miss class comparison. b) Electrode 54 for S3, located along the central sulcus and selected during the MI vs. MI+Key comparison, shows a higher and protracted mean HG response from Feedback start for successful Concurrent trials as compared to successful MI-only activity. This is mirrored by the Key-only related HG activity. c) Posteriorly located electrode 28 in S4 shows a marked difference in miss vs hit for the concurrent BCI output pre and post feedback cue. This activation pattern maintains itself until late in the trials at which point, HG activation for the hit cases inverses.

The last electrode for subject 4, lies along posterior parietal areas and primarily reflects difference in the success and failure for the concurrent MI+Key cases. Here, the variances of the HG activity, let alone the mean activity, post target presentation and feedback start are mostly separated from each other. As these areas can be related to attention and movement planning, these differences might be in response to perceived error or unexpected state aberrance.

Five electrodes were selected from among the second pass group. The first, for subject 1, is electrode 10 (Figure 18-a), lying along the same Left Parietal Strip as the original control electrode and indicated in relation to motor imagery success. Despite being somewhat anterior and superior to the control electrode, it shows very similar differences in the HG activation related to success for all three behavior classes as originally seen at the control electrode. For MI only, the hit versus miss difference is clearly tuned to the feedback period. This holds for the key case as well, though the hit/miss activation pattern is inverted. It is possible then, that this activation is in response to or tied to the MI onset, as the primary failure type for key presses for subject 1 was due to HG activation

that pushed the cursor vertically out of target bounds, though the cursor x-coordinates were appropriate for success. This is again seen for the MI+Key miss vs. hits and possibly arises from TC4 misses, where again MI activation prevented proper downwards cursor movements.

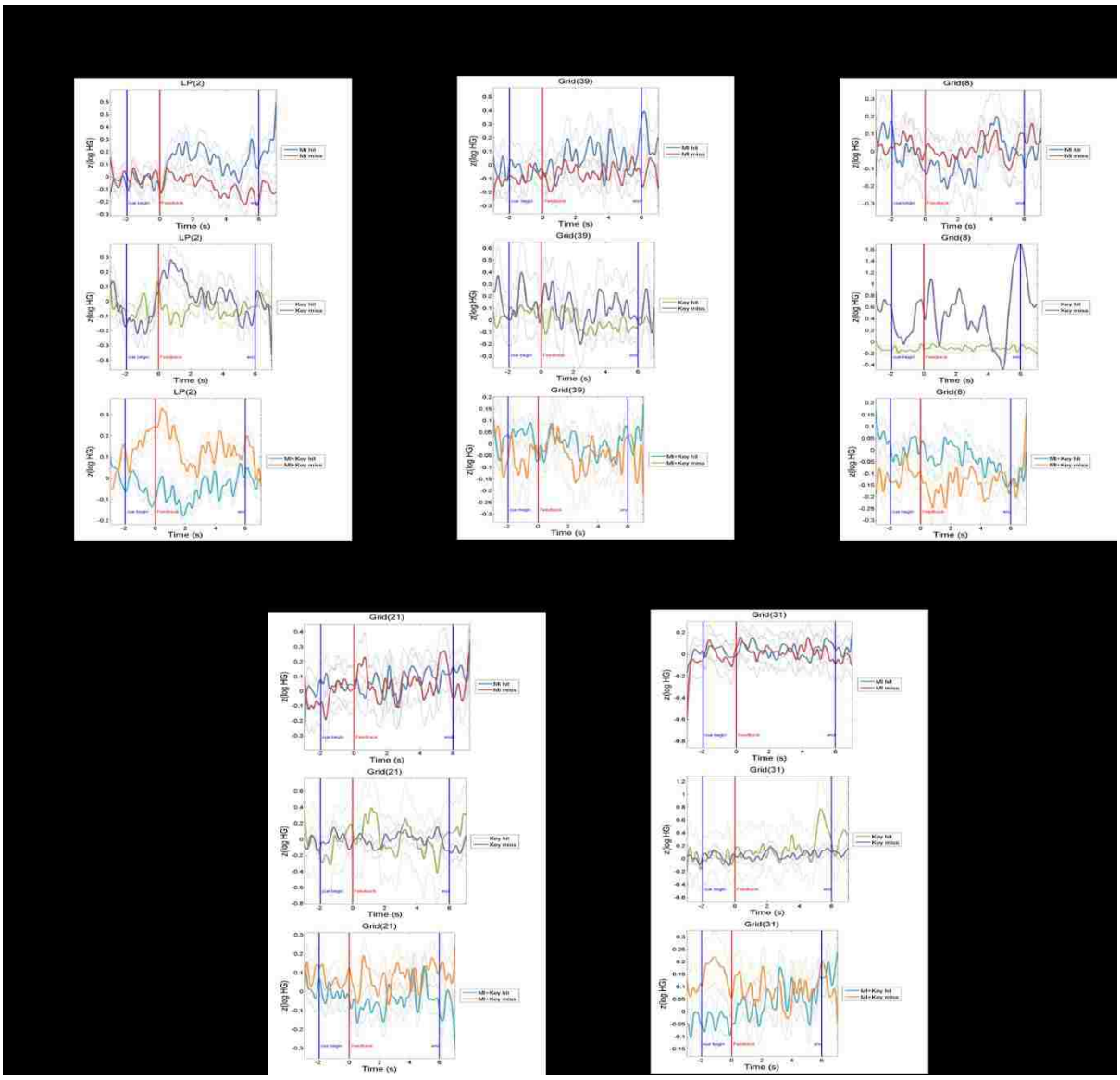

Figure 18 - Mean HG Activation for Second Pass electrodes of interest. Mean HG activity a sample of electrodes selected from Table 2-II are shown for each trial across all output behaviors as in figures 6 and 8. Relevant task cues are marked in time on each plot. For each mean HG signal, the standard error of the mean is also plot in dotted relief. Subject specific trends are further discussed in text. a) Electrode 10 for subject 1 showed significance during MI hit vs. miss. b) For subject 2, electrode 39 was indicated for success vs. failure for both MI and MI+Key. c) Electrode 8, along temporal lobe for subject 5, was indicated for MI+Key behaviors, but shows marked differences for Key only miss. d) Electrode 21 for subject 4 was indicated for multiple MI+Key classes. e) Electrode 31 for subject 4 was the only electrode across both passes that was indicated for a Key only behavior.

For subject 5, we looked more closely at electrode 8 (Figure 18-c) which lies at the end of the superior temporal gyrus. Though not active at all during motor movement as per the screening, it is indicated for significance during the success and failure for MI+Key. While the difference in the means of this behavior class are clear with a lower aggregate response in the miss case, the activation pattern for the Key only hit versus miss classes, is far more pronounced. The large positive HG activation starting from target onset and ending exactly at end of feedback with a peak almost 2 standard deviations (as per the z-score) away from baseline would seem like a fluke but are seen in neighboring electrodes as well specifically for the key only miss case. This behavior was also seen in the Keyboard miss activation plot for the control electrode.

Finally, electrode 31 for subject 4 was the only electrode across both passes that pinged for significance for the Key only success versus fail. This electrode was barely active during motor activity and is thus unlikely to be related to any pure motor related behaviors. However, as seen in Figure 18-e below, there is a distinct peak at the end of the trial aligning closely in time with the rare cursor contact with target along the horizontal axis. This peak does not arise for any other success behavior nor does it arise for any general key press in the other mixed behaviors. Additionally, as seen in Figure 18-d, electrode 21 was indicated in multiple MI+Key classes, but does not show high degree of significant difference between the behaviors, though there is a convergence between Key hit and MI+Key miss.

8.3.4 Distributed Cortical Changes over time.

An attempt was made to also characterize distributed cortical changes in regards to learning or 'training' for each subject as per each output behavior class. While cortical response changes shown in Figure 19 above are quite small, a similar effect is seen for all subjects in regards to a slight decrease in frontal activity, where covered by grid electrodes. In addition, subject 3 actually shows a marked increase in cortical activity around the control electrode, especially for the +MI output. In addition subjects 1 and 5 show increase activity along the temporal lobe in keeping with previously shown cortical changes during BCI learning. (Wander et al., 2013) However, at less than 0.5 z-score, none of these are strong enough effects to claim this trend would hold up with continued training and performance improvements.

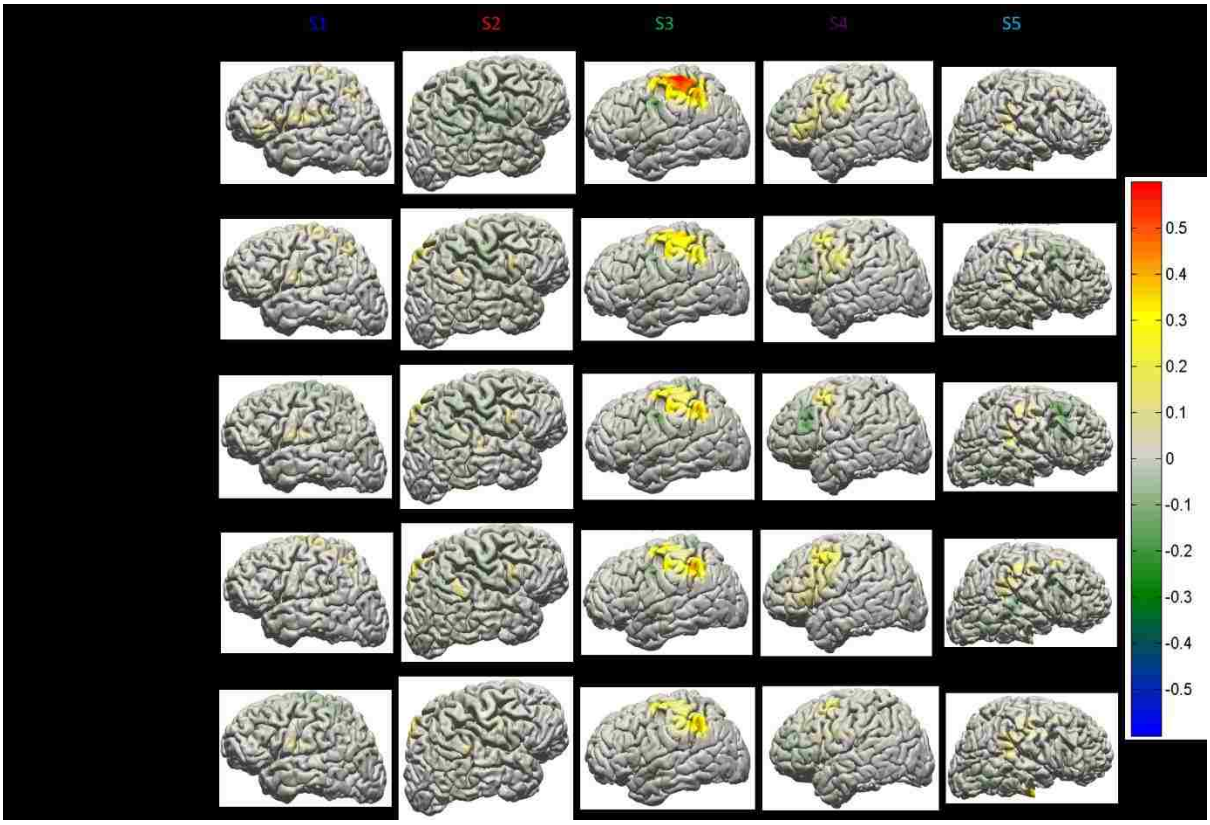

Figure 19 - Difference in HG Activation for late vs. early trials. Cortical Changes Mean HG differences mapped across cortical areas covered by grid electrodes for late vs early trials (pre-trained vs. post-trained states) for each activity (target category) type. HG response is amplified at many cortical areas, with pronounced magnification around the control electrode for (+) MI as seen for subject 3. Otherwise, a slight decrease in activity is seen as light green shades for most other activities.

8.4 Discussion

In our experiment, subjects performed a BCI task which required the bimanual concurrent and independent use of BCI control with overt finger movements of the opposite hand. We have demonstrated here that subjects were able to perform the concurrent BCI control task, though significant interference did occur from activations from the opposing hand. However, rather than the ipsilateral finger movements (key presses) being the primary source of noise, it was often the contralaterally driven HG activation that impeded success for Overt Motor only trials. Nevertheless, subjects were able to consistently coordinate control simultaneously to hit 'corner' targets. This should not be surprising as, much like with traditional bimanual feedback and rehabilitation tasks(Peper et al., 2013), the necessity for coordination may engender improved control especially if the motor cortex is indeed optimized for bimanual activity (Ganguly et al., 2009; Kadivar et al., 2011). While bimanual motor behavior, i.e., reach and grasps, limb kinematics, etc., have been studied quite

extensively for both human and animal models, to our knowledge there has yet to be a demonstration of concurrent bimanual BCI control and movement execution, especially utilizing a semi-invasive interface model like ECoG. In the non-invasive BCI control setting, some cases, including our own, have been reported where the concurrent production of movement execution has not significantly disrupted the performance of EEG-based BCIs (Cheung et al., 2012; Leeb et al., 2013). However, incongruous movements outside the bimanual setting has been shown to have a differing response profile as compared to traditional EEG-BCI activity (Seeber et al., 2015). Nevertheless, as mentioned previously, concurrent control has, however, been reported in two non-human primate studies using intracortical single-unit recordings. In the first (Orsborn et al., 2014), one monkey performed an isometric force task, pressing a force plate to match a desired value, while performing a previously over-trained center-out 2D BCI control task. Initially, the addition of the concurrent control significantly decreased BCI performance. An important note, however, is that unlike our task, in which the output behaviors were meant to be congruous and actively coordinated for success, the monkey's secondary behavior had no relation to BMI success and was an isometric force hold and not a movement coordination process. Following in the footsteps of this first primate study, (Milovanovic et al., 2015) one more monkey performed a target pursuit task, now utilizing an isometric wrist torqueing behavior on a lever as the controller for one dimension of cursor movement with the BCI behavior controlling the second dimension. Like with our subjects, though with significantly more training or experimental time and food reward, the monkey was able to perform the task and gain concurrent control. This then extrapolates quite nicely to our case, except that instead of a held wrist torque, our subjects used continuous key presses.

8.5 Bimanual Considerations for ECoG BCI

Here, we have demonstrated the potential for human subjects to control BCI devices concurrently and independently to the execution of natural movements. Though not with the significance or degree as that of the single unit studies mentioned in previous chapters, our short-term results with these five subjects suggests that the brain is capable of dissociating specific motor related responses from the behavior to which they were initially correlated specifically in order to represent the activity of a newly acquired effector such as a BCI. As previously shown for motor movement as well as simple 1-D cursor BCIs (Tim Blakely et al. 2009; Leuthardt, Miller, et al. 2006 & 2007), the use of specific feedback during the control period enhances the "self-control of brain

activity." However, the difficulty in the task combined with transient distractions in the experimental environment often lead subjects to not effect good "BCI Control", in that they could modulate their signal to a point, but were unable to excel at the task (see accuracy vs. precision and related decreases over time). Thus, there is an immediate concern of the actual applicability to an individual with an existing deficit. If the task is too hard to learn, might the performance of a subject obfuscate the general feasibility or utility of this type of control schema and might dexterous bimanual coordination be too lofty of a goal to achieve with current ECoG-based BCIs. To that extent, the following chapter attempts to examine this very issue and gets at the heart of our motivation.

Chapter 9: BCI for Rehabilitation – A Case of Stroke.

As mentioned throughout this document, much of the research on brain-computer interfaces (BCIs) has focused on developing assistive brain-controlled devices for patients with severe neuromuscular disorders, such as amyotrophic lateral sclerosis (ALS), brain-stem stroke, and spinal cord injury, all of which result in degradation of volitional motor abilities (Curran and Stokes, 2003). Traditionally, BCI technologies have been applied to cases in which there is little or no motor ability. However, there is a much larger population of patients that retain some residual motor function, even with degradation, who could benefit significantly from BCIs (Buma et al., 2010). In addition, looking further into the future, can BCIs also be used to augment a healthy-functioning motor system? For example, can individuals with deficit use BCIs simultaneously with overt coordinated motor activity, e.g., for bimanual control? Additionally, how do the unique cortical networks adapt in such a hybrid BCI-manual control?

Here we show that a subject with lifelong hemiparesis implanted with electrocorticographic (ECoG) electrodes can learn to perform a 2-D BCI center-out cursor task in which one dimension of control is modulated by motor imagery-related ECoG activity and the other dimension is controlled by overt natural movement. We explore the effects of confounding ipsilateral and contralateral neural activation due to natural movements on BCI control. We also investigate task-related adaptation across cortical areas in the hybrid BCI-manual control task and its relationship with overt motor behavior.

9.1 Experimental Setup

9.1.1 Subject Zero: A Case of Hemiparesis

Much like the subjects from Chapter 7, this patient with intractable epilepsy was implanted with platinum subdural ECoG electrodes for the purpose of seizure focus localization at the Harborview Medical Center. Electrodes were placed by medical staff over the right hemisphere as per the clinical indication. 8x8 electrode grid was made of 3mm diameter platinum pads spaced at 1cm center-to-center and embedded in silastic (AdTech). Before experimentation, all protocols were explained verbally and summarized in writing. The patient provided written informed consent to participate as a subject for research activity during clinical monitoring. All experiments and

procedures performed were approved by the Institutional Review Board at the University of Washington.

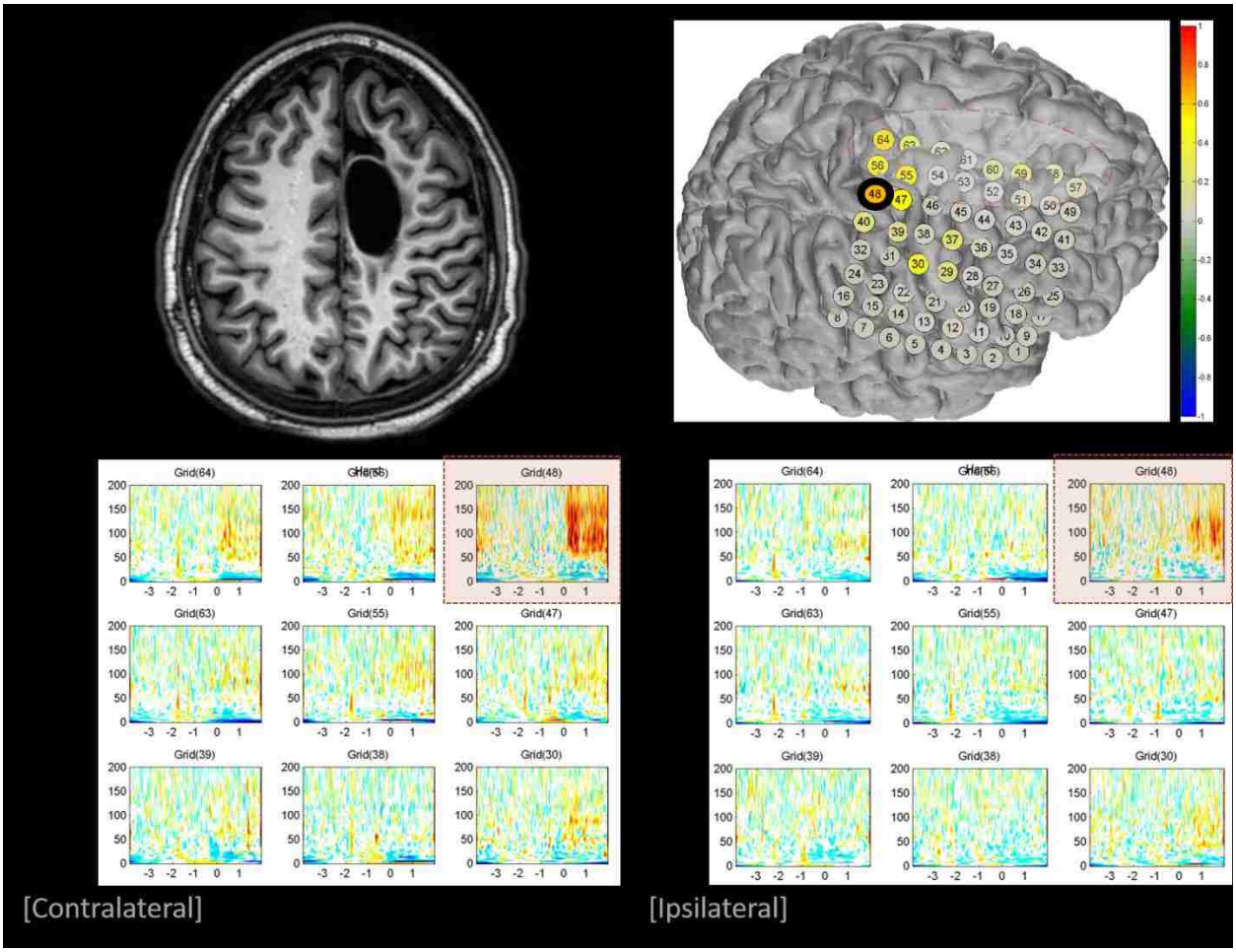

Figure 20 - ECoG Implant and Initial Screening. (a) MRI axial slice view (110/187) of the subject's brain, reflected about the y-axis from original clinical view, indicating possible porencephalic cyst corresponding to perinatal infarction of the right MCA. (b) Cortical reconstruction of subject's brain with ECoG implant generated from pre/post-op MRI and CT scans (Wander et al., 2013). The ECoG electrodes consist of 3mm diameter platinum pads spaced at 1cm center-to-center and embedded in silastic (AdTech). Subject was implanted with one 8x8 grid over the central sulcus, one 1x8 strip over the frontal lobe, and one 2x8 strip along the interior. Only the 8x8 grid electrodes were used for experimental purposes. Subject was visually cued to move their left hand, wrist, tongue, and shoulder at 3 second intervals. High Gamma (HG) power (70-100Hz) at each electrode was examined for significant differences between activity and rest conditions. The colored circles show the average responses for left hand movements, which are contralateral to grid. The electrode labeled 48 (in a putative hand motor region) had the highest significance and was chosen for use in BCI control. Similar screening was done with motor imagery as well as with movements ipsilateral to the implanted hemisphere. (c) & (d) Contralateral vs. ipsilateral time-frequency analysis for z-scored HG power responses mapped across a set of grid electrodes. The HG response over time supports initial selection of electrode 48 (highlighted in light red). Most electrodes are quiescent to ipsilateral hand movement. There is activity at electrode 48 for ipsilateraleral movement but this activity is muted and somewhat delayed compared to the contralateral case.

Relative placement of the implant can be seen in Figure 20-b. Subject was an 18-year-old right-handed male with lifelong hemiparesis due to a perinatal infarct involving the right MCA. Imaging was suggestive of a porencephalic cyst (Figure 20-a). Visual fields were essentially normal. Facial symmetry and sensation also presented as normal, and tongue was midline. Motor examination showed, on the right, normal tone, bulk, strength, and dexterity in the upper and lower extremity, while on the left, subject had moderate spastic hemiparesis of the upper and lower extremity. Subject could move the left wrist with very limited clawlike grasping ability of the hand (due in part to spasticity) and showed some mirrored movements on the contralateral side indicating possible conjoinment or entrainment of motor hand behavior. Subject could not move left side limb independent of the right, and also demonstrated mirrored movement of left limb when moving right side limb. Subject was able to lift the arm and ambulated with a hemiparetic gait. Sensory exam revealed mild decrease in fine touch and, perhaps, temperature on the left side. Subject was nevertheless able to identify coins by touch. Despite some difficulties and no prior experience, subject was eager and engaged, frequently asking questions and providing observations on experimental procedure throughout recording activities.

9.1.2 Recordings

Experimental recordings were taken at the patient's bedside without interrupting the primary clinical recordings. Data was acquired at 1200Hz using four synchronized sixteen-channel g.USBamps (GugerTec) connected to a high-performance Sager computer. Data was anonymized in accordance with Health Insurance Portability and Accountability Act (HIPAA). Cortical potentials were referenced against a scalp electrode, digitized and processed using the BCI2000 (Schalk et al., 2004) software suite.

9.1.3 Data Processing

All channels recorded from the electrocorticographic grid were common average re-referenced by subtracting the average signal recorded at all electrodes. This was done in an attempt to remove any common noise introduced by activity recorded at the scalp reference electrode due to electrical noise in the hospital environment. The re-referenced signals were band pass filtered for the high-gamma (HG) band (70-200 Hz) using a fourth-order Butterworth filter. The square of the magnitude of the Hilbert Transform was then used to calculate a time-variant estimate of band-power. Data was then log transformed to obtain approximately normally distributed data for proper

statistical analyses. To account for differences between recording sessions, this log-power estimate was further z-normalized with respect to the rest (behaviorally quiescent) periods for each channel and session. This signal is referred to in the paper as HG activation.

9.1.4 Screening Process

Before attempting on-line control, subject performed an overt motor screening exercise, in addition to clinical motor evaluation. Typically, subjects are visually prompted to move their hand or tongue for 3s with a 3s rest period in between each movement. This is repeated about 20 times. Subjects then repeat the task, imagining the prompted movement without executing an overt motion. In our case, the subject was also cued to attempt to move their left wrist and shoulder in addition to hand and tongue. HG activation at each electrode was examined for significant differences between activity and rest conditions (Figure 20). The electrode with the highest significance in a putative hand motor region was then chosen as a candidate for use in BCI control.

9.1.5 BCI Training

Initial BCI training was done on a 1-D center out cursor task using overt hand movements to control the vertical movement of the cursor. Control of the cursor was derived from HG activation at a single electrode during movement of the left wrist/hand. Subject reported difficulty in movements and struggled greatly with the task with minimal successful trials. Clinical staff also frequently interrupted to check on subject. Separate overt training was abandoned in favor of directly training with motor imagery in the primary task.

9.1.6 Concurrent BCI Center-out Cursor Task

Subject performed a 2-D center-out cursor dwell BCI task using left hand motor imagery to control the vertical movement of the cursor and right hand keyboard presses to control horizontal movement (Figure 21-a). 'Brain control' of the cursor was driven by spectral power changes in HG at a single electrode during motor imagery. Eight targets distributed radially were presented at random (Figure 21-b). The patient was instructed to imagine moving his left hand (contralateral with respect to hemispheric coverage) when presented with targets in the upper half of the screen (up targets). When presented with targets in the bottom half of the screen (down targets), they were instructed to rest or not engage in motor imagery.

Due to the use of a single hand for right & left key presses, targets can be re-categorized by activity type where T1 requires purely left hand motor imagery (LMI), T2 requires concurrent

activation of LMI and right-hand (RH) movements, T3 utilizes only RH key presses, T4 requires relaxing, or release, of LMI with concurrent RH key presses, and, finally, T5 requires overall rest (relaxation of LMI) to achieve downwards movement towards the desired target. The cursor's vertical velocity (speed and direction) was updated every 40ms and driven by changes in HG activity at the control electrode as calculated by an autoregressive filter using the previous 500ms of recorded data.

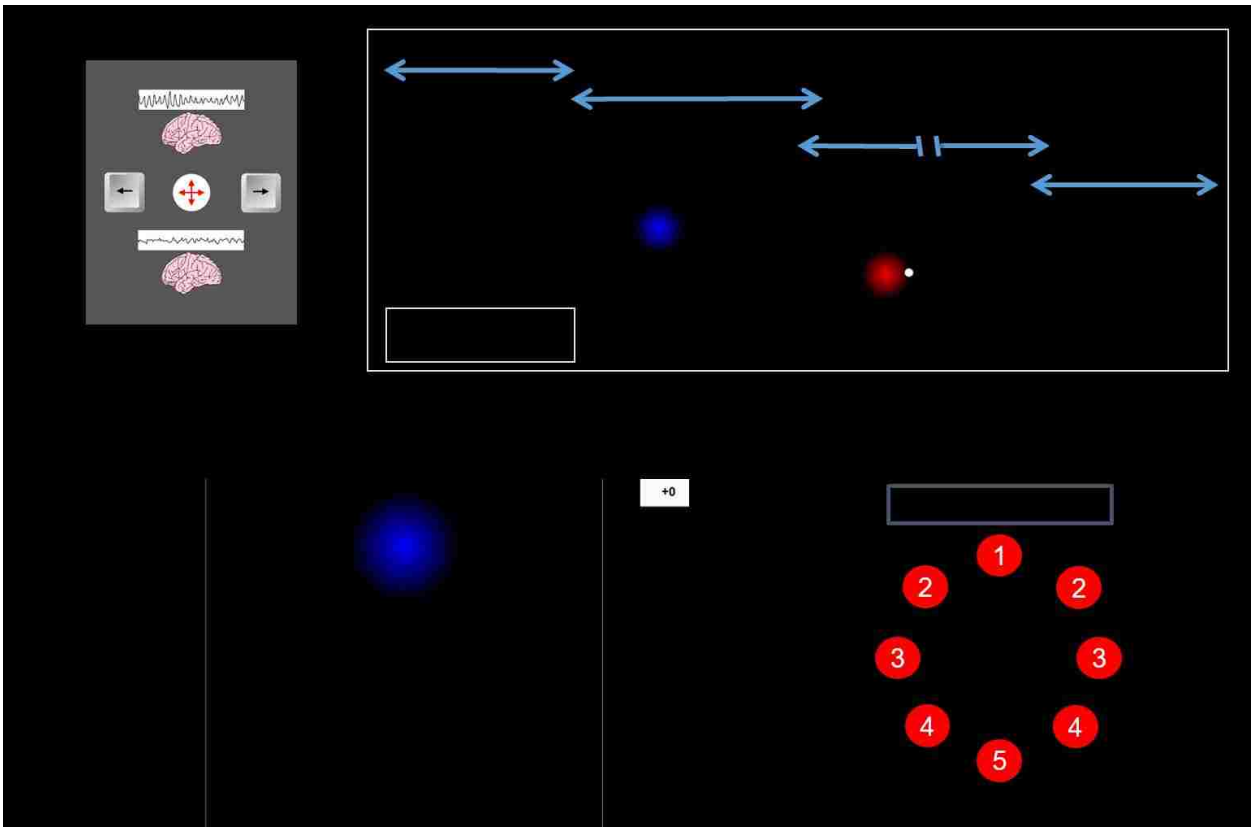

Figure 21 - Center-Out and Cursor Dwell BCI Task. (a) Sequence of steps in a trial. Subject performed a 2-D center-out cursor dwell BCI task using left hand motor imagery (LMI) to control the vertical movement of the cursor and keyboard presses with the right hand (RH) to control horizontal movement (b). 'Brain control' of vertical cursor movement was driven by HG spectral power changes of a single electrode (electrode 48) during modulation of motor imagery. Each trial started with the target being cued in one of the 8 locations (see (d)). Two seconds later, the feedback period began with cursor at the center of the screen. The subject was given control for six seconds, followed by a blanking of the screen. The inter-trial interval was one second with some jitter. (c) The task window with a running score in the top right corner based on cursor distance to the center of the target after contact with target. Score was calculated through each run to provide subject with a running motivating tally. Task difficulty could be modulated by decreasing target radius size. (d) Targets shown relative to initial cursor position and re-categorized by 'height' from 1 to 5.

Horizontal movement of the cursor was mapped to overt presses of the right or left arrows keys by the right hand. Consistent motor activation was insured by imposing "gravity" on the cursor towards the center in the horizontal axis, requiring the subject to continuously press a key to keep the cursor

moving in the desired direction. In the horizontal direction, the cursor x-position was updated at 30Hz; with each update, the cursor position moved (|right - left key presses| * key press distance) – gravity distance, where key press distance is 1.39% and gravity reversal distance is 0.0005% of the total workspace 0-1 (AU). To reach a diagonal target, subject would need to exhibit and maintain concurrent control. To aid with subject engagement, a running score was provided based upon targets hit and cursor distance from the center of the target. Task difficulty could be adjusted by changing the diameter of each target based on a difficulty slider (1 to 5, 1 being smallest diameter and highest difficulty) Duration of recording sessions was dictated by the subject's willingness and capability to participate at the time of experimentation and as per clinical constraints.

9.2 Results

The subject volunteered in multiple experimental recording sessions over four days. The initial session consisted of a series of basic functional screening tasks in which the subject was visually cued to perform gross motor behaviors or imagined motor activities. As indicated, due to a perinatal infarction in the right middle cerebral artery (MCA), the subject had lifelong hemiparesis which drastically impeded motor function on his left side. Functional screening of residual motor ability helped determine electrodes that exhibited statistically significant increase in HG activity during modulation as compared to rest (Miller et al., 2010). Electrode 48 was selected based on the magnitude of the observed power change corresponding to wrist and hand movement as seen in Figure 20-b, previously.

ECoG signals from electrode 48 were used in the initial BCI training for a 1-D vertical center-out task, with vertical cursor velocity entrained in this case to the HG activation due to overt movement of the subject's left wrist and hand. The subject then performed a more complex 2-D concurrent BCI-movement task which did not require movement of the left side (Figure 21). The subject was randomly presented with one of 8 targets, evenly distributed radially about the center of the screen. To reach the target, the subject modulated HG activity to control the vertical velocity of the cursor while simultaneously using their right hand to press the right-arrow or left-arrow keys to control the horizontal position of the cursor. The subject was instructed to aim for the center of the target and dwell in place as much as possible. To motivate the subject, a discrete score window was shown, where the score was derived from the proximity of the cursor to target center. To ensure

continuous hand movement, a "gravity" element caused the cursor to drift towards the center along the horizontal axis, requiring continuous key presses to maintain horizontal movement or dwell.

The subject's behavior throughout the task requires coordinated simultaneous control of left hand motor imagery (LMI) and right hand overt movement (RH) for pressing the keys. In the following discussion of the task, the eight targets are numbered as shown in Figure 21. Targets requiring only an increase of HG activity (LMI only) are referred to as "up targets" or target type T1; targets requiring only a decrease of HG activity (LMI only) are referred to as "down targets" or T5; targets requiring simultaneous increase of HG activity and overt keyboard presses (LMI+RH) are referred to as "up diagonals" or T2, while targets requiring simultaneous decrease of HG activity and overt keyboard presses (LMI+RH) are referred to as "down diagonals" or T4. Finally, targets requiring only horizontal cursor movement using the keyboard (RH only) are referred to as "horizontals" or T3.

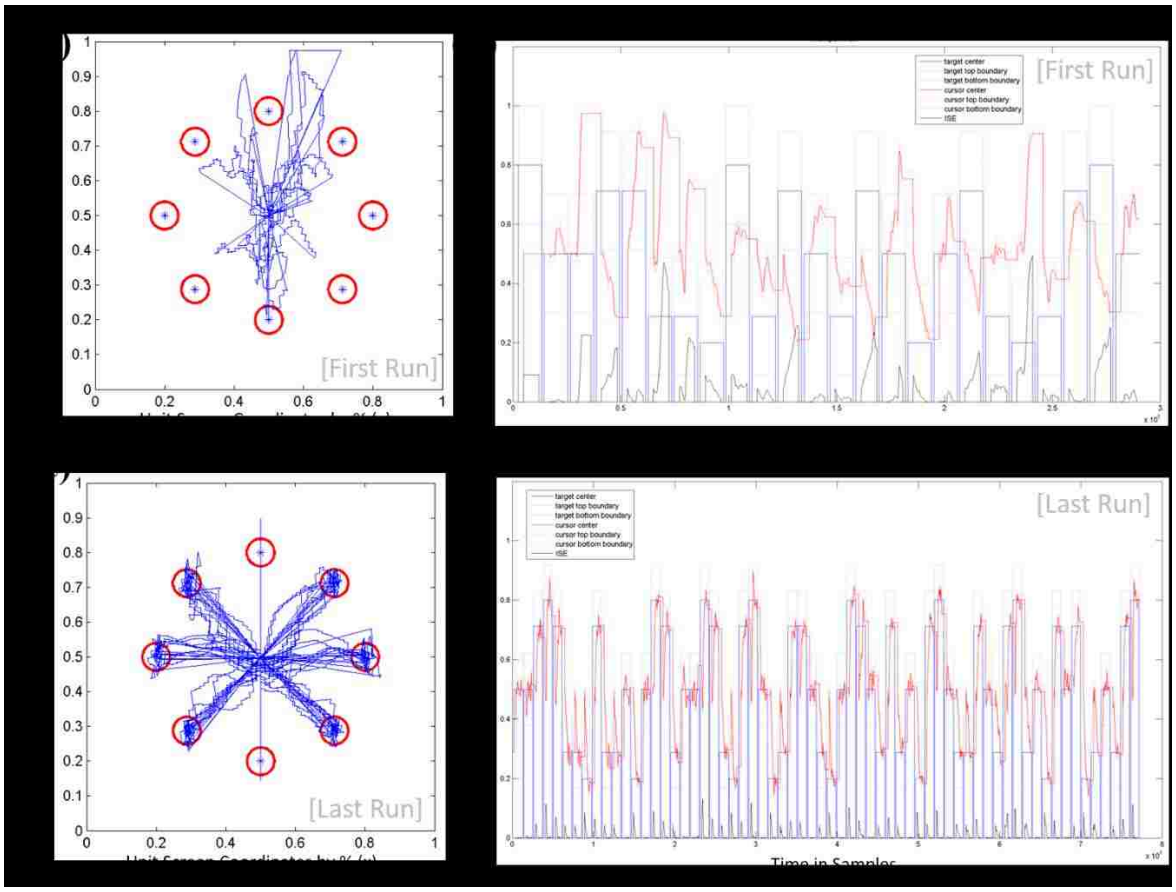

Figure 22 - Concurrent BCI Performance: Learning to Control the Cursor in 2D. (a) & (c) Cursor trajectories for each trial in the first (a) and last run (c). A marked improvement in cursor control can be seen in (c) compared to (a). (b) \& (d) Y coordinate position of cursor center (red line) relative to target center (blue line) for first (b) and last run (d). The integrated squared error (ISE) between these two positions shown at the bottom in black - note the dramatic reduction in ISE in the final run.

9.2.1 Behavioral Performance

The subject performed 16 runs of 24-64 trials of the BCI task amounting to roughly 461 total BCI trials over 3 sessions split over 2 days. In all trials, the score was tallied and reported to the subject. Initially, the subject was able to hit less than 50% of targets but with practice, the accuracy improved quickly to near 100%. Figure 22, above illustrates the overall performance improvement over time. The subject's marked improvement in cursor control over the course of the sessions can be seen by comparing the cursor traces from the first run to that of the very last run, as well as the plots of the vertical coordinate of the cursor in relation to the target center and boundaries in Figure 22-b&d. The integrated square error (ISE) of the distance from cursor to center of target is greatly minimized in the final run.

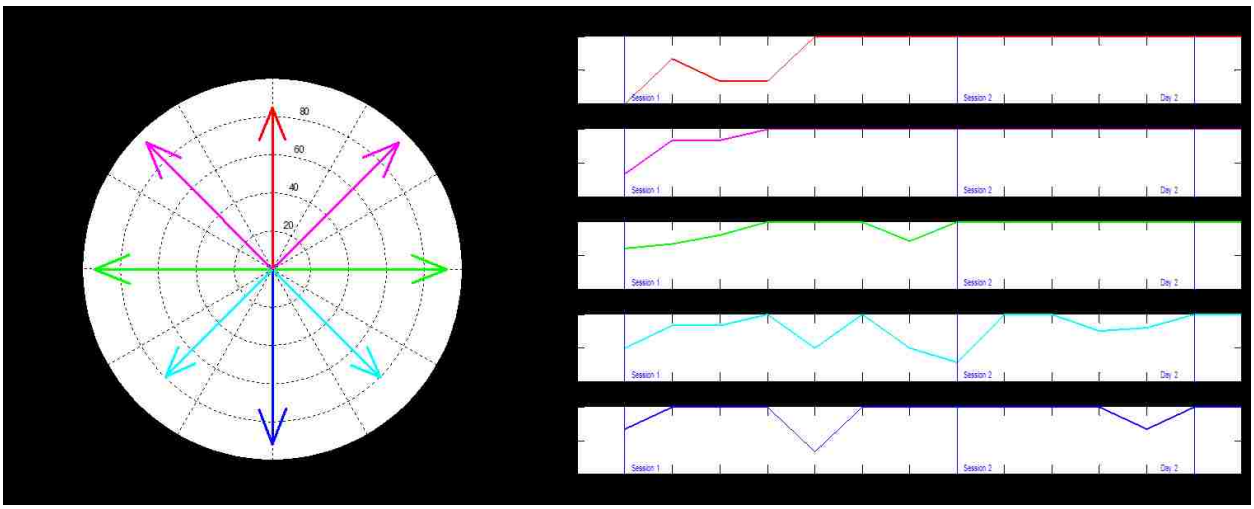

Figure 23 - Concurrent BCI Performance by Target. (a) Radial plot showing directional accuracy for each target type. The symmetry across left and right sides allows for collapsing the trials into 5 target categories. (b) Average accuracy for the five target categories across all runs (Session 1 left, Session 2 right). Note the improvement in performance for all target categories in Session 2.

Overall, the subject was able to achieve high accuracies across all targets, significantly above chance, as illustrated in Figure 23. As expected, the subject was most successful in acquiring the keyboard only targets, the few misses being attributed to inexperience with the gravity element and fatigue towards the end of some trials. Targets across each of the conditions (LMI up, LMI+RH up, RH, LMI+RH down, LMI down) were achieved without any significant difference between the right and left key presses, validating our grouping of the left and right side targets into the classes T1-5. Initially, the subject struggled with overall LMI modulation, as seen in Figure 23-b. By session 2, however, the only targets the subject occasionally struggled with were the LMI downwards ones (T4 & T5).

Accuracies for LMI upwards (T1 & T2) and LMI neutral (T3) peaked at 100%. By day 2, all targets were attained with 100% accuracy, the score being the only determinant of difference between the states.

9.2.2 Volitional Modulation of HG at Control Electrode.

We hypothesized that the subject's improvement in performance over time should be reflected in the HG activation patterns at the control electrode 48. The trial-by-trial HG activation for this electrode over time for each trial is plotted for each target in Figure 24, as seen below. Individual trials are arranged vertically in time and radially by target. Initially, for the upward targets requiring only LMI increase (T1), there is very minimal HG activation of any type across the entire feedback period (upper part of topmost plot in Figure 24). However, after first 20 trials, HG activation increases from the time of the feedback cue for about 2 seconds (peaking around 1 sec) before decreasing to a lower level during the dwell period and returning to baseline during the inter-trial interval.

For down targets (T5), by the end of session 1 and through session 2 and day 2, the subject has learned to decrease HG activation starting from the feedback cue but ending with HG increases during the dwell period at the end of the trials. For RH trials (target type T3), a fast HG increase is seen after the feedback cue due to ipsilateral activation during right hand movements to move the cursor, followed by small HG increases through the dwell period associated with key presses due to the gravity element.

Perhaps the most interesting question with regard to HG activation is how the subject is able to acquire the diagonal targets (T1 and T5) in the presence of ipsilateral HG activation due to RH key presses needed for diagonal movement. The answer can be seen in Figure 24 in the trial-by-trial plots for the diagonal targets: the subject has learned to modulate HG activation to a degree intermediate between the activations for vertical or horizontal movement. This is especially seen in the HG activations for day 2: compare, for example, HG activations on day 2 for downward diagonal cursor movements with activations for purely horizontal and downward cursor movements.

The differences in HG activation patterns for successful ("hit") trials for the different target types after task learning can be seen more clearly in the average activation and standard error plots in Figure 25. A fast HG increase at the start of feedback for up (T1) targets and a suppression of HG activity for down (T5) targets are both consistent with previous 1-D ECoG studies. For the horizontal targets (T3) requiring RH key presses only, HG activation rises quickly but reaches a lower maximal amplitude than T1 and then drops, presumably after reaching the target. For the diagonal targets

(T2 and T4) where the subject is attempting to exert concurrent control with LMI and RH motor behavior, the average HG activation is at an intermediate level between RH key press activation (T3) and activation for motor imagery (T1) or rest (T5). Interestingly, the average activations for all target types converge to approximately the same level towards the end of the trial when the subject is required to dwell the cursor inside the target. These results indicate a remarkable degree of control over HG activation by the subject in the stroke-affected hemisphere.

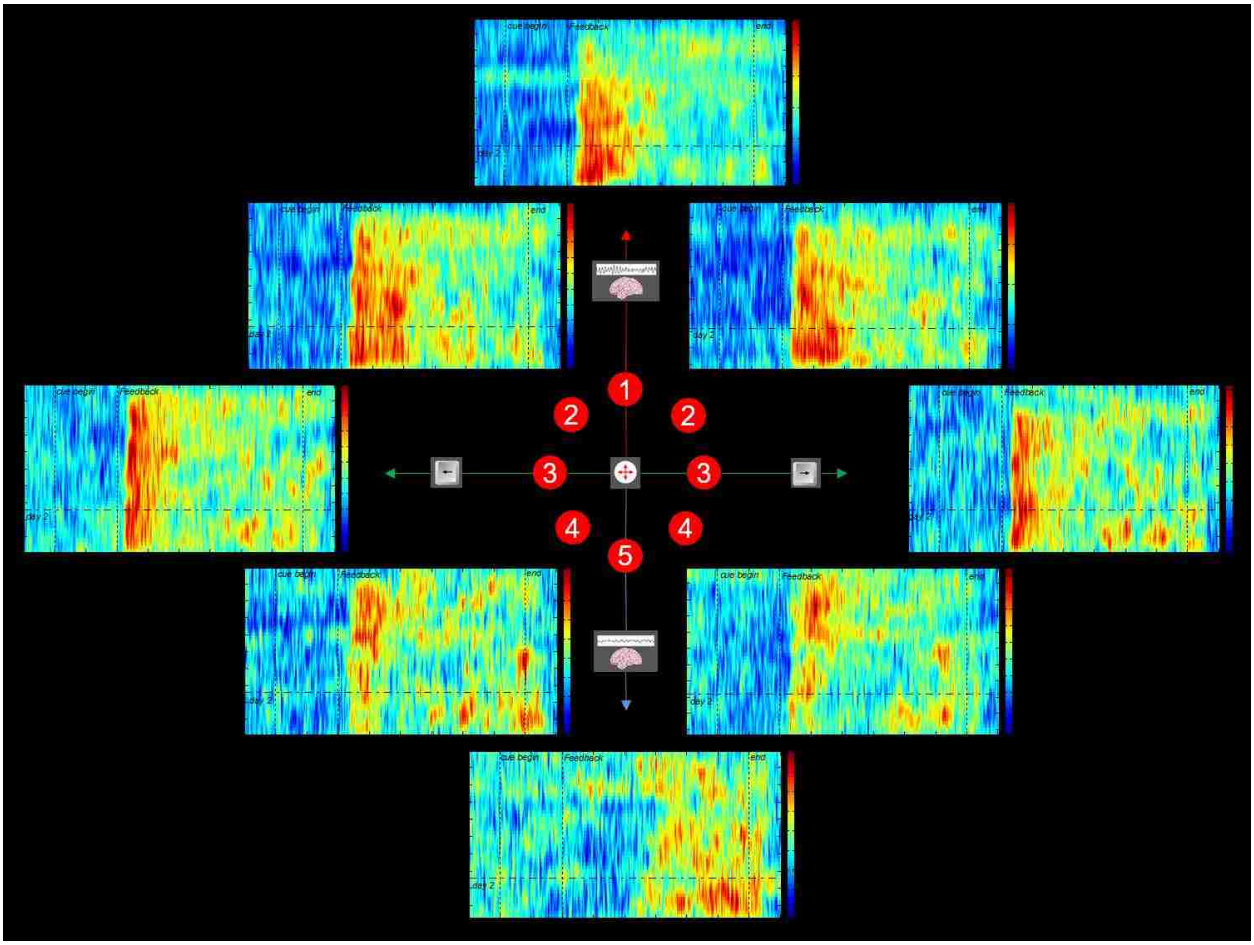

Figure 24 - BCI Task Learning as revealed by Trial-by-Trial High Gamma (HG) Activation at the Control Electrode. In each of the 8 plots corresponding to the 8 possible targets, high gamma (HG) band (70-200 Hz) power changes over time (X axis) are plotted across trials (Y axis) from top (early trials) to bottom (late trials). For target T1 (requiring LMI only), the subject initially had little or no HG activation, leading to poor performance. Later trials show a progressive increase (red) in HG activation after the feedback cue, indicating purposeful modulation and leading to higher performance. A similar effect is seen of the T5 plot, where a progressive reduction (blue) in HG activation is seen, leading to better control of downward cursor movement. For the diagonal target types T2 and T4, HG activation increases over trials or decreases over trials as necessary to boost performance - note that in both cases, ipsilateral activation due to right hand key presses persists over the course of a trial.

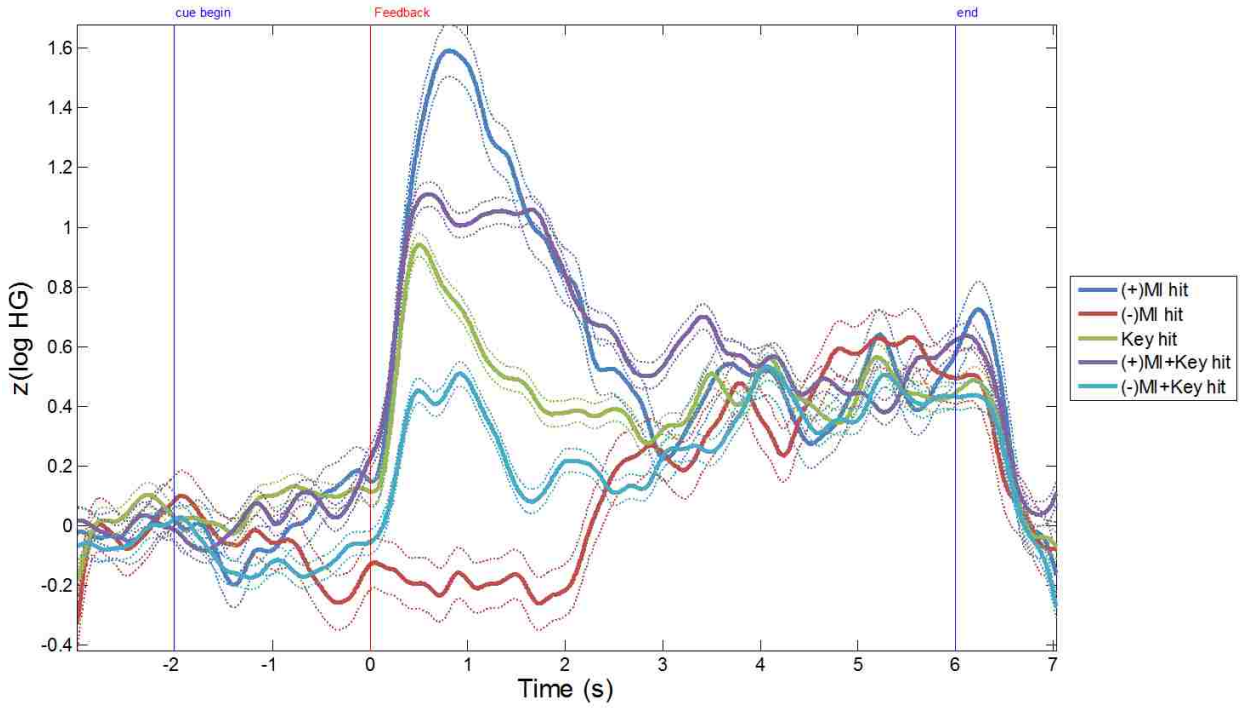

Figure 25 - Mean HG activity at the Control Electrode after BCI Task Learning. The average HG activation for each of the 5 target types T1-T5 is shown for day 2, with standard error plotted using dotted lines. All trials were successful or 'hit' trials. Note the expected increase versus suppression of HG activation for T1 targets (denoted by "(+)MI" for motor imagery) versus T5 targets ("(-)MI" for rest) respectively. For the T3 targets, which require only right hand key presses, we see ispilateral activation in the control electrode (green plot). For the diagonal targets (T2 and T4), the subject has learned to activate the control electrode at intermediate levels (see lines labeled (" (+/-)MI+Key")) between key press activation and activation for motor imagery or rest. Note that for all target types, the activations converge to the same common level towards the end of the trial when the subject was required to dwell the cursor inside the target.

9.2.3 Task Modulated Activity in Electrodes near the Control Electrode

We found that electrodes close to the control electrode exhibited similar activation patterns as the control electrode. Specifically, electrodes 64, 56, 47, and 39, which fall along or immediately adjacent to the central sulcus, also showed task-related HG activation during the screening task (see Figure 20). The HG stratification by target type seen at the control electrode 48 (Figure 25) are also exhibited by electrodes 64, 56, & 40, though the maximum amplitudes are lower and there is not as significant a difference between the T4 and T5 trials. Channels 39, 47, & 55 exhibited a significant HG rise for T1 targets, but negligible HG suppression for T5 trials, with channels 47 and 55 even showing a slight increase in HG for all target classes starting from the beginning of feedback. Channel 32, a channel one electrode away from the control electrode, however, showed a very different activation pattern, with increased HG for all upward targets utilizing LMI behavior but not for any target category in which RH behavior is active. These results suggest that cortical networks can commandeer

the activities of large neuronal populations in regions near the control electrode to precisely shape the activity at the control electrode in order to increase the reliability of control during the BCI-task.

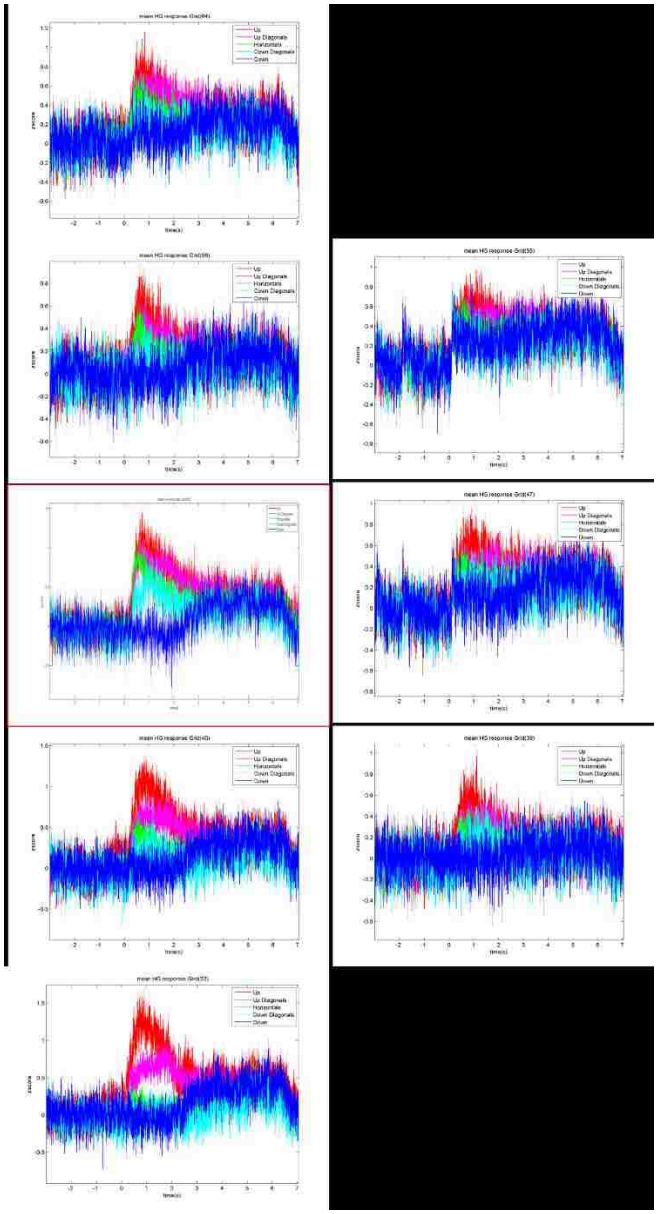

Figure 26 - HG Activation for Electrodes surrounding Control. HG activation across all target categories is averaged, respectively. Standard error for the z-normalized signals are calculated and plotted for channels immediately neighboring the control electrode. Plots are spatially laid out as per grid orientation seen in Figure 20. The general activation patterns seen at the control electrode, outlined in red, are seen in electrodes 64, 56, & 40. In these cases, there is some suppression of HG for T5 targets with a staggered level of activation for T1-T4 based upon the degree of LMI involvement. Channels 39, 47, & 55 indicate some level of HG activation for T1 cases, but demonstrate negligible HG suppression for T5 trials. In fact, there may be a general non-significant HG activation for all target trials. Channel 32 shows a very different activation pattern, with increased HG for all upward targets utilizing LMI behavior but not for any target category in which RH behavior is active. Unlike at the control channel, there is a directional separation of HG activation akin to a simpler 1-D cursor task.

9.2.4 Adaptation in non-motor cortical areas

Additional examination of the HG activities at electrodes further from the control electrode also yielded some surprising results. Figure 27 shows the average HG activation and standard error across all target categories for four electrodes (57, 16, 1, 40) from putatively non-motor cortical areas.

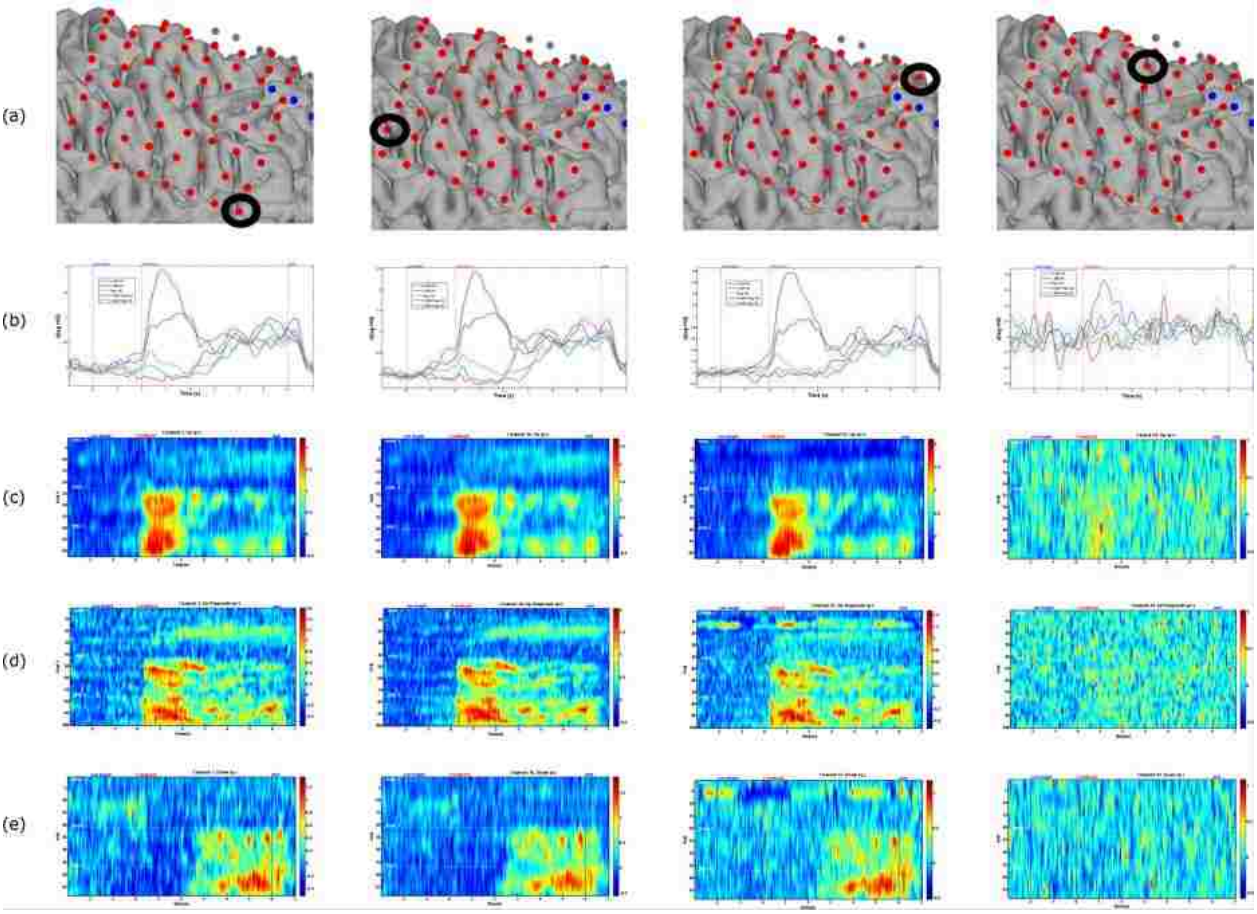

Figure 27 - Examples of HG Activation for other electrodes across cortical areas. Examples of HG Activation for non-Control electrodes across cortical areas. (a) Data for three non-control electrodes (circled) with highly similar activation patterns in different cortical areas (separated by column). A fourth electrode is provided as a counter-example of quiescence or lack of task-related activation. (b) The second row of panels shows the average HG activation (post learning) across all target categories, along with standard error. In the first three cases, there is an increased HG activation for all upward targets involving LMI behavior but low activations for other target categories in which RH behavior is active. (c) The third row shows plots of trial-by-trial HG activation for "up" targets (type T1), with earlier trials at the top of the plot. Note the remarkably similar activation patterns for the three different electrodes, with a notable increase in HG activation (red) in the later trials (from Session 2). (d) The fourth row of plots shows trial-by-trial HG activation for target type T2 trials; there is no significant HG activity until the later trials from Session 2. (e) The last row shows the trial-by-trial HG activation for "down" targets (type T5), with a notable increase only in day 2 late in trial time corresponding with the convergence of HG across target types in (b) during the dwell/hold phase.

These electrodes lie in frontal, occipital and temporal parts of the ECoG grid as seen in Figure 20. The final electrode is provided as contrast for a non-task relevant area (as per observed activation patterns). Despite being distant from each other, the first three electrodes exhibited an increased average HG activation for all upward targets utilizing LMI behavior but not for any target category in which RH behavior is active (second column of panels in Figure 27). This type of activation pattern was also seen in an electrode closer to the control electrode (channel 32) as mentioned above. These same electrodes from non-motor cortical areas also showed remarkably similar trial-by-trial HG activation patterns (last two columns of plots in Figure 27), suggesting that the subject's high performance in the concurrent BCI-motor task was achieved by an orchestration of distant neuronal populations across diverse cortical areas.

9.2.5 Neural Correlates of Concurrent BCI Learning across Cortical Areas

What changes occurs across cortical areas as the subject learns to control the concurrent BCI in the 2D cursor control task? We compared the z-scored mean HG activation for Day 1 versus Day 2 trials, representing pre-learning and post-learning states, for all electrodes in the ECoG grid. Figure 28 shows the difference in mean HG activation between pre- and post-learned states for each of the 5 target types. Overall, the HG response was amplified across many cortical areas, with a pronounced increase by Day 2 at and near the control electrode as expected for upward targets. The decrease in activity (green) in some frontal areas for downward (T4 and T5) targets and the additional HG increase in putative non-motor locations (as seen in Figure 27) appear to be consistent with previous results on ECoG BCI learning (Wander et al., 2013).

9.3 Relevance and Related Work

Significant work has been done on all levels of BCI systems to both improve functionality and understand the neural processes at work (Murphy et al., 2016). Though a variety of cortical areas and structures have been examined for BCI control, these assume an intrinsic absence of functional motor ability (Daly et al., 2013). The most successful examples from the Brain-Gate project (Jarosiewicz et al., 2013) or the impressive control of the Modular Prosthetic Limb (MPL) in Pittsburgh were performed by tetraplegic patients (Schwartz et al., 2006). Even when multiple cortical areas (via multiple localized multicellular groups) are utilized for high-dimensional dynamic control, there is essentially one singular motor actor to which all relevant cortical systems become entrained. It is unclear, then, how effective these systems would continue to be in the presence of other residual

natural motor behaviors. However, work by Orsborn, Carmena, and colleagues (Orsborn et al., 2014)has shown that in cases of simultaneous control of BCI and overt movement, in their case a force hold behavior during a cursor task, monkeys were able to gain proficiency with the paradigm and their neuroprosthetic control skills were not completely disrupted by performing the simultaneous task, with the neural adaptation possibly facilitating the formation of a BCI-specific network. Other results from experiments in monkeys by Milovanovic, Moritz, and colleagues (Milovanovic et al., 2015) have shown that neural activity from a single hemisphere can be effectively decoupled to simultaneously control a BCI and ongoing wrist movement.

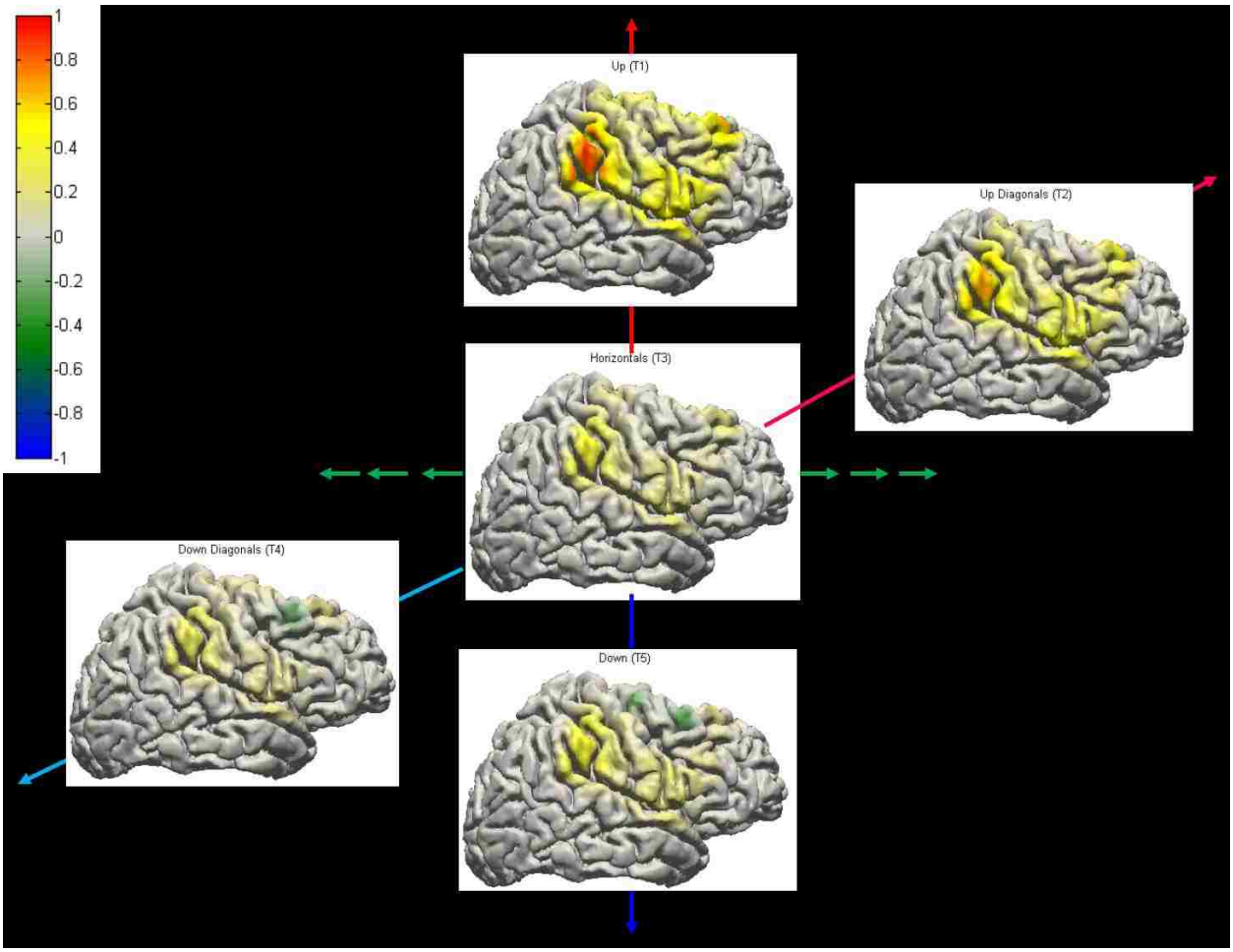

Figure 28 - Changes in Cortical Activation from Early to Late Trials. Each brain map shows the mean HG activation changes for Day 1 vs. Day 2 (Pre-learned vs. Post-learned states) for each of the five target types T1 through T5 (indicated by the 5 different colored arrows). As expected, there is an amplification of HG response around the control electrode, especially for up (T1) targets. The decrease in activity (green) in some frontal areas for downward (T4 and T5) targets along with an increase in activity (yellow) in some putative non-motor areas can be compared to previous results on ECoG BCI learning (Wander et al., 2013)

Other groups have examined the practicality of using unaffected cerebral hemispheres for non-invasive BCI control in stroke patients (Bundy et al., 2012)} and individuals with cerebral palsy (Faller et al., 2013), in both cases utilizing multi-hemispheric electroencephalographic (EEG) recordings to showcase the ability to co-opt an area to function as the primary BCI controller while monitoring contralateral activity. Previous work by our group, as described in Chapter 6, demonstrated that human subjects can learn a simultaneous BCI-motor control task using EEG, with interference from ipsilateral movements similar to what we have reported here for ECoG (Cheung et al., 2012). BCI studies involving stroke patients typically utilize EEG, as it is rare to find stroke patients with ECoG implants (Leuthardt, Miller, et al., 2006) or more invasive microelectrode arrays (Jarosiewicz et al., 2013). In the majority of the EEG cases, feasibility of BCI for stroke rehabilitation (or spinal cord injury (Faller et al., 2013)) is shown either by incorporating a complex FES (Daly et al., 2009) or haptic feedback system (Gomez-Rodriguez, Peterst, et al., 2010) or utilizing very complicated 'whole brain' classification approaches with the smeared EEG signals (Prasad et al., 2010), often with limited gains. Some studies focus simply on communication with a BCI (Birbaumer, 2006) based on signals from the hemisphere unaffected by stroke (Bundy et al., 2012). Two prior studies using ECoG from patients with chronic stroke, have shown that it is possible to detect similar arm- (Gomez-Rodriguez, Grosse-Wentrup, et al., 2010) and hand-movement (Spüler et al., 2014) intentions from the damaged cortical zone and one further case has utilized this method to effect control of a robotic hand (Yanagisawa et al., 2011). However, coordinated control by pairing the damaged areas with the intact contralateral motor regions has not previously been shown.

9.4 Discussion

For BCIs to be functional in the real world, even for simple tasks like opening a jar, patients need to be able to utilize a BCI in coordination with their residual motor capabilities. Our results show that for a person with significant hemiparesis, the stroke-affected hemisphere can learn to control an ECoG BCI in coordination with ipsilateral hand movements and successfully complete a 2D center-out task. A diverse population of cortical networks in the stroke-affected hemisphere were recruited and entrained to achieve reliable 2D control in the presence of ipsilateral activation due to hand movements.

Part of the successful acquisition of control in our patient can likely be attributed to early reorganization of the cortex after the perinatal stroke, as underscored by ipsilateral HG activity

observed during motor behavior screening. Whether these results also generalize to other chronic stroke models remains to be seen. Previous studies from our group and others have shown limited ipsilateral representation of movement in ECoG in non-stroke-affected subjects (Zanos, Miller and Ojemann, 2008; Scherer et al., 2009; Darvas et al., 2010). Additionally, in nonhuman primate models, it has been shown that as cortical networks are optimized for bimanual limb control, there is a limited representation of ipsilateral limb kinematics in neural populations (Ganguly and Carmena, 2009). In LFP/ECoG recordings, this has been seen as detectable ipsilateral HG responses and a boosted beta response (Zanos, Miller and Ojemann, 2008) (with different ERD/ERS relationships (Blankertz et al., 2010)). Such ipsilateral activity could be a source of noise for BCI control (Prasad et al., 2010) or add more information to aid a bimanual task (Cheung et al., 2012).

However, the confound in our subject is that these movements were heavily constrained to the equivalent movements of the right side. Thus, to actually effect any overt limb movement, the patient had to also move their right side. This, however, was not the case for isolated hand and wrist movements on the left side. Interactions with various objects and external manipulation of the left hand and fingers, though not naturally dexterous, were found to be visually independent from the right hand with cortical activity centered on electrode 48. This selection was supported as isolated manipulation of the right hand, showed a similar, though delayed and less intense, HG activation at electrode 48 (Figure 20). From the surprisingly robust cortical response for the left hand, it was decided to use recordings from electrode 48 as the controller input for the BCI task.

However, based on the observed ipsilateral effect, we hypothesized that it would be difficult for the patient to actually perform the bimanual parts of the task, namely, the diagonal targets (T2/T4). As seen in Figure 23, this is indeed the case, as performance and overall accuracy is extremely low for not only the diagonal cases, but any movement utilizing keyboard presses of the right hand. Thus, even for horizontal targets, in which the cursor should not be actively driven in the y+/y- directions (but this movement was not constrained), the ipsilateral motor activations serve as a confound for the system, preventing pure right and left movement along the horizontal (x+/x-). Nevertheless, much like traditional bimanual feedback and rehabilitation tasks (Peper *et al.*, 2013), the patient learned to coordinate BCI control with hand movements and became proficient, with near straight diagonal trajectories as seen in the final run in Figure 22.

Our study also sheds light on possible cortex-wide mechanisms underlying the proficiency in the concurrent BCI-motor control task. By Day 2, the HG response at the control electrode for diagonal T2 targets is closer to the response for upwards T1 targets, while the HG response for target type T4 is closer to type T5 (Figure 24). Comparing the mean HG profiles during cursor control around the control electrode (Figure 25) versus other non-motor areas sheds further light on possible mechanisms of learning (Figure 28). As seen in Figure 27, these non-motor areas become engaged in Day 2 and may play an important role in helping regulate HG activation at the control electrode. Some of these non-motor areas appear to align with areas previously implicated in motor and BCI learning (Wander et al., 2013), but a more precise comparison is difficult due to the limited coverage of the grid as well as the stroke-related characteristics of this subject.

In conclusion, the high degree of accuracy in concurrent BCI control in coordination with existing motor capabilities suggests that concurrent BCI-manual control for stroke patients can be both valuable and feasible for long-term rehabilitation and therapy. While no physical improvements were noted in the patient as a result of BCI use, the improvement in lateral coordination through BCI when coupled with a traditional rehabilitation regimen could potentially be a powerful future tool. In addition, as noninvasive and ECoG technologies continue to improve, the coupling of HG activation with existing control paradigms (Smith et al., 2014) could open the door to a host of novel avenues of inquiry (Wander and Rao, 2014) for patients with similar neuromuscular deficits.

9.5 Expanding beyond cursors.

Though there are distinct limitations to the scope of this case and its generalizability to other chronic stroke models, the fact that a subject with hemiparesis is able to effect such a high degree of control of a BCI cursor interface and that too in coordination with their existing intact physiology, suggests that this avenue of study of invasive BCI with stroke patients is both valuable and feasible for long term rehabilitation and therapy. However, this task framework does not actually get us beyond the cursor model, even though it is analogous to limb reaching as per NHP studies on which the center-out task is largely based (Ganguly and Carmena, 2009; Orsborn et al., 2014; Shenoy and Carmena, 2014). For true dexterous bimanual control of a hand robotic or prosthetic system, more degrees of freedom will be needed. To that extent, having a better resolution of the related cortical areas, as well as a better framework for application and control will be needed.

Chapter 10: Resolving Hands: Macro vs. Micro ECoG

Electrocorticographic (ECoG) signals recorded from the brain surface provide a powerful semi-invasive source of brain signals for direct control of hand prosthetics (Moran, 2010; Buzsáki, Anastassiou and Koch, 2012). Whether ECoG offers sufficient spatial resolution to allow accurate decoding of dexterous hand movements remains an important open question. In this chapter, we explore the limits of useful information contained in ECoG signals as captured by a variety of clinical and research grids from multiple subjects performing a host of hand manipulation tasks. Microgrids (µgrids) provide higher spatial resolution (in the mm range) compared to conventional ECoG grids (resolution in the cm range) but their utility for decoding fine-grained movements has been relatively unexplored. We applied a variety of classification techniques to µECoG data and compared decoding performance with macrogrid data. Using off-the-shelf methods such as support vector machines for classification, we show that µgrid recordings allow decoding accuracies of up to 97% for gross finger movements as well as near 90% accuracy across 7 grasping classes. Our results suggest that compared to macrogrids, µECoG may provide sufficient information to allow high-fidelity control of individual finger and grasp movements, opening the door to practical brain-computer interfaces for hand prosthetics.

10.1 Significance

Brain-computer interface (BCI) platforms can be broken down into the following components: signal acquisition, signal processing, and device output. Signal acquisition can be either non-invasive or invasive. Among the many electrophysiological modes, semi-invasive electrocorticography (ECoG), strikes a good balance between signal quality and recording robustness, while also allowing study of neural dynamics over distributed cortical areas (Moran, 2010). Current ECoG-based BCI paradigms screen for gross high frequency activity during certain modalities of movement. Electrodes showing activity correlated with periods of movement have their changes in high frequency mapped to a control signal; increasing spectral power beyond a linear threshold triggers the control signal output. This technique, while viable for simple control mappings, provides only a binary output of a positive or negative result. Typically, each electrode can provide only one control signal, meaning multiple degrees of freedom require multiplexing the identified control features. This leads to complications when controlling two or three degrees of freedom from two or three control features and the near

impossibility of controlling high-dimensional systems. Controlling modern prosthetics in this way could be an effort in futility, as some manipulators precisely mimic more than 20 degrees of freedom present in the human hand(Kumar, Xu and Todorov, 2013). However, previous studies of the central and peripheral motor nervous systems suggest the presence of synergistic activations of musculoskeletal groups during coordinated movement, and that these "motor primitives" may be present at the level of the spinal column and possibly in higher levels of CNS (Blakely et al., 2009). This might be one avenue of investigation for dexterous movement with BCI.

However, capturing these dynamics can challenging (Bundy et al., 2014). Our group has previously shown that high gamma (75-200Hz) activity in primary motor cortex as recorded by standard electrocorticography (ECoG) shows high spatial preference for individual digit movements during overt finger flexion (Scherer et al., 2009). In contrast, the average spatial activity in this medium during object grasping appears to show little unique spatial organization relative to the grasps performed (Pistohl et al., 2012). However, this may be a factor of scale, as leveraging high resolution (3mm-spacing and below) ECoG grids can allow for better classification of finger movement (Wang et al., 2009). In this study, we demonstrate the comparative robustness of µECoG for classification and BCI use as compared to standard clinical recordings. Furthermore, we show µECoG can allow for the spatial separation and identification of fingers during more complex grasping and hand manipulation behaviors. In addition, we show that the theoretical utility of even clinical ECoG can be improved with just a slight decrease in scale. There remains an open question as to whether 'synergies' or similar lower-dimensional postural components would distinguishable with ECoG, but it is clear that the resolution of standard ECoG grids should continue to be improved to one day utilize this schema for dexterous biomimetic volition control by a user of a virtual or robotic hand.

10.2 Methods

10.2.1 Subjects

As with the previously described ECoG studies, patients with intractable epilepsy were implanted with platinum subdural ECoG electrodes for the purpose of seizure focus localization at the University of Washington's Harborview Medical Center or the Seattle Children's Hospital. Electrodes were placed by medical staff over the right hemisphere as per the clinical indications. The primary 8x8 electrode arrays consisted of 3mm diameter platinum pads spaced at either 1cm or 7.5

mm center-to-center and embedded in silastic (AdTech). In some cases, additional strips of electrodes were placed based upon clinical need. Patients provided informed consent to participate as subjects for research activities during clinical monitoring under UW and SCH IRBs. Relative placement of the implants for each subject can be seen in Figure 29. Subject demographics and research involvement for this study can be seen in Table 4. Three additional subjects underwent intraoperative procedures as described in the following sections. Relative implant sizes can be seen in Figure 30-a.

Table 4 – Demographic information for implanted subjects. Listed for each subject are the implant type (macro, micro or mini based upon implant spacing and size), the hand manipulation tasks performed, as well as which hand was recorded by the CyberGlove. For Macro-5, no hand recording was possible due to IV needles. One patient from each group of implant type was used for comparison by classification analysis and is indicated in italics.

Subject ID	Age	Gender	Grid Spacing	Task Type			DataGlove
				Finger Flexion	Grasping	Hand Posture	
Macro-1	11	M	1cm	5+pinch	6 objects	--	R
Macro-2	12	M	1cm	--	6 objects	--	R
Macro-3	50	F	1cm	t,i+pinch	6 objects	5 poses	L
Macro-4	*45*	*F*	*1cm*	*5+pinch*	*6 objects*	--	*R*
Macro-5	34	F	1cm	--	6 objects	--	--
Macro-6	19	M	1cm	--	6 objects	--	L
Macro-7	19	M	1cm	--	6 objects	--	L
Mini-1	*11*	*F*	*7.5mm*	*t,i+pinch*	*6 objects*	*5 poses*	*R*
Mini-2	16	F	7.5mm	--	3 objects	--	R
Micro-1	*49*	*F*	*3mm*	*5+pinch*	*6 objects*	--	*R*
Micro-2	38	F	3mm	5+pinch	6 objects	--	R
Micro-3	30	M	3mm	5+pinch	6 objects	5 poses	R

10.2.2 Signal Recording

Experimental recordings were taken at the patients' bedsides without interrupting the primary clinical recordings. As per previous work from our group, data were acquired at 1200Hz using four synchronized sixteen-channel g.USBamps (GugerTec) connected to a high-performance Sager laptop computer (Blakely et al., 2009). Data were anonymized in accordance with Health Insurance Portability and Accountability Act mandate. Cortical potentials were referenced against a scalp electrode and digitized and processed in the BCI2000 software suite (Schalk et al., 2004). Additionally, hand movements were captured using a Cyberglove II system. For each subject, the hand contralateral to hemisphere of implant was recorded. Data were synchronized with ECoG within the same software setup. In some few cases, due to clinical intervention, the glove could not be worn by subject or had to be removed during the recording session. This is reported in Table 4.

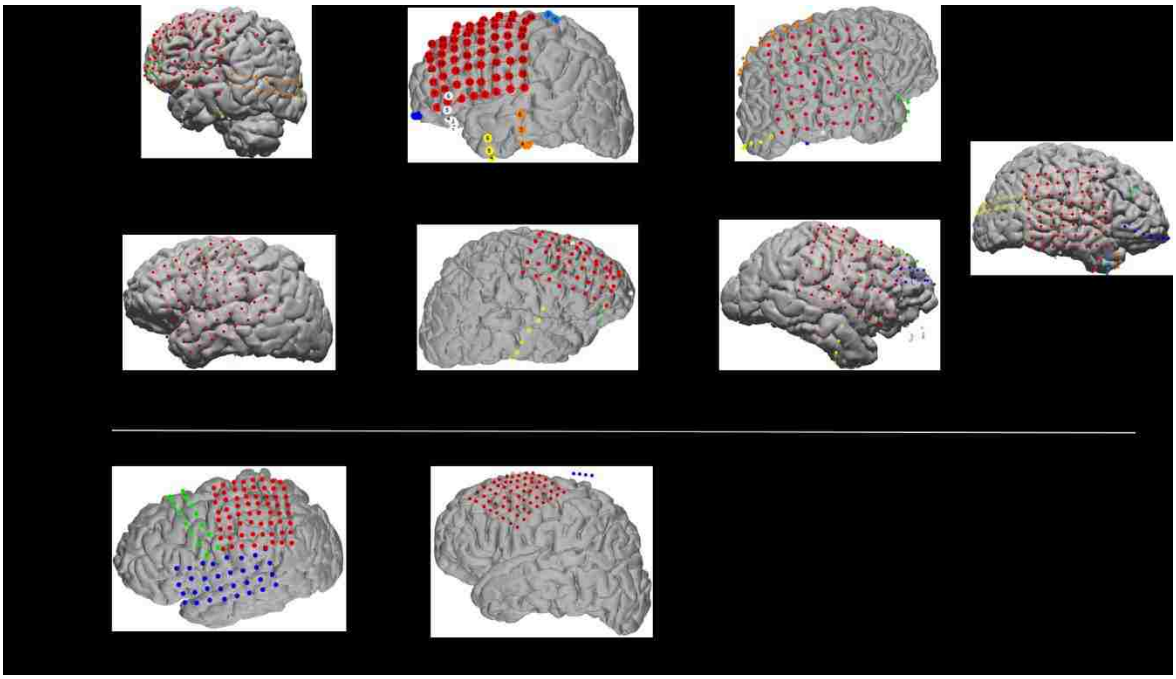

Figure 29 - Clinical ECoG Implants by Subject. (a) Implant location for subjects with standard (1cm spacing) clinical ECoG arrays. Patient MR and CT scans were used to create 3D head model reconstructions showing the spatial arrangement of the implanted array in relation to the cortical tissue below. (b) Implant locations for subjects with 7.5mm spaced clinical arrays (in red).

10.2.3 Awake Craniotomy µECoG implants

Three subjects were implanted with µECoG arrays during intraoperative surgical sessions. For inclusion in this study, the subjects had to have a surgical necessity for an awake craniotomy with epileptic lesions near sensorimotor cortex, in addition to being able to respond to visual cues during the intraoperative session. In an ideal situation, a subjects' craniotomy window would have been large enough to expose primary sensorimotor cortex. This would allow stimulation mapping of the area to directly map areas of motor cortex eliciting hand movement. Unfortunately, the craniotomy window was typically inferior to hand motor cortex and without exposing areas associated with hand movement. Thus, the grids were guided by the surgeon by sliding the implant subdurally in the direction corresponding to the most likely area associated with superior central sulcus. To aid in this process, a quick-mapping technique based on traditional behavioral screening tasks(Wander et al., 2013) used by our group was performed. This involved recording all 64 electrodes while the subject rested for 5 seconds. After the rest period, the subject was instructed to open and close their hand, hopefully activating areas of cortex associated with gross motor movement. Recording ended after

10s and was processed for changes in high gamma (75-200Hz) between the rest period and hand movement. The results were visually displayed to the researcher and surgeon, as seen in Figure 30-d. If the grid showed no activity, the grid was moved to the next most likely area based on pre-operative MRI images.

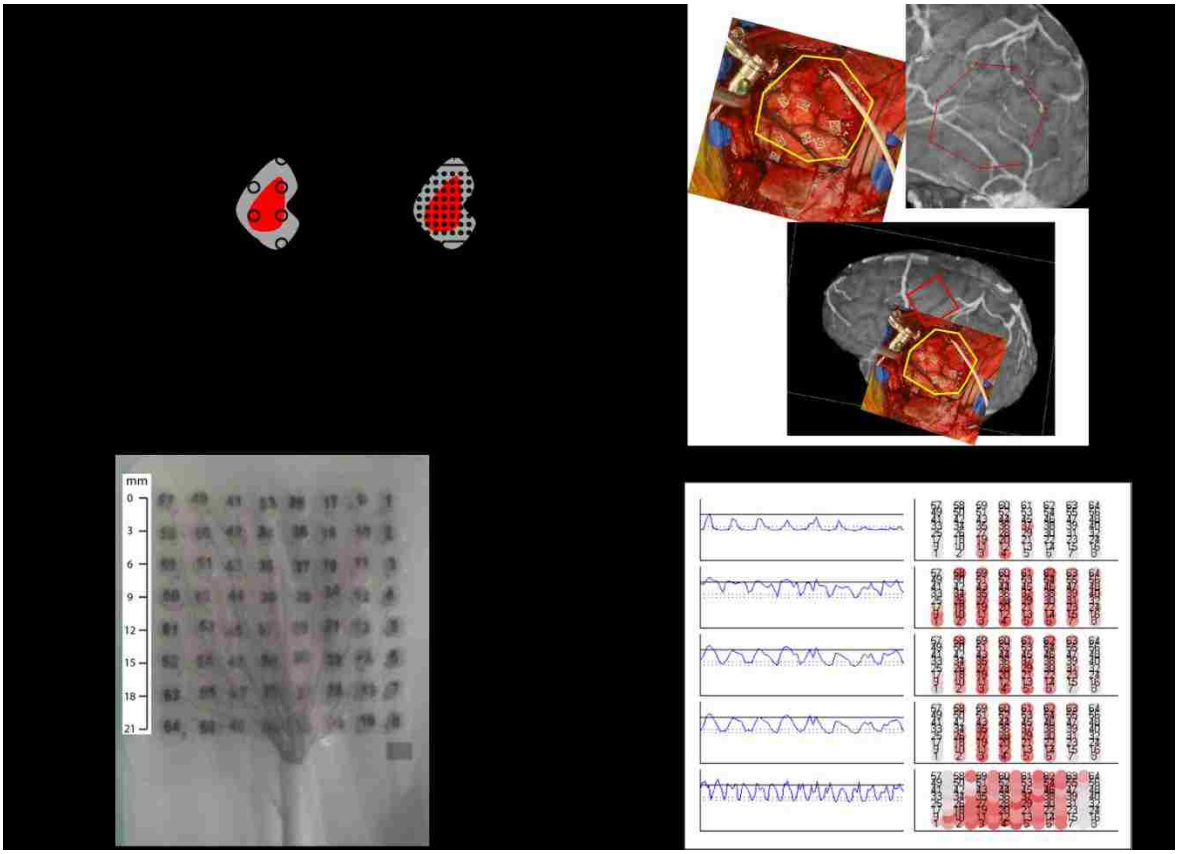

Figure 30 – The Microgrid Implants. a) Relative size of the microgrid. Standard clinical grids (left) have 3mm platinum disks spaced at 10mm center-to-center. The µgrid utilized contained 64 1.5mm diameter electrodes spaced at 3mm. b) Example of microgrid implant. Scale shown next to standard clinical forceps. All 64 contacts come out in a single wire split into four 16-contact pig-tails. Each pigtail was plugged into a single biosignal amplifier. c) Upper-left: intraoperative photo of the craniotomy of Subject 2850af, with artificial landmarks highlighted in yellow. The lead coming from the microgrid can be seen in white. The vasculature from the intraoperative photo was aligned with the vasculature in a pre-operative magnetic resonance angiogram (MRA, upper-right). Estimated artificial landmark location is highlighted in red. After alignment, 3 dimensional grid location is estimated to cover primary sensorimotor cortex (red square, lower). d) Screenshot of the quickmap program used to identify whether the grid was over motor cortex. Left columns show the unrolled grid (channels 1-64) vs RSA-value. The lowest dotted line in each plot indicates zero correlation with activity, followed by RSA=.1 above it, with the solid line at 0.5 RSA. Values above .1 indicate weak positive correlation, and values approaching 0.5 indicate strong correlation. Right column shows a graphical representation of the grid, with a redder color indicating a stronger correlation. To ensure that noise did not contaminate the results, the raw signal (top row) was re-referenced four different ways to try to eliminate noise and identify signal: common average, amplifier bank, corner-reference, and pairwise referencing (2nd through bottom, respectively).

As the craniotomy window did not expose the central sulcus, it was important to also create an accurate estimation of the grid's location beyond the behavioral screen. Pre-operative MR angiograms were performed. A cortical surface is generated from this volume using the Freesurfer reconstruction pipeline (Fischl, 2012). As intra-operative CT scans are not part of the clinical procedure, grid position relative to the craniotomy window was measured from the base of the grid at the hillock of PDMS material, see Figure 30-b, to the edge of the dural opening. Taking into account the direction of the visible wire in intraoperative photos and aligning the photo's vasculature to that of the MR angiogram, we are able to estimate the position of the grid over the reconstructed cortical anatomy in conjunction with the quick map process. Figure 30-c shows the results of the reconstruction and estimation of cortical location for one subject.

10.2.4 Visually Cued Hand Manipulation Tasks

At the beginning of each recording session, standard clinical subjects performed an overt motor screening exercise, in addition to clinical motor evaluation. Typically, subjects were visually prompted to move their hand or tongue for three seconds with a three second rest period in between each movement. This was repeated about 20 times. Subjects then repeat the task, except imagining the prompted movement without executing an overt motion. This was similar for the intraoperative subjects; after they were brought out of deep anesthesia and quick-mapping confirmed that the grid was over an area that showed increases in high gamma during hand movement, a screen was placed comfortably within visual range of the subject and the data-glove was put on the subjects' right hand. The subjects were instructed to flex their outstretched hand into a fist when they saw a picture of a hand appear on the screen, and relax when it disappeared. Each cue was presented for three seconds followed by three seconds of rest, repeated a total of 10 times.

Following the gross motor screening, subjects participated in a series of additional visually cued response tasks designed to elicit highly stereotyped but unique movements either for each finger digit or in relation to particular hand grasp types. In the finger flexion task, a white silhouette of a hand was presented to the subject ('rest' phase). After two seconds, one of the five digits was colored or the index and thumb was highlighted (see Figure 31-a). The subject was instructed to flex the corresponding finger on their right hand. After another two seconds, the highlight was removed and the subject rested. This sequence was repeated 15 times for each of the six stimuli. In the object grasping task, six prototypical hand grasps were elicited as seen in Figure 31-b. In this case, however,

the visual cue was shown to the researcher who then selected the object and handed it to the subject in their bed. This prevented a reach and grasp phase, requiring the subject only to see the object, shape their hand, and hold it until removed by the researcher. After a two to three second interval, another object was provided. This was repeated 10-15 times for each object/grasp type. To elicit more unique and dynamic hand movements, one additional task was added for later procedures. In this task, subjects were first instructed on one of six hand poses: an open palm, a fist, thumbs up gesture, a cowabunga gesture (also known as the Hawaiian shaka or 'hang loose'), a grasped claw with all fingers bent, and a dynamic curling closed motion splaying fingers open and then closing from little finger to thumb. Subjects were cued visually with the word for the posture and given a six second compliance window. After a 2-3 second rest period, another cue was provided. This was repeated 10-15 times for each pose. Differences in procedure length and administration was dependent on subject compliance and availability (see Table 4).

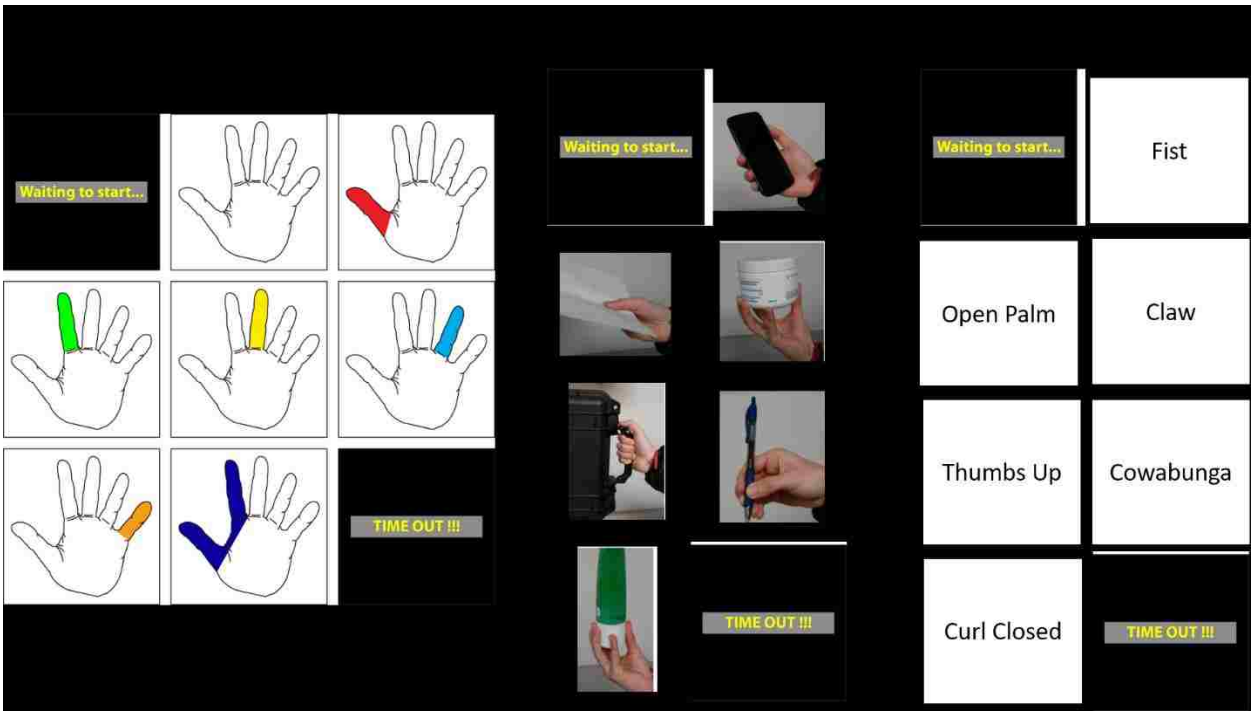

Figure 31 – Visual Cues for Hand Manipulations Tasks. a) Finger Flexion - During rest periods, an empty silhouette of a hand was presented to the subject (top middle). Every two seconds one of five digits (or index and thumb for pinch) was highlighted for two seconds. Subjects were instructed to flex the indicated digit during cue presentation. b) Object Grasping – In this case, cue is presented to the researcher. Over five second intervals, an object is shown and then handed by the researcher to subject. Subject shapes their hand and holds object until removed at the end of the cue period. c) Hand Postures – As with the original task, subjects were cued to shape their target hand into one of five postures and one dynamic movement (curl). Subjects were previously instructed on expected hand postures.

10.2.5 Data Processing and Signal Analysis

All channels recorded from the electrocorticographic grid were common average re-referenced by subtracting the average signal recorded at all electrodes. This was done in an attempt to remove any common noise introduced by activity recorded at the scalp reference electrode in the electrically noisy hospital environment. As per previous ECoG studies from our group, the re-referenced signals were band pass filtered for the high-gamma (HG) range (70-200 Hz) using a fourth-order Butterworth filter (Darvas et al., 2010). The square of the magnitude of the Hilbert Transform was then used to calculate a time-variant estimate of band-power (Wander et al., 2013). Data were then log transformed in order to become approximately normally distributed for proper statistical analyses (Blakely et al., 2009). To account for differences between recording sessions, this log-power estimate was further z-normalized with respect to the rest (behaviorally quiescent) periods for each channel and session. This signal is heretofore discussed as the HG signal or HG activation. Similar extrapolation was done for the lower frequency beta range (8-32 Hz) as well, though not used for primary analyses.

As the trial numbers and durations were often not balanced, either due to subject compliance or available experimental time in the clinical setting, it is useful to use an alternative statistical measure to compare subject specific activation. For every electrode and movement type, we calculated a high and low activation weight by comparing the distributions of HG and beta for each movement type with the corresponding rest distributions. This provides an activity metric based upon the signed, squared cross-correlation value, a measure of how much of the variance in power across both movement and rest epochs was accounted for by the difference in the mean power between movement and rest epochs (Miller et al., 2007). For convenience, this is referred to as the RSA values (HG or β RSA). These can be used as additional features to measure and compare task-related cortical activity across subjects (Miller et al., 2007).

10.2.6 Classification of Hand Movements

10.2.6a Feature Creation & Selection

For direct comparison of activity and representation across the resolution types, a classification framework was created based upon three subjects, one from each implant type (see Table 1). Features for classification were constructed from the HG signal by taking the mean of the

log power over a number of different window lengths. From the glove data, 107ms was measured as the shortest duration of a single directional finger movement by any subject—i.e., the quickest they moved their finger down or up was 107ms. This was chosen as the shortest window, as it was the quickest response captured but may yet be a potentially reasonable granularity for controlling movement of a prosthetic device (Velliste et al., 2008). 186ms was the shortest directional movement measured from the 'macrogrid' patient (standard clinical implant). We hypothesized that larger windows would increase performance due to the fact that more samples would be contained in each feature (Drucker et al., 1997). In a real-world BCI, however, this would lead to a tradeoff between accuracy and responsiveness, however, as it would take longer to make these more accurate predictions. We determined that four actions per second would be near the lower limit of useful responsiveness for granularities of finger movement yet more than enough for a single grasping behavior, and thus limited the largest window to 250ms.

In order to achieve as accurate labels as possible, movement classes were labeled based upon the onset of movement as detected by the CyberGlove. Rest classes were labeled as beginning after the presentation of the rest instruction and ending after the presentation of the following movement instruction. The onset time was padded to allow for the completion of the preceding finger or hand movement. A small number of epochs were present in which the subject performed the wrong action or was provided the wrong object; these were verified by hand and omitted.

10.2.6b Algorithm

An SVM classifier with linear and RBF kernels was selected for classification. Though potentially slower than a pure regression based linear classier, SVM was chosen because it is fairly simple and commonly used algorithm in the BCI community and generally provides high performance, especially for multiple classes. The linear and RBF kernels did not yield significantly different results, and only the results of the linear kernel are shown. The scikit-learn implementations of the algorithm was used (Abraham et al., 2014; Sofiyanti, Fitmawati and Roza, 2015).

10.2.6c Tasks

Two classification tasks each were constructed for finger movements as well as for grasping. The first was a 7-class problem and was to distinguish between rest and the individual finger movements (plus pinch). Although the patients moved the indicated finger up and down during each trial, this task was merely to distinguish which finger was being moved. The second task was a 12-

class problem. It consisted of rest class, as well as the up and down class for each finger (plus pinch). The two classification tasks were performed on each subject, with features constructed over the three different windows. The data in each were a 64-column matrix consisting of the log power in the high gamma band at each electrode. There were as many rows as there were samples. The number of samples varied, however, as the patients did not move their fingers for precisely the same amount of time in each trial, and due to the fact that as the window size increases the number of samples decreases. Further, due to the fewer microgrid samples, response error in the intraoperative session, there were not enough examples of all classes to perform 5-fold cross validation on some tasks. In addition, for the 7.5mm case, the subject only performed thumb, index, and pinch actions, so the finger tasks were adapted to 4 and 6 classes, respectively.

For the grasping behaviors, the first task was also a 7-class problem to distinguish between rest and the individual grasp/object types. However, after review of both glove recordings and task feedback, it was determined that there may be significant overlap in the grasp types and thus the 'object' types were collapsed to 3 for a 4-class problem. This would also serve to boost the sampling size of the data. From here, classification proceeded as with the fingers, but with 250ms as the only window.

10.3 Results

10.3.1 Finger Flexion

Figure 32 and Figure 33 show the results of the finger flexion task for all subjects as well as the microgrid cases. Every digit movement for Micro-1 shows at least three electrodes with mean z-scores above 0.5, and all but thumb have nine or more. The pattern of activity of high gamma activity associated with each digit movement is clearly spatially distributed for Micro-1 and Micro-2. The first had significant thumb activity on the inferior edge of the grid (left column in Figure 32), while index, middle, ring, and pinky progressing further superior along the grid. This is explicitly outlined in Figure 38 for more clarity. Micro-2 had one issue, in that half of the grid (33-64) dropped out due to connector issues for that block. Nevertheless, there is thumb-related activity in the middle of the grid, with each subsequent digit appearing along the posterior edge of the grid from inferior to superior, respectively. Due to the relatively quiet responses for many subjects, as per low zero-meaned z-score HG values, it can be useful to get a general idea of activity change from rest by examining the HG RSA for these same electrodes.

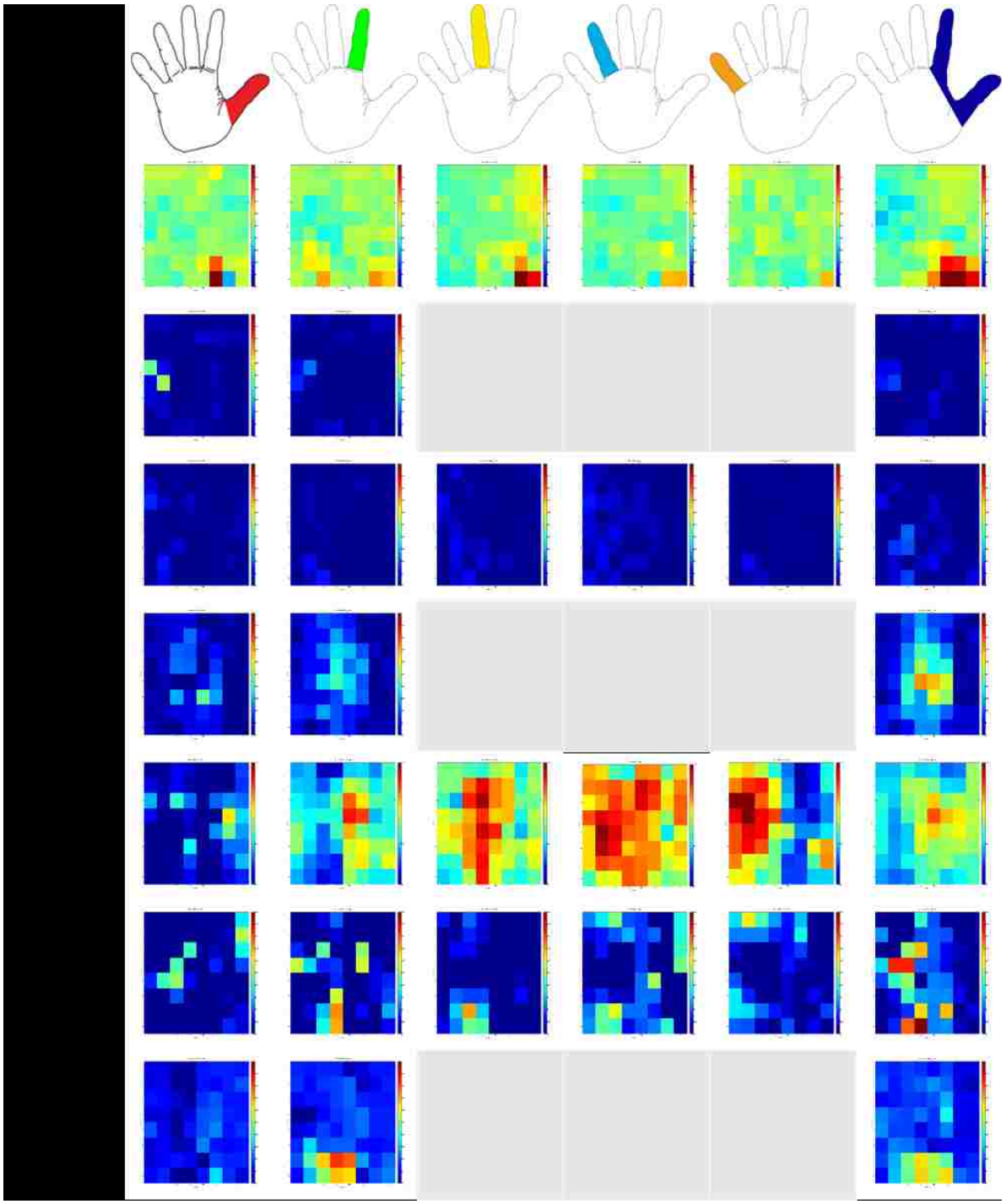

Figure 32 - HG response for Finger Flexion. For each subject the HG signal at each electrode is zero-meaned and z-normed and plotted in relative spatial orientation for each finger type. Heatmap scale is 0 to 1.5 (z-norms) such that task-relevant electrodes can be easily identified and compared across subjects. In case of greyed out windows, the subject only performed thumb, index, and pinch movements.

The trend for Micro-2 is confirmed here, though, is not as robust as in Micro 1. Pinch activity for all three microgrid subjects showed surprising patterns of cortical activation. In both cases, areas

of cortex that increased in activity during thumb and index appear in pinch. (HG RSA boosts the case for Micro-3). Areas that are associated with middle, ring and pinky finger are not co-activated to the level of index and thumb. An overlay example for Micro 1 can be seen in Figure 38-a.

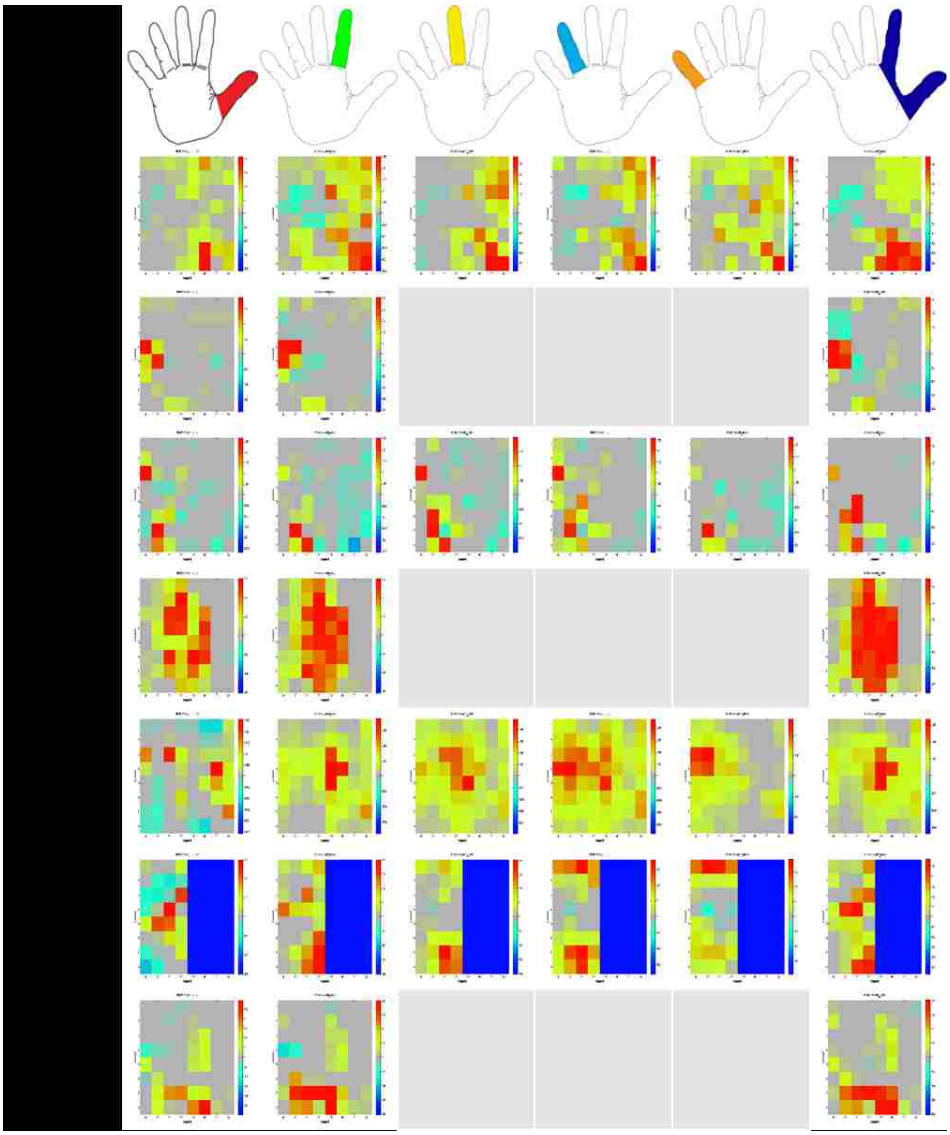

Figure 33 - Active Electrodes during Finger Flexion. For each subject, the HG RSA metric at each electrode is plotted in relative spatial orientation for each finger type. Heatmap is self-scaled by subject RSA values to show the degree of activity versus rest for each subject. In case of greyed out windows, the subject only performed thumb, index, and pinch movements.

For the standard clinical grids, the HG raster is relatively quiescent except for in the case of Macro-1 (0dd118). However, for this subject, the HG response is essentially the same across all finger movements, though it is boosted in the pinch case. Due to the scale and placement of the grid (Figure 29), it is possible some of this is due to sensory activation during pinch. Regardless, there is no

discernable spatial mapping unlike the microgrids. Referring to the HG RSA raster for these subjects, it is clear that there is some task related activation, though it is not unique nor robust across the finger types at this scale or analysis mode.

For Mini-1 (6cc87c), with the smaller 7.5 mm clinical grid, the overall trend is similar to Macro-1 with an amplified response for the pinch case, but still robust finger and thumb related activation. Unfortunately, without the other fingers, it is hard to make any claims about the capturing of any specific spatial localizations. However, several studies from our lab have previously examined the cortical dynamics during finger flexion (Shenoy et al., 2007; Kubánek et al., 2009; Scherer et al., 2009; Wang et al., 2010). For the purposes of this study, the finger flexion recordings are primarily used to contrast the object grasping findings and provide an additional testing and comparison set for classification.

10.3.2 Object Grasping

Figure 34 and Figure 35 show the results of the object grasping task for all subjects as well as the microgrid cases. The additional subjects performing the grasping task underscores the SNR difference with the microgrid cases. Even with poor compliance from the microgrid subjects in the complex intraoperative environment, reflected as mostly thumb and palmar interactions with the objects, the strength of the response is significantly louder than many of the macrogrid case.

Here again, the HG RSA values help make better sense of the overall HG response. For Micro 1, the grasping behavior is localized to the previously seen ring and pinky areas with some activity around the middle finger. For Micro 3, the activation pattern seems quite random. Unfortunately, further analysis showed a marked amount of external noise in the recording during that particular session. Micro-2, however, shows a marked amount of activation, especially with the objects which require a more precise grasp control and finger curl or closure (pen, case, and phone).

For the standard clinical grids, the HG raster is again relatively quiescent except for in the case of Macro-1 (0dd118), Macro-5 (8afafd), and Macro-2 (3745d1). However, the loud general activations, though with peaks centered on the same electrodes as before and supported by the RSA map, is indicative of a possible noise source during the task execution for these patients. Nevertheless, all show 2-4 localized spots of robust HG activity. These were also active during the gross motor activations, indicating that these are most likely representing the physical “blob” that is the hand motor knob.

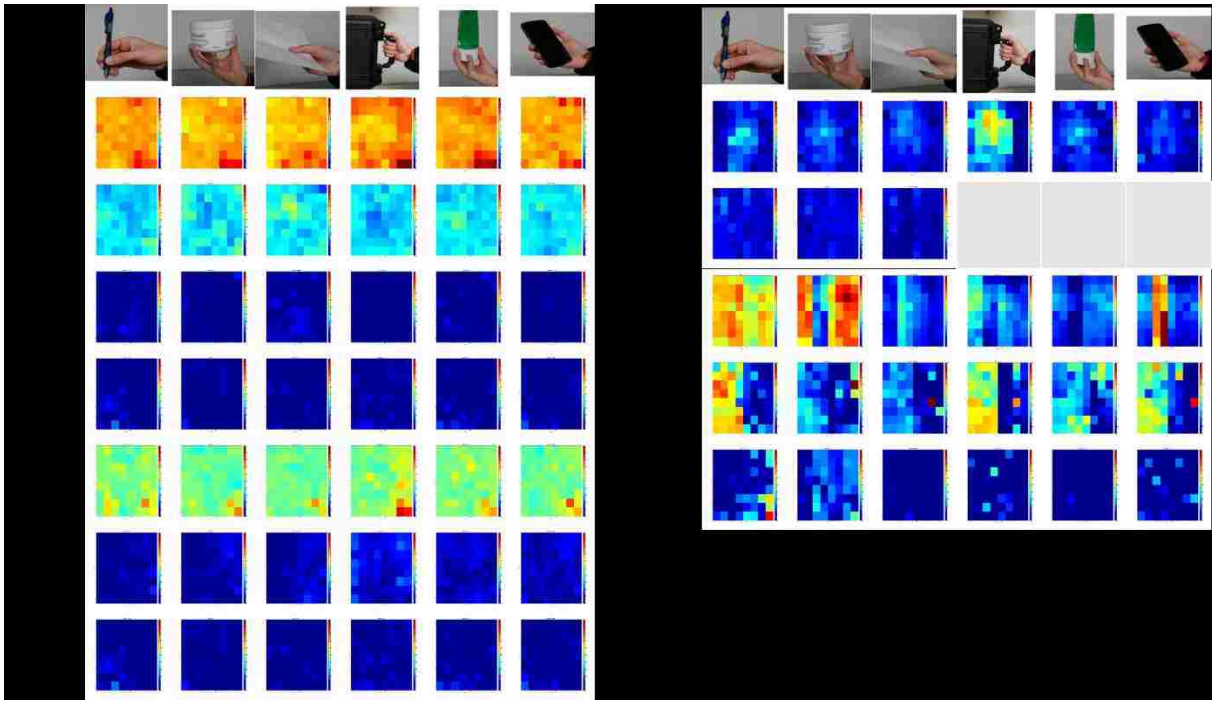

Figure 34 - HG Response for Objects Grasping. For each subject the HG signal at each electrode is zero-meaned and z-normed and plotted in relative spatial orientation for each grasp type. Heatmap scale is 0 to 1.5 (z-norms) such that task-relevant electrodes can be easily identified and compared across subjects. In case of greyed out windows, the subject only performed three grasp types. All subjects in the set on the left have 1cm spacing grids.

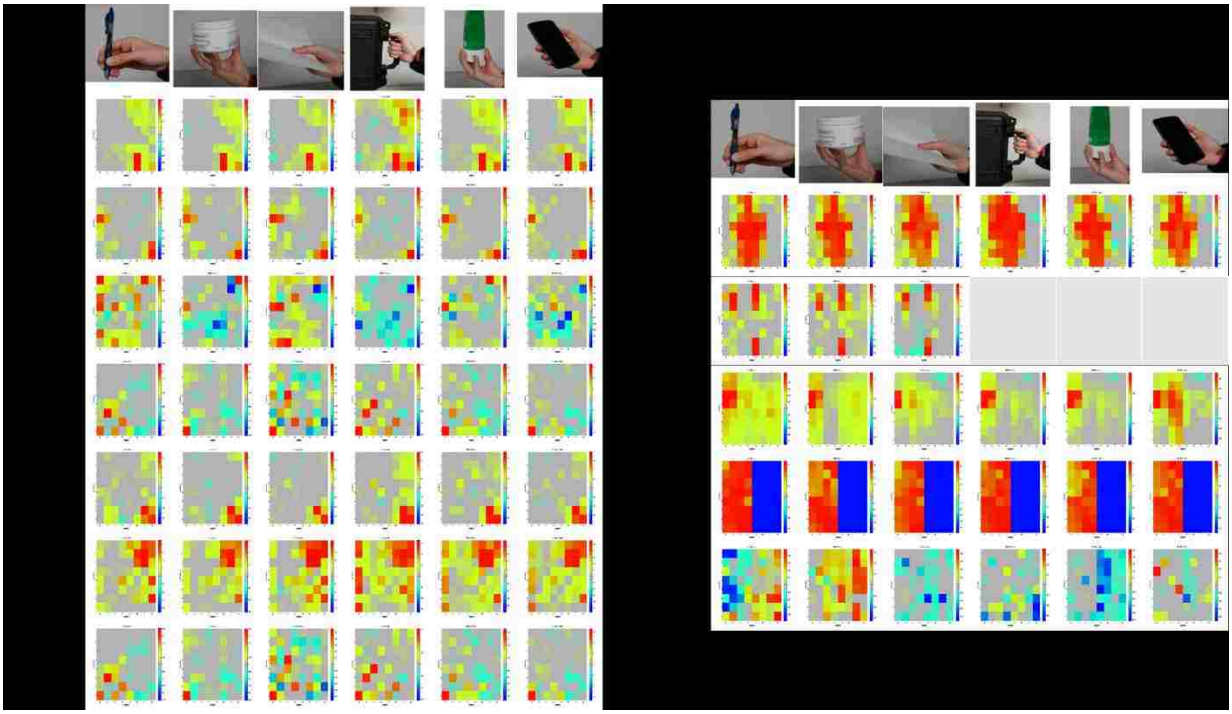

Figure 35 - Active Electrodes for Hand Grasping. For each subject, the HG RSA metric at each electrode is plotted in relative spatial orientation for each grasp type. Heatmap is self-scaled by subject RSA values to show the degree of activity versus rest for each subject. In case of greyed out windows, the subject only performed three grasp types.

Finally, it is important to note that the activation for 6cc87c mimics that as during finger flexion, but is actually less intense except in for grasping the case. Examining the glove behavior, shows that most of the variance in the joint movements actually comes from thumb and lower palm. The lower activation, thus might be from a less robust hand interaction as well as the reduction of movements, since there were multiple finger flexions per cue previously as compared to one fairly small hand movement for this subject.

10.3.3 Hand Postures

The overall reduced activation for Mini-1 (6cc87c) holds true during the hand postures, though it does scale nicely with movement. Open palm shows almost no significant activation, though the potential stabilizing of the palm is distinct from rest (as seen with the HG RSA). However, activation increases for the moving curl posture as well as the more extreme claw. Furthermore, as compared with the finger and grasping activations, there seems to be a more tightly thumb-related area when comparing fist, curl and claw, with the more thumb-engaging 'thumbs up' and cowabunga.

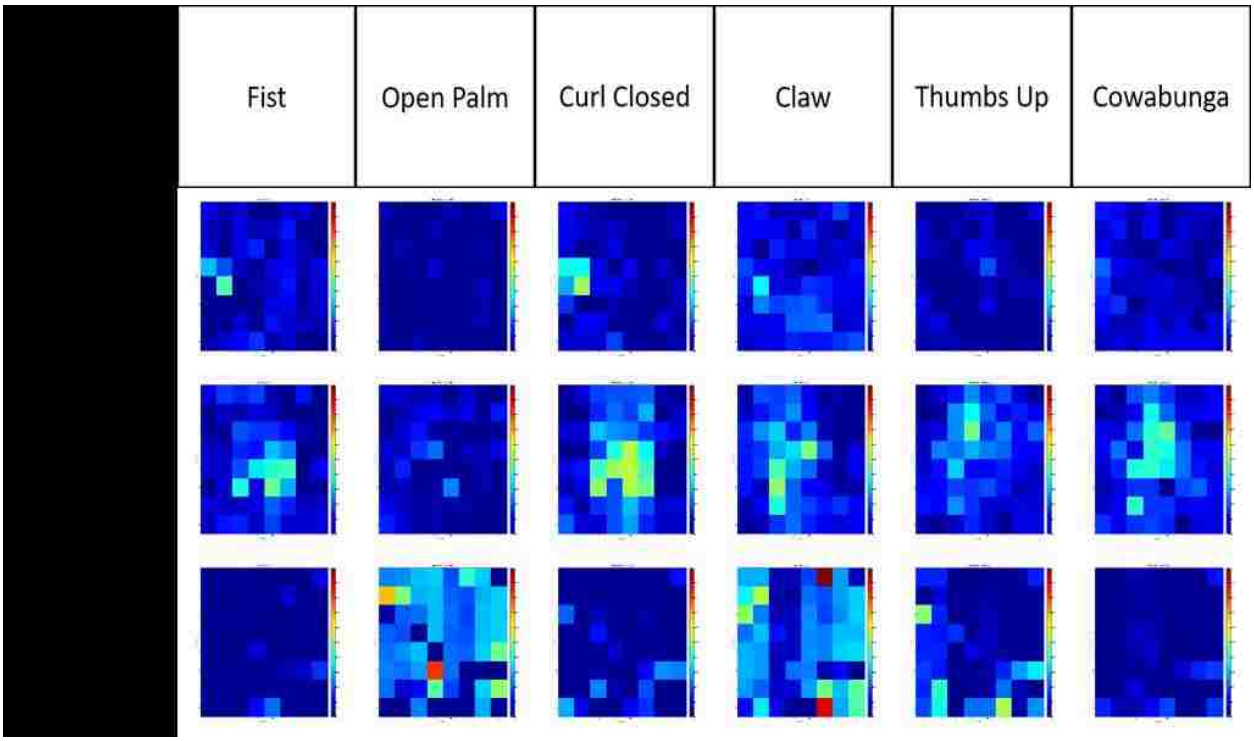

Figure 36 - HG Response for Hand Postures. For each subject the HG signal at each electrode is zero-meaned and z-normed and plotted in relative spatial orientation for each hand posture. Heatmap scale is 0 to 1.5 (z-norms) such that task-relevant electrodes can be easily identified and compared across subjects. Each subject shown has a different grid-type.

This was potentially obfuscated by more general whole hand activations during the object grasping the limited tasks and repetition during finger flexion, though ideally the signal localization would be as robust as that in the Micro-1 case previously. Comparatively, Macro-3 (6b68ef) shows what would be expected for a standard clinical grid with only a couple electrodes strongly activated during the fist and curl cases centered in a 2x2cm zone, representing, as before, the general hand knob area.

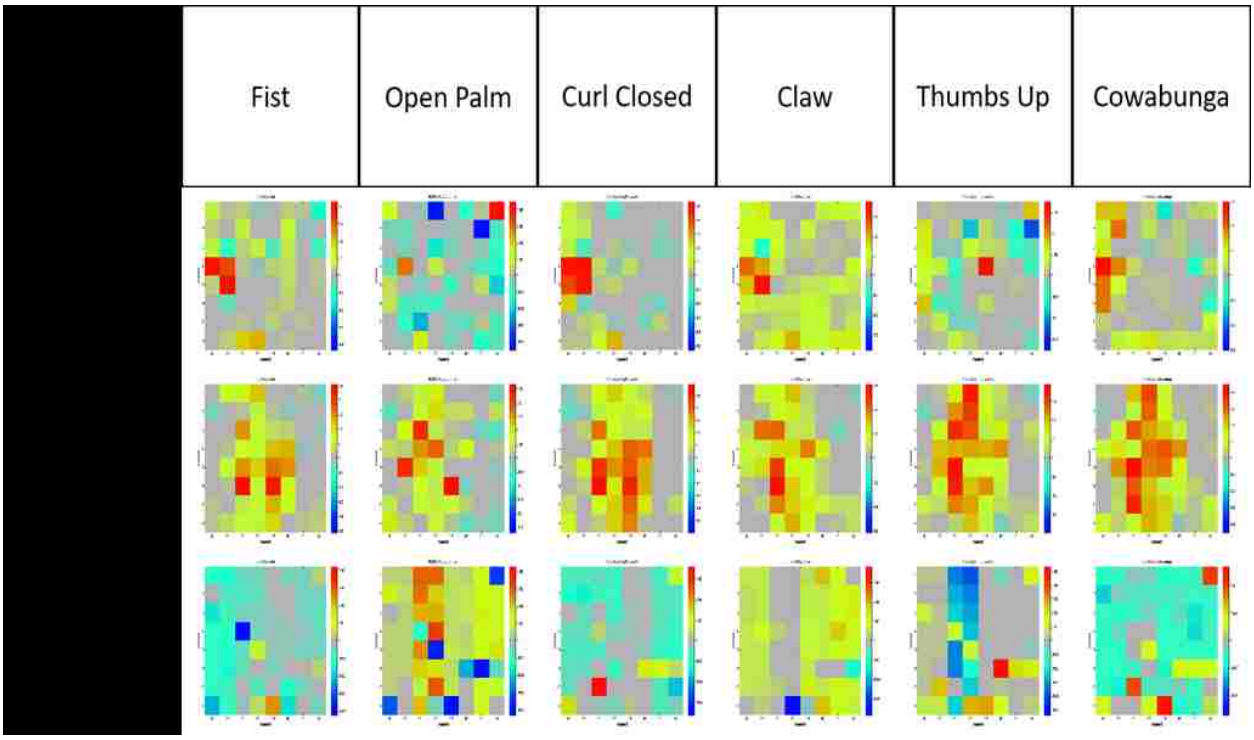

Figure 37 - Active Electrodes for Hand Postures. For each subject, the HG RSA metric at each electrode is plotted in relative spatial orientation for each hand posture. Each Heatmap is self-scaled by subject RSA values to show the degree of activity versus rest for each subject. Each subject shown has a different grid-type.

10.3.4 Active Electrodes & Theoretical Utility

As described previously, the signed, squared cross-correlation measure (RSA) can show how many electrodes are active during task compliance. For each subject and task type, the HG and β RSAs were calculated for all electrodes. For each electrode with significant task-relevant activity (non-zero HG or β RSA), an aggregate time-frequency representation from 0-200 Hz for each task class was built to examine the frequency power change and distribution over time (Figure 38-b). This was then compared to the z-scored HG and the digital flexion dynamics from the Cyberglove data (Fig. 10a) to determine the validity of the task-relevant activity for each electrode (Blakely et al., 2008).

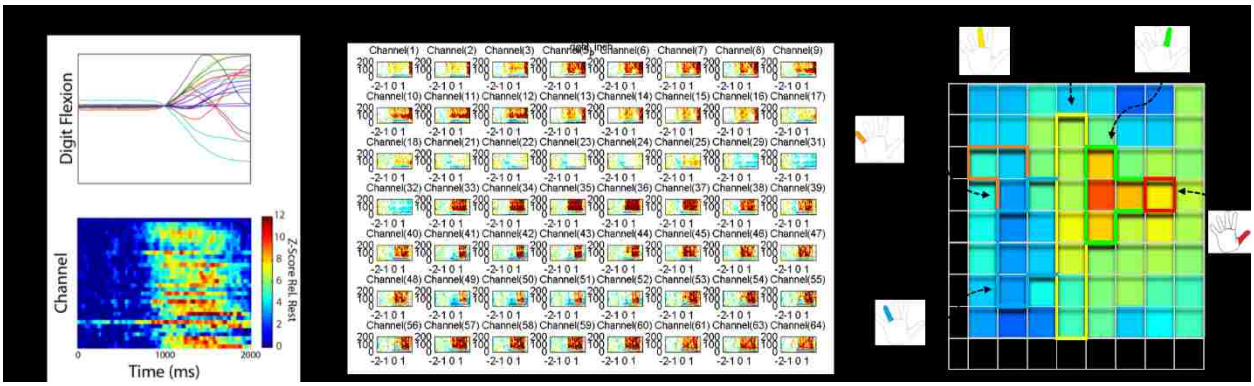

Figure 38 – Characterizing Active Electrodes. a) An example of zero-mean z-scored HG is shown for pinching behavior of Micro-1. The top plot is a trace of joint trajectories during the task. Below is the channel raster of HG over time for each electrode. b) Time-frequency representations of frequency band-power from 0-200 HZ over the pinch period for RSA-significant electrodes for Micro-1. c) A potential spatial map for finger localization is overlay on Micro-1's HG activity during pinching.

Additionally, this process helps validate finger localization spatial maps such as seen in Figure 38-c. The electrodes showing correlation in onset and/or duration were tabulated as 'active electrodes' as seen in Table 5. This also serves to provide a gut check for the activity plots in the previous figures. In the case of Macro-1 (0dd118), the HG and RSA plots both indicate a high degree of activity, however, there are only around 3-6 active, relevant electrodes for this subject.

Table 5 – Active Electrodes and Theoretical Utility. Active electrodes are identified from comparison of RSA significance, HG response, and digit flexion. (Beta || HG RSA > 0). The TU metric for each subject is then tabulated as the ratio of active electrodes to viable recording electrodes.

Table 2 - Active Electrodes (Beta || HG RSA > 0)					
Subject ID	**Grid Spacing**	**Task Type**			**Theoretical Utility**
		Finger Flexion	**Grasping**	**Hand Posture**	
Macro-1	1cm	6	3	--	0.07
Macro-2	1cm	--	2	--	0.03
Macro-3	1cm	13	14	31	0.30
Macro-4	*1cm*	*17*	*17*	--	*0.27*
Macro-5	1cm	--	34	--	0.53
Macro-6	1cm	--	24	--	0.38
Macro-7	1cm	--	17	--	0.27
Mini-1	*7.5mm*	*47*	*50*	*42*	*0.72*
Mini-2	7.5mm	--	17	--	0.27
Micro-1	*3mm*	*56*	*64*	--	*0.94*
Micro-2	3mm	32	32	--	0.50
Micro-3	3mm	53	2	27	0.43

The ratio of the active electrodes to the number of valid channels (channels initially screened to be of appropriate recording quality and SNR) is determined as the 'Theoretical Utility' of each

subject's recording and grid, shown in Table 2. This is primarily used as a metric of data quality and to confirm the selection of subjects for classification and comparison and prevent garbage in, garbage out. Note, however, even though Macro-4 (77da65) does not have the highest TU for the macrogrids, this subject performed a full finger flexion task. Had Macro-3 (6b68ef) performed a full complement of finger movements, they would have been chosen for classification.

10.3.5 Classification Performance

Classification performance across the various classification tasks is shown in Table 3, below. The number given is the mean ratio correct across five-fold cross-validation using features constructed over the given window. It is important to note that these numbers on their own are somewhat misleading because of an unequal distribution of classes. In the presentation of the task to the patient, each instruction to move any finger or perform a grasp was preceded by a duration of time where they were instructed to rest. This means that there are significantly more data labeled rest than any particular movement. For this reason random performance would not be expected to produce a mean ratio correct of 1/7. Also note that the differing numbers of samples between the grid patients is due to two factors. First, as explained above, a significant portion of the microgrid data had to be discarded prior to analysis based on faulty contacts during the awake craniotomy or other issues related to the intraoperative setting. Second, the subjects took different amounts of time to move their fingers or flexed multiple times after cue, resulting in different numbers of samples generated during feature selection. Those marked as a dash did not contain enough data points from each class to perform 5-fold cross-validation. The classifiers generating the matrices were trained on a random 80% of the data and tested on the remaining 20%. The times shown correspond to the amount of time over which the log power in the high gamma band was averaged in order to produce features. The macrogrid remained essentially unclassifiable, while the microgrid yielded accuracy as high as 93% on the 12-class problem and 97% on the seven-class problem. Surprisingly, the minigrid (7.5mm) also showed as high as 90% for classification of fingers, though this is for a much simpler 4 class set in which the thumb and index are quite separable and pinch and rest are also quite unique. The performance for the grasp classes drops to 50% which, while not quite as poor as with the macrogrid, is quite bad considering that this is also for the collapsed classes which should have more data and useable observations. SVMs using an RBF rather than a linear kernel did not significantly increase the classification accuracy (data not shown).

Grid Type (spacing)	Classification Task (classes)	SVM Window Length (ms)		
		107	186	250
micro (3mm)	Gross Finger Movement (7)	0.940	0.970	0.969
	Finger Direction (12)	0.842	0.926	--
	Object Gripping (7)	--	--	0.889
	Simple Grasps (4)	--	--	0.980
mini (7.5mm)	Gross Finger Movement (4)	0.832	0.866	0.902
	Finger Direction (6)	0.820	0.891	--
	Object Gripping (7)	--	--	0.508
	Simple Grasps (4)	--	--	0.533
macro (1cm)	Gross Finger Movement (7)	0.389	0.406	0.389
	Finger Direction (12)	0.400	0.431	--
	Object Gripping (7)	--	--	0.152
	Simple Grasps (4)	--	--	0.521

Table 6 - Classifier Performance for Hand Manipulation Tasks. Results are shown for Support Vector Machine (SVM) classification across a series of classification tasks. The finger tasks consisted of distinguishing between rest, pinch, and gross finger movement or distinguishing between rest, pinch, and the direction of movement for each finger. The grasp tasks consisted of distinguishing between all 6 object grasps and rest or a collapsed set of 3 objects/grasps and rest. Numbers given are the mean ratio correct across 5-fold cross validation. Times shown are the size of the window over which the ECoG signal was averaged during feature generation. The first task was simply to distinguish between rest, pinch, and movement of the five fingers. Note that the microgrid drastically outperforms the macrogrid, and that performances for finger classification generally increases with window size.

10.4 So What?

These results show that ECoG macrogrids do not capture enough information to consistently and accurately predict dexterous hand movements. This is shown based both on a measure of the utility of the recorded data and utilizing machine learning techniques at reasonable granularities for prosthetic control to compare the wide disparity in information density between macro- and microgrids. While such information might eventually be captured using more advanced techniques or developing new algorithms(Murphy et al., 2016), we instead advocate the adoption of the ECoG microgrid for motor-related BCI development as a realistic and significant means of acquiring an ideal signal for control while maintaining the invasiveness-SNR tradeoff (Moran, 2010). All of the analyses performed were in parallel to existing BCI studies utilizing many of the same subjects and thus the direct applicability to BCI was never far from mind. For example, the time windows chosen for feature construction were selected to provide reasonable response time if afforded by a prosthetic. The classification techniques were chosen because they require minimal tuning (Spüler et al., 2014). This

means that in research settings classifiers could realistically be trained as the patients were connected to a prosthetic without needing lengthy grid searches over the parameter space.

However, this analysis does not quite indicate whether or not a simple finger movement task or semi-static grasping flexion such as the ones analyzed here would be sufficient to train a regressor or other system to correctly output arbitrarily complex movements in the future. The dimensionality reduction of the brain-space before analysis likely impedes any immediate translation back to movements beyond what was presented as training data. Even if computational power accessible in a practical BCI setting was not an issue, and if all the dimensions of the brain data were passed to the algorithm, it would still not be guaranteed to accurately predict arbitrary movements. To understand why this might be so, imagine if a regressor were given all dimensions and was able to correctly recreate thumb and forefinger movement; it would surely be able to recreate the thumb and forefinger pinch. However, it is currently unknown if complex composite motions such as a two-finger pinch are composed only of the cortical superposition of a thumb and forefinger movement. This is certainly not the case when examining components of the muscular physiological representation (synergies) (Santello, Flanders and Soechting, 1998; Desmurget et al., 2014). It is an open research question as to whether or not such movements in fact are encoded as more complex informational cascades between motor areas, etc. in which case the training task would have to be significantly more complex in order to be capable of generating arbitrary future movements (Wong et al., 2013). Nevertheless, the ability to localize spatially and identify individual movements in the microscale even with the challenges of the intraoperative recordings is promising as it reflects the potential expandability of ECoG as a recording modality (Wander and Rao, 2014).

Of course, while this study makes a compelling case for the promising role of ECoG microgrids as a foundation for sophisticated BCIs, several caveats remain. First, it is important to note that these studies were carried out on individual, separate subjects. It is possible that a particular macrogrid patient is simply not a strong candidate for ECoG-based BCI, regardless of the spatial resolution of the grid (Wander et al., 2013). A patient with both a macro- and a micro- grid or an overlapping system, as seen in some animal implants (Viventi *et al.*, 2011; Orsborn *et al.*, 2015), would be extremely informative for our purposes; however, due to clinical protocol and practical considerations, we have not yet been able to realize this arrangement at UW unlike at some other institutions (Bleichner et al., 2016). Second, it is possible that more advanced algorithmic techniques

or more nuanced feature selection would be able to capture sufficient information from a macrogrid to decompose complex hand movements. Stronger conclusions could be also be drawn from an analysis of additional subjects with 'better' coverage and higher TUs. Other avenues to be pursued include a more in-depth examination of the temporal component of the data to see if there is a temporal distribution in the grips that could be used in concordance with the spatial representation or one could examine the phase coherence of high-gamma during the different grip phases (Darvas, Ojemann and Sorensen, 2009). Further work is also needed on chronic long-term recordings with these types of grids. Even with these considerations, however, we believe ECoG microgrids remain an extremely promising way forward. The strength of our analysis is to show that a microgrid combined with off-the-shelf implementations of classification and regression algorithms allow for robust characterization of hand movements for further utilization in a BCI framework. μECoG is a promising technique that brings sophisticated BCIs one step closer to reality.

Chapter 11: Conclusion

For individuals with neuromuscular impairments, brain-computer interfaces (BCIs) provide the potential for neurologic restoration or improved interactions with their daily environments (Daly et al., 2013). Whether through schemes for rehabilitation (Daly & Wolpaw, 2008; Pfurtscheller, Muller-Putz, Scherer, & Neuper, 2008) or direct replacement of lost sensorimotor function (Bensmaia & Miller, 2014; Daly et al., 2013; Velliste et al., 2008) or communicative ability (Birbaumer, 2006; Wolpaw et al., 2002a), the field has given hope of improved neural function to millions of individuals (Wolpaw & Wolpaw, 2012). For those with CNS injury or limb amputation, one proposed and commonly tested mode of BCI control involves recording cortical signals and translating derived signal features correlated with executed or imagined movements to devices designed for functional restoration in the absence of natural effectors (Wang et al., 2013). Unfortunately, the requirements for real world control, such as natural movement with hands, or hand analogs, for daily tasks such as opening a jar with two hands can be inordinately complex. In these cases, especially ones requiring more dexterity and manipulation such as playing the piano, BCIs must be functional in a more bimanual context with patients potentially utilizing their interface in coordination with other motor behavior.

However, due to the nature of the typical target populations, for example patients with amyotrophic lateral sclerosis (ALS) or brainstem stroke or spinal cord injury, in which there is significant degradation of volitional physical motor ability, much of the research on BCIs has focused on developing assistive devices for situations in which there is no motor ability remaining (Curran and Stokes, 2003). Yet, there is a large population of patients that retain some residual motor function, who could benefit significantly from a targeted BCI that incorporates this residual function, especially in a bimanual control schema (Buma et al., 2010). Our work as described in this dissertation attempts to bridge that gap and provide a framework for consideration in the development of future BCI technologies. In addition, we provide a context regarding expanding the traditional ECoG modality. When combined together, our hope is that thinking about bimanual aspects of control and motor representation will provide a better context in which high-resolution ECoG signals are processed and translated to robotic control (for example within the Adroit framework developed by

Emo Todorov and the GridLab). However, until then, there is significant additional work to be done before true dexterous bimanual control is possible.

Final Thoughts on Bimanuality

The bimanual process of BCI control and overt hand control seems extremely unnatural behaviorally and required several degrees of mental abstraction on the part of the "successful" users. Nevertheless, as we make the assumption that motor-BCI interactions are not that dissimilar from complex motor tasks, this type of coordination might not be unnatural for the underlying motor networks involved, especially for upper limb control. Natural movements almost always require the coordination of different limbs (for example, during walking the legs are coordinated for gait while the arms swing in particular rhythmicity). When we observe only how an individual's two arms might move, we can see that there is a natural tendency to move both arms in some correlated fashion. Yet, we can also clearly operate each arm or hand alone.

In general, arm movements can be divided into three categories:

1) Unimanual movements, where only one of the arms moves. Some movements are typically unimanual, such as writing or drawing.

2) Symmetric bimanual movements, where both arms move together or in opposite directions around a plane of symmetry. Examples of symmetric limb movements are hand clapping, walking, hand movements associated with speech.

3) Non-symmetric bimanual movements, where the two hands move in a nonsymmetric fashion, for example: tying shoelaces, playing the piano or violin, and some kinds of dancing.

If one executes a movement involving more than one limb – one actually performs at least two movements. To that extent, inter-limb-coordination may be considered as generation of a "unitary motor action" from elements of several movements. For bimanual movements, typically the more different the movement executed simultaneously by the two hands, the greater the difficulty. For example, it is very easy to draw a triangle or a circle using one hand. But, to draw a triangle with one hand and simultaneously draw a circle with the other is quite tricky. However, drawing two circles (or triangles) simultaneously, using both hands separately for each is substantially easier. This simple observation may indicate some of the restrictions and preferences of the motor system as this suggests that there are different types of bimanual movements and that they are not merely the sum

of two unimanual movements. Based on the described complexity of the system in question, this is not totally absurd and, in fact, these are included in the concept of coordination.

To execute any movement, the motor system might compute or generate desired values of endpoints for each point in time for each muscle, joint and limb. This type of complex computation as we would normally consider it is, no doubt, a time-consuming process. Therefore, it also reasonable that the nervous system contains an internal representation of compound bimanual movements as unitary motor actions. An important feature of the system is the redundancy in the degrees of freedom. Namely, each movement can be executed in several different ways. Bernstein (Bernstein, 1967) defined motor coordination as "the process of mastering redundant degrees of freedom of the moving organ, in other words its conversion to a controllable system." In other words, this mastery means finding some optimal time-efficient algorithms to control a high degree of freedom (DF) system. This "controllable system" is a real time computational one. Therefore, minimization of the time required for each computation during the movement is of prime importance. Let us assume that "easy" motor tasks (like symmetrical bimanual movements) are less demanding computationally, while harder tasks requires more complex, time-consuming computation. To apply this approach to definitions of difficulty for "bimanual coordination," we may define coordination requiring less computations – as "easier." Looking at the same issue in terms of DF, we may describe "difficulty" as follows: the number of DF of a movement proportional to the number of joints associated with it. In relation to bimanual coordination, we introduce the term: "Functional DF (FDF)," which is the actual number of independent uses of the joints while a certain movement is executed. This is to indicate that the system may be designed to reduce the actual number of DF while executing a certain movement. Note that the number of independently moving joints is always equal to or less than the anatomical number of joints in the given limb ($DF \geq FDF$). The difficulty in bimanual coordination is, therefore, proportional to the level of interlimb independence in the movement: namely, it is proportional to the FDF.

In summary, we suggest that the level of difficulty of interlimb coordination reflects the need to increase the number of controlled degrees of freedom in order to execute the particular movement. To demonstrate the interesting impact of such an approach, especially with BCI and manual coordination, let us briefly consider an example from robotics. What are the differences between robots and humans from a bio/mechanical point of view? The most striking difference is the

perfectly smooth and very rapid performance of multi-joint and multi-limb manipulations by humans as compared with many robots. A primary advantage of the biological brain is its ability to coordinate the joints in both time and space in a highly dynamically efficient mode. While the timing problem is readily solved in robotics, the space problem (where to place the joint) remains a restricting factor. To generate a finer movement by a robot (particularly in space) – we need to increase the number of DF. Consequently, the cost in computational demands rises exponentially! These computational problems limit the possible number of joints in standard artificial systems. In simplistic terms, one could say that the robots are limited by the fact that the number of FDF is always equal to the DF (the sum of the degrees of freedom of the joints). The biological brain, however, seems to be able to reduce the number of DF to number of FDF according to functional demands. This means that our higher cognitive centers do not have to continuously calculate the coordinates for each joint, but only for those independent joints for which we must make dynamic changes due to environmental constraints (as per sensory feedback). This is extremely relevant to the BCI control problem as we extrapolate beyond cursors to systems with innately higher degrees of freedom that also require higher levels of abstraction from the user for optimal dexterous control. Overall, the field of neural engineering or neuroprosthetic control has only just started to open Pandora's box in regards to the factors that will allow for truly functional, effective BCI applications. A bimanual approach is but one more important aspect that may lead us out of the rabbit hole and towards a more integrative and successful solution.

Bibliography

Abraham, A. *et al.* (2014) 'Machine Learning for Neuroimaging with Scikit-Learn', *Frontiers in neuroinformatics*, 8(February), p. 14. doi: 10.3389/fninf.2014.00014.

Adams, J. A. (1971) 'A Closed-Loop Theory of Motor Learning', *Journal of Motor Behavior*, 3(2), pp. 111–150. doi: 10.1080/00222895.1971.10734898.

Adkins-Muir, D. L. and Jones, T. A. (2003) 'Cortical electrical stimulation combined with rehabilitative training: Enhanced functional recovery and dendritic plasticity following focal cortical ischemia in rats', *Neurological Research*. Taylor & Francis, 25(8), pp. 780–788. doi: 10.1179/016164103771953853.

Adkins, D. L. *et al.* (2006) 'Epidural cortical stimulation enhances motor function after sensorimotor cortical infarcts in rats', *Experimental Neurology*, 200(2), pp. 356–370. doi: 10.1016/j.expneurol.2006.02.131.

Adkins, D. L., Hsu, J. E. and Jones, T. A. (2008) 'Motor cortical stimulation promotes synaptic plasticity and behavioral improvements following sensorimotor cortex lesions', *Experimental Neurology*, 212(1), pp. 14–28. doi: 10.1016/j.expneurol.2008.01.031.

Alnajjar, F. *et al.* (2013) 'Muscle synergy space: learning model to create an optimal muscle synergy', *Frontiers in Computational Neuroscience*, 7, p. 136. doi: 10.3389/fncom.2013.00136.

Alnajjar, F. *et al.* (2015) 'Sensory synergy as environmental input integration', *Frontiers in Neuroscience*, 8. doi: 10.3389/fnins.2014.00436.

Amorim, M.-A., Isableu, B. and Jarraya, M. (2006) 'Embodied spatial transformations: "Body analogy" for the mental rotation of objects.', *Journal of Experimental Psychology: General*, 135(3), pp. 327–347. doi: 10.1037/0096-3445.135.3.327.

Ang, K. K. *et al.* (2010) 'Clinical study of neurorehabilitation in stroke using EEG-based motor imagery brain-computer interface with robotic feedback', *2010 Annual International Conference of the IEEE Engineering in Medicine and Biology Society, EMBC'10*, 2010, pp. 5549–5552. doi: 10.1109/IEMBS.2010.5626782.

Battaglia, P. W., Jacobs, R. A. and Aslin, R. N. (2003) 'Bayesian integration of visual and auditory signals for spatial localization', *Journal of the Optical Society of America A*. OSA, 20(7), p. 1391. doi: 10.1364/JOSAA.20.001391.

Bejot, Y. *et al.* (2008) 'Trends in incidence, risk factors, and survival in symptomatic lacunar stroke in dijon, france, from 1989 to 2006: A population-based study', *Stroke*, 39(7), pp. 1945–1951. doi: 10.1161/STROKEAHA.107.510933.

Bennett, K. M. and Lemon, R. N. (1994) 'The influence of single monkey cortico-motoneuronal cells at different levels of activity in target muscles.', *The Journal of physiology*, 477 (Pt 2(2), pp. 291–307. doi: 10.1113/jphysiol.1994.sp020191.

Bensmaia, S. J. and Miller, L. E. (2014) 'Restoring sensorimotor function through intracortical interfaces: progress and looming challenges', *Nature Reviews Neuroscience*. Nature Publishing Group, 15(5), pp. 313–325. doi: 10.1038/nrn3724.

Bernstein, N. (1967) *Coordination and regulation of movement*. Long Island City, NY: Permagon Press.

Birbaumer, N. *et al.* (2000) 'The thought translation device (TTD) for completely paralyzed patients', *IEEE Transactions on Rehabilitation Engineering*, 8(2), pp. 190–193. doi: 10.1109/86.847812.

Birbaumer, N. (2006) 'Breaking the silence: Brain-computer interfaces (BCI) for communication and motor control', *Psychophysiology*, 43(6), pp. 517–532. doi: 10.1111/j.1469-8986.2006.00456.x.

Blakely, T. *et al.* (2008) 'Localization and classification of phonemes using high spatial resolution electrocorticography (ECoG) grids', *Conference proceedings : ...Annual International Conference of the IEEE Engineering in Medicine and Biology Society. IEEE Engineering in Medicine and Biology Society. Annual Conference*, 2008, pp. 4964–4967. doi: 10.1109/IEMBS.2008.4650328 [doi].

Blakely, T. *et al.* (2009) 'Robust, long-term control of an electrocorticographic brain-computer interface with fixed parameters', *Neurosurgical Focus*, 27(1), p. E13. doi: 10.3171/2009.4.FOCUS0977.

Blakely, T. (2013) 'Decoding Coordinated Hand Movement in Human Primary Motor Cortex Using High Resolution Electrocorticography', *Department of Bioengineering, University of Washington*, Dissertati.

Blakemore, S. J., Wolpert, D. M. and Frith, C. (2000) 'Why can't you tickle yourself?', *Neuroreport*, 11(11), pp. R11-6. doi: 10.1097/00001756-200008030-00002.

Blankertz, B. *et al.* (2010) 'The Berlin brain-computer interface: Non-medical uses of BCI technology', *Frontiers in Neuroscience*, 4(DEC), p. 198. doi: 10.3389/fnins.2010.00198.

Bleichner, M. G. *et al.* (2016) 'Give me a sign: decoding four complex hand gestures based on high-density ECoG', *Brain Structure and Function*. Springer Berlin Heidelberg, 221(1), pp. 203–216. doi: 10.1007/s00429-014-0902-x.

Brinkman, C. (1981) 'Lesions in supplementary motor area interfere with a monkey's performance of a bimanual coordination task', *Neuroscience Letters*, 27(3), pp. 267–270. doi: 10.1016/0304-3940(81)90441-9.

Broccard, F. D. *et al.* (2014) 'Closed-loop brain-machine-body interfaces for noninvasive rehabilitation of movement disorders', *Annals of Biomedical Engineering*, 42(8), pp. 1573–1593. doi: 10.1007/s10439-014-1032-6.

Brouwer, A. M. and van Erp, J. B. F. (2010) 'A tactile P300 brain-computer interface', *Frontiers in Neuroscience*, 4(MAY), p. 19. doi: 10.3389/fnins.2010.00019.

Buma, F. E. *et al.* (2010) 'Review: Functional Neuroimaging Studies of Early Upper Limb Recovery After Stroke: A Systematic Review of the Literature', *Neurorehabilitation and Neural Repair*, 24(7), pp. 589–608. doi: 10.1177/1545968310364058.

Bundy, D. T. *et al.* (2012) 'Using ipsilateral motor signals in the unaffected cerebral hemisphere as a signal platform for brain–computer interfaces in hemiplegic stroke survivors', *Journal of Neural Engineering*, 9(3), p. 36011. doi: 10.1088/1741-2560/9/3/036011.

Bundy, D. T. *et al.* (2014) 'Characterization of the effects of the human dura on macro- and micro-electrocorticographic recordings', *Journal of Neural Engineering*, 11(1), p. 16006. doi: 10.1088/1741-2560/11/1/016006.

Buzsaki, G. (2006) *Rhythms of the Brain*. Oxford University Press.

Buzsáki, G., Anastassiou, C. a and Koch, C. (2012) 'The origin of extracellular fields and currents--EEG, ECoG, LFP and spikes.', *Nature reviews. Neuroscience*, 13(6), pp. 407–20. doi: 10.1038/nrn3241.

Carmena, J. M. *et al.* (2003) 'Learning to control a brain-machine interface for reaching and grasping by primates.', *PLoS biology*, 1(2), p. E42. doi: 10.1371/journal.pbio.0000042.

Cheung, W. *et al.* (2012) 'Simultaneous brain-computer interfacing and motor control: Expanding the reach of non-invasive BCIs', *Proceedings of the Annual International Conference of the IEEE Engineering in Medicine and Biology Society, EMBS*. IEEE, 2012, pp. 6715–6718. doi: 10.1109/EMBC.2012.6347535.

Clark, A. (2013) 'Whatever next? Predictive brains, situated agents, and the future of cognitive science', *Behavioral and Brain Sciences*. Cambridge University Press, 36(3), pp. 181–204. doi: 10.1017/S0140525X12000477.

Collinger, J. L. *et al.* (2013) 'High-performance neuroprosthetic control by an individual with tetraplegia', *The Lancet*, 381(9866), pp. 557–564. doi: 10.1016/S0140-6736(12)61816-9.

Coronado, V. G. *et al.* (2011) 'Surveillance for traumatic brain injury-related deaths--United States, 1997-2007.', *Morbidity and mortality weekly report. Surveillance summaries (Washington, D.C. : 2002)*, 60(5), pp. 1–32. doi: 2011-723-011/21044.

Curran, E. A. and Stokes, M. J. (2003) 'Learning to control brain activity: A review of the production and control of EEG components for driving brain-computer interface (BCI) systems', *Brain and Cognition*, 51(3), pp. 326–336. doi: 10.1016/S0278-2626(03)00036-8.

Daly, I. *et al.* (2013) 'On the control of brain-computer interfaces by users with cerebral palsy', *Clinical Neurophysiology*. International Federation of Clinical Neurophysiology, 124(9), pp. 1787–1797. doi: 10.1016/j.clinph.2013.02.118.

Daly, J. J. *et al.* (2009) 'Feasibility of a New Application of Noninvasive Brain Computer Interface (BCI): A Case Study of Training for Recovery of Volitional Motor Control After Stroke', *Journal of Neurologic Physical Therapy*, 33(4), pp. 203–211. doi: 10.1097/NPT.0b013e3181c1fc0b.

Daly, J. J. and Wolpaw, J. R. (2008) 'Brain-computer interfaces in neurological rehabilitation', *The Lancet Neurology*. Elsevier Ltd, 7(11), pp. 1032–1043. doi: 10.1016/S1474-4422(08)70223-0.

Darvas, F. *et al.* (2004) 'Mapping human brain function with MEG and EEG: methods and validation', *NeuroImage*, 23, pp. S289–S299. doi: 10.1016/j.neuroimage.2004.07.014.

Darvas, F. *et al.* (2010) 'High gamma mapping using EEG', *NeuroImage*. Elsevier Inc., 49(1), pp. 930–938. doi: 10.1016/j.neuroimage.2009.08.041.

Darvas, F., Ojemann, J. G. and Sorensen, L. B. (2009) 'Bi-phase locking - a tool for probing non-linear interaction in the human brain', *NeuroImage*. Elsevier Inc., 46(1), pp. 123–132. doi: 10.1016/j.neuroimage.2009.01.034.

Demain, S. *et al.* (2013) 'A narrative review on haptic devices: relating the physiology and psychophysical properties of the hand to devices for rehabilitation in central nervous system disorders', *Disability and Rehabilitation: Assistive Technology*, 8(3), pp. 181–189. doi: 10.3109/17483107.2012.697532.

Desmurget, M. *et al.* (2014) 'Neural representations of ethologically relevant hand/mouth synergies in the human precentral gyrus', *Proceedings of the National Academy of Sciences*, 111(15), pp. 5718–5722. doi: 10.1073/pnas.1321909111.

Dewhurst, D. J. (1967) 'Neuromuscular control system', *IEEE Transactions on Biomedical Engineering*, 14(3), p. S. 167-171.

Doble, J. E. *et al.* (2003) 'Impairment, Activity, Participation, Life Satisfaction, and Survival in Persons With Locked-In Syndrome for Over a Decade: Follow-Up on a Previously Reported Cohort', *The Journal of head trauma rehabilitation*. LWW, 18(5), pp. 435–444.

Doya, K. *et al.* (2007) *Bayesian Brain: Probabilistic Approaches to Neural Coding*, *Dynamical Systems*. Edited by K. Doya. Cambridge, Mass.: Cambridge, Mass. : MIT Press. doi: 10.7551/mitpress/9780262042383.001.0001.

Drucker, H. *et al.* (1997) 'Support vector regression machines', *Advances in Neural Information Processing Systems*, 1, pp. 155–161. doi: 10.1.1.10.4845.

Eisen, A. *et al.* (2015) 'Does dysfunction of the mirror neuron system contribute to symptoms in amyotrophic lateral sclerosis?', *Clinical Neurophysiology*, 126(7), pp. 1288–1294. doi: 10.1016/j.clinph.2015.02.003.

Eng, D. P. *et al.* (2011) 'Spatial and temporal movement characteristics after robotic training of arm and hand: A case study of a person with incomplete spinal cord injury', *IEEE International Conference on Intelligent Robots and Systems*. Ieee, pp. 1711–1716. doi: 10.1109/IROS.2011.6048735.

Evarts, E. V (1973) 'Motor cortex reflexes associated with learned movement', *Science (New York, N.Y.)*, 179(4072), pp. 501–503. doi: 10.1126/science.179.4072.501.

Fajen, B. R. and Matthis, J. S. (2011) 'Direct perception of action-scaled affordances: The shrinking gap problem.', *Journal of Experimental Psychology: Human Perception and Performance*, 37(5), pp. 1442–1457. doi: 10.1037/a0023510.

Fajen, B. R. and Warren, W. H. (2003) 'Behavioral dynamics of steering, obstable avoidance, and route selection.', *Journal of Experimental Psychology: Human Perception and Performance*, 29(2), pp. 343–362. doi: 10.1037/0096-1523.29.2.343.

Faller, J. *et al.* (2013) 'Online co-adaptive brain-computer interfacing: Preliminary results in individuals with spinal cord injury', *International IEEE/EMBS Conference on Neural Engineering, NER*, 3, pp. 977–980. doi:

10.1109/NER.2013.6696099.

Faradji, F., Ward, R. K. and Birch, G. E. (2009) 'Plausibility assessment of a 2-state self-paced mental task-based BCI using the no-control performance analysis', *Journal of Neuroscience Methods*, 180(2), pp. 330–339. doi: 10.1016/j.jneumeth.2009.03.011.

Faul, M. *et al.* (2010) 'Traumatic brain injury in the United States: emergency department visits, hospitalizations, and deaths', *Centers for Disease Control and Prevention, National Center for Injury Prevention and Control*, pp. 891–904. doi: 10.1016/B978-0-444-52910-7.00011-8.

Felton, E. A. *et al.* (2007) 'Electrocorticographically controlled brain–computer interfaces using motor and sensory imagery in patients with temporary subdural electrode implants', *Journal of Neurosurgery*. American Association of Neurological Surgeons, 106(3), pp. 495–500. doi: 10.3171/jns.2007.106.3.495.

Fetz, E. E. (1969) 'Operant Conditioning of Cortical Unit Activity', *Science*, 163(3870), pp. 955–958. doi: 10.1126/science.163.3870.955.

Fetz, E. E. and Baker, M. A. (1973) 'Operantly conditioned patterns on precentral unit activity and correlated responses in adjacent cells and contralateral muscles.', *Journal of Neurophysiology*, 36(2).

Fischl, B. (2012) 'FreeSurfer', *NeuroImage*, 62(2), pp. 774–781. doi: 10.1016/j.neuroimage.2012.01.021.

Flor, H. *et al.* (1995) 'Phantom-limb pain as a perceptual correlate of cortical reorganization following arm amputation', *Nature*, 375(6531), pp. 482–484. doi: 10.1038/375482a0.

Friedrich, E. V. C., Scherer, R. and Neuper, C. (2012) 'The effect of distinct mental strategies on classification performance for brain-computer interfaces', *International Journal of Psychophysiology*. Elsevier B.V., 84(1), pp. 86–94. doi: 10.1016/j.ijpsycho.2012.01.014.

Friston, K. (2005) 'A theory of cortical responses', *Philosophical Transactions of the Royal Society B: Biological Sciences*, 360(1456), pp. 815–836. doi: 10.1098/rstb.2005.1622.

Friston, K. (2010) 'The free-energy principle: a unified brain theory?', *Nature Reviews Neuroscience*. Nature Publishing Group, 11(2), pp. 127–138. doi: 10.1038/nrn2787.

Friston, K. (2011) 'What is optimal about motor control?', *Neuron*, 72(3), pp. 488–498. doi: 10.1016/j.neuron.2011.10.018.

Gage, G. J. *et al.* (2005) 'Naive coadaptive cortical control.', *Journal of neural engineering*, 2(2), pp. 52–63. doi: 10.1088/1741-2560/2/2/006.

Ganguly, K. *et al.* (2009) 'Cortical Representation of Ipsilateral Arm Movements in Monkey and Man', *Journal of Neuroscience*, 29(41), pp. 12948–12956. doi: 10.1523/JNEUROSCI.2471-09.2009.

Ganguly, K. *et al.* (2011) 'Reversible large-scale modification of cortical networks during neuroprosthetic control', *Nature Neuroscience*, 14(5), pp. 662–667. doi: 10.1038/nn.2797.

Ganguly, K. and Carmena, J. M. (2009) 'Emergence of a stable cortical map for neuroprosthetic control', *PLoS Biology*, 7(7), p. e1000153. doi: 10.1371/journal.pbio.1000153.

George, D. and Hawkins, J. (2009) 'Towards a mathematical theory of cortical micro-circuits', *PLoS Computational Biology*, 5(10). doi: 10.1371/journal.pcbi.1000532.

Gibson, E. J. (1979) *The ecological approach to visual perception*, *of Experimental Psychology Human Perception and*. Houghton Mifflin.

Gilja, V. *et al.* (2011) 'Challenges and opportunities for next-generation intracortically based neural prostheses.', *IEEE transactions on bio-medical engineering*, 58(7), pp. 1891–9. doi: 10.1109/TBME.2011.2107553.

Gilja, V. *et al.* (2012) 'A high-performance neural prosthesis enabled by control algorithm design', *Nature Neuroscience*, 15(12), pp. 1752–1757. doi: 10.1038/nn.3265.

Goldreich, D. (2007) 'A Bayesian perceptual model replicates the cutaneous rabbit and other tactile spatiotemporal illusions', *PLoS ONE*, 2(3), p. e333. doi: 10.1371/journal.pone.0000333.

Goldreich, D. and Tong, J. (2013) 'Prediction, postdiction, and perceptual length contraction: A bayesian low-speed prior captures the cutaneous rabbit and related illusions', *Frontiers in Psychology*, 4(MAY). doi: 10.3389/fpsyg.2013.00221.

Gomez-Rodriguez, M., Peterst, J., *et al.* (2010) 'Closing the sensorimotor loop: Haptic feedback facilitates decoding of arm movement imagery', *Conference Proceedings - IEEE International Conference on Systems, Man and Cybernetics*, 8(3), pp. 121–126. doi: 10.1109/ICSMC.2010.5642217.

Gomez-Rodriguez, M., Grosse-Wentrup, M., *et al.* (2010) 'Epidural ECoG online decoding of arm movement intention in hemiparesis', *Proceedings - Workshop on Brain Decoding: Pattern Recognition Challenges in Neuroimaging, WBD 2010 - In Conjunction with theInternational Conference on Pattern Recognition, ICPR 2010*, pp. 36–39. doi: 10.1109/WBD.2010.17.

Green, A. M. and Kalaska, J. F. (2011) 'Learning to move machines with the mind', *Trends in Neurosciences*. Elsevier Ltd, 34(2), pp. 61–75. doi: 10.1016/j.tins.2010.11.003.

Grensham, G. E., Stason, W. B. and Duncan, P. W. (1995) 'Post-Stroke Rehabilitation'.

Harvey, R. L. and Nudo, R. J. (2007) 'Cortical Brain Stimulation: A Potential Therapeutic Agent for Upper Limb Motor Recovery Following Stroke', *Topics in Stroke Rehabilitation*. Taylor & Francis, 14(6), pp. 54–67. doi: 10.1310/tsr1406-54.

HENRY, F. M. and HARRISON, J. S. (1961) 'Refractoriness of a Fast Movement', *Perceptual and Motor Skills*, 13(3), pp. 351–354. doi: 10.2466/pms.1961.13.3.351.

Hill, N. J. *et al.* (2012) 'Recording Human Electrocorticographic (ECoG) Signals for Neuroscientific Research and Real-time Functional Cortical Mapping', *Journal of Visualized Experiments*. JoVE, (64), p. e3993. doi: 10.3791/3993.

Hochberg, L. R. *et al.* (2006) 'Neuronal ensemble control of prosthetic devices by a human with tetraplegia', *Nature*. Nature Publishing Group, 442(7099), pp. 164–171. doi: 10.1038/nature04970.

Huang, M. *et al.* (2008) 'Cortical Stimulation for Upper Limb Recovery Following Ischemic Stroke: A Small Phase II Pilot Study of a Fully Implanted Stimulator', *Topics in Stroke Rehabilitation*. Taylor & Francis, 15(2), pp. 160–172. doi: 10.1310/tsr1502-160.

Hudson, T. E., Maloney, L. T. and Landy, M. S. (2008) 'Optimal compensation for temporal uncertainty in movement planning', *PLoS Computational Biology*. Public Library of Science, 4(7), pp. 1–9. doi: 10.1371/journal.pcbi.1000130.

Jackson, A., Baker, S. N. and Fetz, E. E. (2006) 'Tests for presynaptic modulation of corticospinal terminals from peripheral afferents and pyramidal tract in the macaque', *The Journal of Physiology*. Blackwell Publishing Ltd, 573(1), pp. 107–120. doi: 10.1113/jphysiol.2005.100537.

Jacobs, R. A. and Fine, I. (1999) 'Experience-dependent integration of texture and motion cues to depth', *Vision Research*, 39(24), pp. 4062–4075. doi: 10.1016/S0042-6989(99)00120-0.

Jarosiewicz, B. *et al.* (2013) 'Advantages of closed-loop calibration in intracortical brain–computer interfaces for people with tetraplegia', *Journal of Neural Engineering*, 10(4), p. 46012. doi: 10.1088/1741-2560/10/4/046012.

Jelliffe (1910) *Vergleichende Lokalisationslehre der Grosshirnrinde*, *The Journal of Nervous and Mental Disease*. Leipzig: J.A. Barth. doi: 10.1097/00005053-191012000-00013.

Jensen, O. *et al.* (2011) 'Using brain-computer interfaces and brain-state dependent stimulation as tools in cognitive neuroscience', *Frontiers in Psychology*, 2(MAY), p. 100. doi: 10.3389/fpsyg.2011.00100.

Johnson, L. A. *et al.* (2012) 'Sleep spindles are locally modulated by training on a brain-computer interface.', *Proceedings of the National Academy of Sciences of the United States of America*. National Academy of Sciences, 109(45), pp. 18583–8. doi: 10.1073/pnas.1207532109.

Kadivar, Z. *et al.* (2011) 'Comparison of reaching kinematics during mirror and parallel robot assisted movements', *Studies in Health Technology and Informatics*, 163, pp. 247–253. doi: 10.3233/978-1-60750-706-2-247.

Kandel, E. R. (2012) *Principles of neural science*. New York: McGraw-Hill.

Kapeller, C. *et al.* (2014) 'Single trial detection of hand poses in human ECoG using CSP based feature extraction', *Conference proceedings : ... Annual International Conference of the IEEE Engineering in Medicine and Biology Society. IEEE Engineering in Medicine and Biology Society. Annual Conference*, 2014, pp. 4599–4602. doi: 10.1109/EMBC.2014.6944648.

Kawato, M. (1999) 'Internal models for motor control and trajectory planning', *Current Opinion in Neurobiology*, 9(6), pp. 718–727. doi: 10.1016/S0959-4388(99)00028-8.

Kipke, D. R. *et al.* (2008) 'Advanced Neurotechnologies for Chronic Neural Interfaces: New Horizons and Clinical Opportunities', *Journal of Neuroscience*, 28(46).

Knill, D. C. (2005) 'Reaching for visual cues to depth: The brain combines depth cues differently for motor control and perception', *Journal of Vision*, 5(2), p. 2. doi: 10.1167/5.2.2.

Knill, D. C. (2007) 'Learning Bayesian priors for depth perception.', *Journal of vision*, 7(8), p. 13. doi: 10.1167/7.8.13.

Knill, D. C. and Pouget, A. (2004) 'The Bayesian brain: The role of uncertainty in neural coding and computation', *Trends in Neurosciences*, 27(12), pp. 712–719. doi: 10.1016/j.tins.2004.10.007.

Körding, K. P. and Wolpert, D. M. (2004) 'Bayesian integration in sensorimotor learning', *Nature*, 427(6971), pp. 244–247. doi: 10.1038/nature02169.

Krusienski, D. J. and Shih, J. J. (2011) 'Control of a Visual Keyboard Using an Electrocorticographic Brain–Computer Interface', *Neurorehabilitation and Neural Repair*. SAGE PublicationsSage CA: Los Angeles, CA, 25(4), pp. 323–331. doi: 10.1177/1545968310382425.

Kubánek, J. *et al.* (2009) 'Decoding flexion of individual fingers using electrocorticographic signals in humans', *Journal of Neural Engineering*, 6(6), p. 66001. doi: 10.1088/1741-2560/6/6/066001.

Kübler, A. *et al.* (2001) 'Brain–computer communication: Unlocking the locked in.', *Psychological Bulletin*. American Psychological Association, 127(3), pp. 358–375. doi: 10.1037/0033-2909.127.3.358.

Kumar, V., Xu, Z. and Todorov, E. (2013) 'Fast, strong and compliant pneumatic actuation for dexterous tendon-driven hands', *Proceedings - IEEE International Conference on Robotics and Automation*, pp. 1512–1519. doi: 10.1109/ICRA.2013.6630771.

Lancaster, J. L. *et al.* (1997) 'Automated labeling of the human brain: a preliminary report on the development and evaluation of a forward-transform method.', *Human brain mapping*. NIH Public Access, 5(4), pp. 238–42. doi: 10.1002/(SICI)1097-0193(1997)5:4<238::AID-HBM6>3.0.CO;2-4.

Lancaster, J. L. *et al.* (2000) 'Automated Talairach Atlas labels for functional brain mapping', *Human Brain Mapping*. John Wiley & Sons, Inc., 10(3), pp. 120–131. doi: 10.1002/1097-0193(200007)10:3<120::AID-HBM30>3.0.CO;2-8.

Latash, M. (2008) *Synergy*. Oxford, NY: Oxford University Press.

Latash, M. L. and Anson, J. G. (2006) 'Synergies in Health and Disease', *Physical therapy*, 86(8), pp. 1151–1160. doi: 10.1007/s00421-002-0739-5.

Latash, M. L., Scholz, J. P. and Schöner, G. (2007) 'Toward a New Theory of Motor Synergies', *Motor Control*, 11(3), pp. 276–308. doi: 10.1123/mcj.11.3.276.

Lebedev, M. A. *et al.* (2005) 'Cortical Ensemble Adaptation to Represent Velocity of an Artificial Actuator Controlled by a Brain-Machine Interface', *Journal of Neuroscience*, 25(19).

Leeb, R. *et al.* (2013) 'Thinking penguin: Multimodal brain-computer interface control of a VR game', *IEEE Transactions on Computational Intelligence and AI in Games*, 5(2), pp. 117–128. doi: 10.1109/TCIAIG.2013.2242072.

Leuthardt, E. C. *et al.* (2004) 'A brain–computer interface using electrocorticographic signals in humans', *Journal of Neural Engineering*, 1(2), pp. 63–71. doi: 10.1088/1741-2560/1/2/001.

Leuthardt, E. C., Miller, K. J., *et al.* (2006) 'Electrocorticography-based brain computer interface - The seattle experience', *IEEE Transactions on Neural Systems and Rehabilitation Engineering*, 14(2), pp. 194–198. doi: 10.1109/TNSRE.2006.875536.

Leuthardt, E. C., Schalk, G., *et al.* (2006) 'The emerging world of motor neuroprosthetics: A neurosurgical perspective', *Neurosurgery*, 59(1), pp. 1–13. doi: 10.1227/01.NEU.0000221506.06947.AC.

Levy, R. *et al.* (2008) 'Cortical stimulation for the rehabilitation of patients with hemiparetic stroke: a multicenter feasibility study of safety and efficacy', *Journal of Neurosurgery*. American Association of Neurological Surgeons, 108(4), pp. 707–714. doi: 10.3171/JNS/2008/108/4/0707.

Matthews, P. B. (1986) 'Observations on the automatic compensation of reflex gain on varying the pre-existing level of motor discharge in man.', *J. Physiol*, 374(1986), pp. 73–90. doi: 10.2106/JBJS.F.01133.

Mayka, M. A. *et al.* (2006) 'Three-dimensional locations and boundaries of motor and premotor cortices as defined by functional brain imaging: A meta-analysis', *NeuroImage*, 31(4), pp. 1453–1474. doi: 10.1016/j.neuroimage.2006.02.004.

McFarland, D. J., Lefkowicz, A. T. and Wolpaw, J. R. (1997) 'Design and operation of an EEG-based brain-computer interface with digital signal processing technology', *Behavior Research Methods, Instruments, & Computers*. Springer-Verlag, 29(3), pp. 337–345. doi: 10.3758/BF03200585.

McFarland, D. J., Sarnacki, W. A. and Wolpaw, J. R. (2010) 'Electroencephalographic (EEG) control of three-dimensional movement.', *Journal of neural engineering*, 7(3), p. 36007. doi: 10.1088/1741-2560/7/3/036007.

Mellinger, J. *et al.* (2007) 'An MEG-based brain–computer interface (BCI)', *NeuroImage*, 36(3), pp. 581–593. doi: 10.1016/j.neuroimage.2007.03.019.

Michaels, F. C. and Carello, C. (1981) *Direct perception*, *Century Pschology Series*. Englewood Cliffs, NJ: Prentice-Hall. doi: 10.1002/0470018860.s00170.

Miller, K. J. *et al.* (2007) 'Spectral Changes in Cortical Surface Potentials during Motor Movement', *Journal of Neuroscience*, 27(9), pp. 2424–2432. doi: 10.1523/JNEUROSCI.3886-06.2007.

Miller, K. J. *et al.* (2010) 'Cortical activity during motor execution, motor imagery, and imagery-based online feedback', *Proceedings of the National Academy of Sciences*, 107(9), pp. 4430–4435. doi: 10.1073/pnas.0913697107.

Milovanovic, I. *et al.* (2015) 'Simultaneous and independent control of a brain-computer interface and contralateral limb movement', *Brain-Computer Interfaces*, 2(4), pp. 174–185. doi: 10.1080/2326263X.2015.1080961.

Mitz, a R. and Wise, S. P. (1987) 'The somatotopic organization of the supplementary motor area: intracortical microstimulation mapping.', *The Journal of neuroscience : the official journal of the Society for Neuroscience*, 7(4), pp. 1010–1021.

Moran, D. (2010) 'Evolution of brain-computer interface: Action potentials, local field potentials and electrocorticograms', *Current Opinion in Neurobiology*. Elsevier Ltd, 20(6), pp. 741–745. doi: 10.1016/j.conb.2010.09.010.

Moritz, C. T., Perlmutter, S. I. and Fetz, E. E. (2008) 'Direct control of paralysed muscles by cortical neurons', *Nature*. Nature Publishing Group, 456(7222), pp. 639–642. doi: 10.1038/nature07418.

Mulliken, G. H., Musallam, S. and Andersen, R. A. (2008) 'Decoding Trajectories from Posterior Parietal Cortex Ensembles', *Journal of Neuroscience*, 28(48), pp. 12913–12926. doi: 10.1523/JNEUROSCI.1463-08.2008.

Murphy, M. D. *et al.* (2016) 'Current Challenges Facing the Translation of Brain Computer Interfaces from Preclinical Trials to Use in Human Patients', *Frontiers in Cellular Neuroscience*, 9(January), pp. 1–14. doi: 10.3389/fncel.2015.00497.

Murray, C. J. L. *et al.* (1996) *Global health statistics : a compendium of incidence, prevalence, and mortality estimates for over 200 conditions*, *Global burden of disease and injury series 2*. Published by the Harvard School of Public Health on behalf of the World Health Organization and the World Bank.

Myrden, A. J. B. *et al.* (2011) 'A Brain-Computer Interface Based on Bilateral Transcranial Doppler Ultrasound', *PLoS ONE*, 6(9), p. e24170. doi: 10.1371/journal.pone.0024170.

National Institutes of Health (2009) 'Stroke: challenges, progress and promise', *Retrieved July*, (February). doi: NIH Publication No. 09-6451.

NSCISC (2010) 'National Spinal Cord Injury Statistical Center (NSCISC): Annual report for the Model Spinal Cord Injury systems', *Birmingham*, p. 86.

Of, A. (2013) 'Spinal Cord Injury Facts and Figures at a Glance', *The Journal of Spinal Cord Medicine*, 36(6), pp. 715–716. doi: 10.1179/1079026813Z.000000000230.

Orsborn, A. L. *et al.* (2012) 'Closed-Loop Decoder Adaptation on Intermediate Time-Scales Facilitates Rapid BMI Performance Improvements Independent of Decoder Initialization Conditions', *IEEE Transactions on Neural Systems and Rehabilitation Engineering*, 20(4), pp. 468–477. doi: 10.1109/TNSRE.2012.2185066.

Orsborn, A. L. *et al.* (2014) 'Closed-loop decoder adaptation shapes neural plasticity for skillful neuroprosthetic control', *Neuron*. Elsevier Inc., 82(6), pp. 1380–1393. doi: 10.1016/j.neuron.2014.04.048.

Orsborn, A. L. *et al.* (2015) 'Semi-chronic chamber system for simultaneous subdural electrocorticography, local field potentials, and spike recordings', *International IEEE/EMBS Conference on Neural Engineering, NER*, 2015–July, pp. 398–401. doi: 10.1109/NER.2015.7146643.

Palaniappan, R. *et al.* (2002) 'A new brain-computer interface design using fuzzy ARTMAP', *IEEE Transactions on Neural Systems and Rehabilitation Engineering*, 10(3), pp. 140–148. doi: 10.1109/TNSRE.2002.802854.

Palaniappan, R. (2006) 'Utilizing gamma band to improve mental task based brain-computer interface design', *IEEE Transactions on Neural Systems and Rehabilitation Engineering*, 14(3), pp. 299–303. doi: 10.1109/TNSRE.2006.881539.

Pascual-Leone, A. *et al.* (2005) 'THE PLASTIC HUMAN BRAIN CORTEX', *Annual Review of Neuroscience*. Annual Reviews, 28(1), pp. 377–401. doi: 10.1146/annurev.neuro.27.070203.144216.

Peper, C. (Lieke) E. *et al.* (2013) 'Bimanual training for children with cerebral palsy: Exploring the effects of Lissajous-based computer gaming', *Developmental Neurorehabilitation*, 16(4), pp. 255–265. doi: 10.3109/17518423.2012.760116.

Pfurtscheller, G. *et al.* (2000) 'Brain oscillations control hand orthosis in a tetraplegic', *Neuroscience Letters*, 292(3), pp. 211–214. doi: 10.1016/S0304-3940(00)01471-3.

Pfurtscheller, G. *et al.* (2008) 'Rehabilitation with brain-computer interface systems', *Computer*, 41(10), pp. 58–65. doi: 10.1109/MC.2008.432.

Pfurtscheller, G. (2010) 'The hybrid BCI', *Frontiers in Neuroscience*, 4(April), pp. 1–11. doi: 10.3389/fnpro.2010.00003.

Pistohl, T. *et al.* (2012) 'Decoding natural grasp types from human ECoG', *NeuroImage*. Elsevier Inc., 59(1), pp. 248–260. doi: 10.1016/j.neuroimage.2011.06.084.

Plautz, E. J. *et al.* (2003) 'Post-infarct cortical plasticity and behavioral recovery using concurrent cortical stimulation and rehabilitative training: A feasibility study in primates', *Neurological Research*. Taylor & Francis, 25(8), pp. 801–810. doi: 10.1179/016164103771953880.

Plow, E. B. *et al.* (2009) 'Invasive cortical stimulation to promote recovery of function after stroke: A critical appraisal', *Stroke*, 40(5), pp. 1926–1931. doi: 10.1161/STROKEAHA.108.540823.

Prasad, G. *et al.* (2010) 'Applying a brain-computer interface to support motor imagery practice in people with stroke

for upper limb recovery: a feasibility study', *Journal of NeuroEngineering and Rehabilitation*, 7(1), p. 60. doi: 10.1186/1743-0003-7-60.

Rao, R. P. N. and Ballard, D. H. (1999) 'Predictive coding in the visual cortex: a functional interpretation of some extra-classical receptive-field effects.', *Nature neuroscience*, 2(1), pp. 79–87. doi: 10.1038/4580.

Ray, S. *et al.* (2008) 'Neural Correlates of High-Gamma Oscillations (60–200 Hz) in Macaque Local Field Potentials and Their Potential Implications in Electrocorticography', *Journal of Neuroscience*, 28(45).

Rosenbaum, A. D. (2009) *Human motor control*. San Diego, CA: Academic Press.

Sanders, L. (2016) 'Bayesian reasoning implicated in some mental disorders | Science News', *Science News*, pp. 1–5. doi: 10.1038/nn.4238.2.

Santello, M., Flanders, M. and Soechting, J. F. (1998) 'Postural hand synergies for tool use', *The Journal of Neuroscience*, 18(23), pp. 10105–10115. doi: citeulike-article-id:423192.

Schalk, G. *et al.* (2004) 'BCI2000: A general-purpose brain-computer interface (BCI) system', *IEEE Transactions on Biomedical Engineering*, 51(6), pp. 1034–1043. doi: 10.1109/TBME.2004.827072.

Schalk, G. *et al.* (2008) 'Two-dimensional movement control using electrocorticographic signals in humans', *Journal of Neural Engineering*, 5(1), pp. 75–84. doi: 10.1088/1741-2560/5/1/008.

Scherer, R. *et al.* (2009) 'Classification of contralateral and ipsilateral finger movements for electrocorticographic brain-computer interfaces', *Neurosurgical Focus*, 27(1), p. E12. doi: 10.3171/2009.4.FOCUS0981.

Schieber, M. H. (2011) 'Dissociating motor cortex from the motor', *The Journal of Physiology*. Blackwell Publishing Ltd, 589(23), pp. 5613–5624. doi: 10.1113/jphysiol.2011.215814.

Schlaug, G., Renga, V. and Nair, D. (2008) 'Transcranial Direct Current Stimulation in Stroke Recovery', *Archives of Neurology*. American Medical Association, 65(12), pp. 193–197. doi: 10.1001/archneur.65.12.1571.

Schmidt, R. A. (1975) 'A schema theory of discrete motor skill learning.', *Psychological Review*, 82(4), pp. 225–260. doi: 10.1037/h0076770.

Schmidt, R. A. (1988) *Motor control and learning: A behavioral emphasis (2nd~ed.)*. 5th Editio. Champaign, IL: Human Kinetics. doi: 9780736079617.

Scholz, J. P. *et al.* (2002) 'Understanding finger coordination through analysis of the structure of force variability', *Biological Cybernetics*, 86(1), pp. 29–39. doi: 10.1007/s004220100279.

Schwartz, A. B. *et al.* (2006) 'Brain-Controlled Interfaces: Movement Restoration with Neural Prosthetics', *Neuron*, 52(1), pp. 205–220. doi: 10.1016/j.neuron.2006.09.019.

Seeber, M. *et al.* (2015) 'High and low gamma EEG oscillations in central sensorimotor areas are conversely modulated during the human gait cycle', *NeuroImage*. Elsevier Inc., 112, pp. 318–326. doi: 10.1016/j.neuroimage.2015.03.045.

Shadmehr, R. and Mussa-Ivaldi, F. A. (1994) 'Adaptive representation of dynamics during learning of a motor task.', *Journal of neuroscience*, 14(5 Pt 2), pp. 3208–24. doi: 8182467.

Shain, W. *et al.* (2003) 'Controlling cellular reactive responses around neural prosthetic devices using peripheral and local intervention strategies', *IEEE Transactions on Neural Systems and Rehabilitation Engineering*, pp. 186–188. doi: 10.1109/TNSRE.2003.814800.

Shanechi, M. M. *et al.* (2013) 'A Real-Time Brain-Machine Interface Combining Motor Target and Trajectory Intent Using an Optimal Feedback Control Design', *PLoS ONE*. Edited by W. Zhan. Public Library of Science, 8(4), p. e59049. doi: 10.1371/journal.pone.0059049.

Sheets, R., Stein, J. and Manetz, T. (2006) 'Biodistribution of DNA plasmid vaccines against HIV-1, Ebola, Severe Acute Respiratory Syndrome, or West Nile virus is similar, without integration, despite differing', *Toxicological …*, 91(2), pp. 610–619. doi: 10.1093/toxsci/kfj169.

Shenoy, K. V. and Carmena, J. M. (2014) 'Combining decoder design and neural adaptation in brain-machine interfaces', *Neuron*. Elsevier Inc., 84(4), pp. 665–680. doi: 10.1016/j.neuron.2014.08.038.

Shenoy, P. *et al.* (2007) 'Finger movement classification for an electrocorticographic BCI', *Proceedings of the 3rd International IEEE EMBS Conference on Neural Engineering*. Ieee, pp. 192–195. doi: 10.1109/CNE.2007.369644.

Simeral, J. D. *et al.* (2011) 'Neural control of cursor trajectory and click by a human with tetraplegia 1000 days after implant of an intracortical microelectrode array', *Journal of Neural Engineering*. NIH Public Access, 8(2), p. 25027. doi: 10.1088/1741-2560/8/2/025027.

Sitaram, R. *et al.* (2008) 'fMRI Brain-Computer Interfaces', *IEEE Signal Processing Magazine*, 25(1), pp. 95–106. doi: 10.1109/MSP.2008.4408446.

Smith, E. and Delargy, M. (2005) 'Locked-in syndrome', *British Medical Journal*, 330(February), pp. 3–6. doi: 10.1136/bmj.g7348.

Smith, M. M. *et al.* (2014) 'Non-invasive detection of high gamma band activity during motor imagery', *Frontiers in Human Neuroscience*, 8(October). doi: 10.3389/fnhum.2014.00817.

Sofiyanti, N., Fitmawati, D. I. and Roza, A. A. (2015) 'Stenochlaena Riauensis (Blechnaceae), A new fern species from riau, Indonesia', *Bangladesh Journal of Plant Taxonomy*, 22(2), pp. 137–141. doi: 10.1007/s13398-014-0173-7.2.

Spüler, M. *et al.* (2014) 'Decoding of motor intentions from epidural ECoG recordings in severely paralyzed chronic stroke patients', *Journal of Neural Engineering*. IOP Publishing, 11(6), p. 66008. doi: 10.1088/1741-2560/11/6/066008.

Tassinari, H., Hudson, T. E. and Landy, M. S. (2006) 'Combining Priors and Noisy Visual Cues in a Rapid Pointing Task', *Journal of Neuroscience*, 26(40), pp. 10154–10163. doi: 10.1523/JNEUROSCI.2779-06.2006.

Taub, E., Ellman, S. J. and Berman, A. J. (1966) 'Deafferentation in Monkeys: Effect on Conditioned Grasp Response', *Science*, 151(3710), pp. 593–4. doi: 10.1126/science.151.3710.593.

Taub, E., Goldberg, I. A. and Taub, P. (1975) 'Deafferentation in monkeys: Pointing at a target without visual feedback', *Experimental Neurology*, 46(1), pp. 178–186. doi: 10.1016/0014-4886(75)90040-0.

Thomas, E., Dyson, M. and Clerc, M. (2013) 'An analysis of performance evaluation for motor-imagery based BCI', *Journal of Neural Engineering*. IOP Publishing, 10(3), p. 31001. doi: 10.1088/1741-2560/10/3/031001.

Tobergte, D. R. and Curtis, S. (2013) *Principles of neuroscience*, *Journal of Chemical Information and Modeling*. New York, NY: McGraw-Hill. doi: 10.1017/CBO9781107415324.004.

Tschudi, H. R. (2010) 'Helmholtz Free Energy of a Phase Containing a Sparse Ensemble of Heterophase Clusters with Application to Nucleation Theory', *Journal of Physical Chemistry B*, 114(9), pp. 3219–3235. doi: 10.1021/jp906511z.

Vaid, J. (2002) *Encyclopedia of the Human Brain*, *Encyclopedia of the Human Brain*. Academic Press. doi: 10.1016/B0-12-227210-2/00059-5.

Velliste, M. *et al.* (2008) 'Cortical Control of a Prosthetic Arm for Self-feeding', *Neurosurgery*. Nature Publishing Group, 63(2), pp. 1098–1101. doi: 10.1227/01.NEU.0000335793.88007.CE.

Vidaurre, C. *et al.* (2011) 'Co-adaptive calibration to improve BCI efficiency', *Journal of Neural Engineering*, 8(2), p. 25009. doi: 10.1088/1741-2560/8/2/025009.

Vigneswaran, G. *et al.* (2013) 'M1 corticospinal mirror neurons and their role in movement suppression during action observation', *Current Biology*, 23(3), pp. 236–243. doi: 10.1016/j.cub.2012.12.006.

Viventi, J. *et al.* (2011) 'Flexible, foldable, actively multiplexed, high-density electrode array for mapping brain activity in vivo', *Nature Neuroscience*. Nature Publishing Group, 14(12), pp. 1599–1605. doi: 10.1038/nn.2973.

Wadman, W. J. *et al.* (1979) 'Control of fast goal-directed arm movements', *Journal of Human Movement Studies*, 5, pp. 3–17. doi: 10.1007/BF00236911.

Wander, J. D. *et al.* (2013) 'Distributed cortical adaptation during learning of a brain-computer interface task', *Proceedings of the National Academy of Sciences*, 110(26), pp. 10818–10823. doi: 10.1073/pnas.1221127110.

Wander, J. D. and Rao, R. P. N. (2014) 'Brain-computer interfaces: A powerful tool for scientific inquiry', *Current Opinion in Neurobiology*. Elsevier Ltd, 25, pp. 70–75. doi: 10.1016/j.conb.2013.11.013.

Wang, L. *et al.* (2007) 'Feature extraction of mental task in BCI based on the method of approximate entropy', *Annual International Conference of the IEEE Engineering in Medicine and Biology - Proceedings*, 2007, pp. 1941–1944. doi: 10.1109/IEMBS.2007.4352697.

Wang, W. *et al.* (2009) 'Human motor cortical activity recorded with micro-ECoG electrodes during individual finger movements', *Proceedings of the 31st Annual International Conference of the IEEE Engineering in Medicine and Biology Society: Engineering the Future of Biomedicine, EMBC 2009*, 2009, pp. 586–589. doi: 10.1109/IEMBS.2009.5333704.

Wang, W. *et al.* (2013) 'An Electrocorticographic Brain Interface in an Individual with Tetraplegia', *PLoS ONE*, 8(2), pp. 1–8. doi: 10.1371/journal.pone.0055344.

Wang, Z. *et al.* (2010) 'Decoding finger flexion from electrocorticographic signals using a sparse gaussian process', *Proceedings - International Conference on Pattern Recognition*. Ieee, pp. 3756–3759. doi: 10.1109/ICPR.2010.915.

Warren, W. H. (2006) 'The dynamics of perception and action.', *Psychological Review*, 113(2), pp. 358–389. doi: 10.1037/0033-295X.113.2.358.

Wolpaw, J. R. *et al.* (1991) 'An EEG-based brain-computer interface for cursor control', *Electroencephalography and Clinical Neurophysiology*, 78(3), pp. 252–259. doi: 10.1016/0013-4694(91)90040-B.

Wolpaw, J. R. *et al.* (2000) 'Brain-computer interface technology: A review of the first international meeting', *IEEE Transactions on Rehabilitation Engineering*, 8(2), pp. 164–173. doi: 10.1109/TRE.2000.847807.

Wolpaw, J. R. *et al.* (2002) 'Brain-computer interfaces for communication and control', *Clinical Neurophysiology*, 113(6), pp. 767–791. doi: 10.1016/S1388-2457(02)00057-3.

Wolpaw, J. R. and McFarland, D. J. (1994) 'Multichannel EEG-based brain-computer communication', *Electroencephalography and Clinical Neurophysiology*, 90(6), pp. 444–449. doi: 10.1016/0013-4694(94)90135-X.

Wolpaw, J. R. and McFarland, D. J. (2004) 'Control of a two-dimensional movement signal by a noninvasive brain-computer interface in humans', *Proceedings of the National Academy of Sciences*, 101(51), pp. 17849–17854. doi: 10.1073/pnas.0403504101.

Wolpaw, J. R., McFarland, D. J. and Vaughan, T. M. (2000) 'Brain-computer interface research at the Wadsworth Center', *IEEE Transactions on Rehabilitation Engineering*, 8(2), pp. 222–226. doi: 10.1109/86.847823.

Wolpaw, J. and Wolpaw, E. W. (2012) *Brain-computer interfaces: something new under the sun. In: Wolpaw JR, Wolpaw EW. Brain-computer interfaces: principles and practice*. Oxford University Press, USA.

Wolpert, D., Ghahramani, Z. and Jordan, M. (1995) 'An internal model for sensorimotor integration', *Science*, 269(5232), pp. 1880–1882. doi: 10.1126/science.7569931.

Wong, Y. T. *et al.* (2013) 'Utilizing movement synergies to improve decoding performance for a brain machine interface', *Proceedings of the Annual International Conference of the IEEE Engineering in Medicine and Biology Society, EMBS*, pp. 289–292. doi: 10.1109/EMBC.2013.6609494.

Wood, G. *et al.* (2014) 'On the need to better specify the concept of â€œcontrolâ€ in brain-computer-interfaces/neurofeedback research', *Frontiers in Systems Neuroscience*, 8(September), p. 171. doi: 10.3389/fnsys.2014.00171.

Wu, Y. C. and Voda, J. A. (1985) 'User-friendly communication board for nonverbal, severely physically disabled individuals.', *Archives of physical medicine and rehabilitation*, 66(12), pp. 827–8.

Yanagisawa, T. *et al.* (2011) 'Real-time control of a prosthetic hand using human electrocorticography signals', *Journal of Neurosurgery*, 114(6), pp. 1715–1722. doi: 10.3171/2011.1.JNS101421.

Young, B. M. *et al.* (2016) 'Brain–Computer Interface Training after Stroke Affects Patterns of Brain–Behavior Relationships in Corticospinal Motor Fibers', *Frontiers in Human Neuroscience*, 10(September), p. 457. doi: 10.3389/fnhum.2016.00457.

Zanos, S., Miller, K. J. and Ojemann, J. G. (2008) 'Electrocorticographic spectral changes associated with ipsilateral individual finger and whole hand movement.', *Conference proceedings : ... Annual International Conference of the IEEE Engineering in Medicine and Biology Society. IEEE Engineering in Medicine and Biology Society. Conference*, 2008, pp. 5939–5942. doi: 10.1109/IEMBS.2008.4650569.

VITA

Devapratim Sarma received Bachelor of Science degrees in Bioengineering and Animal Physiology & Neuroscience from the University of California, San Diego in 2009. He was a research associate at the Swartz Center for Computational Neuroscience from 2008-2011. From 2011-2016, he was a graduate researcher with the GRIDlab and Neural Systems Lab in Seattle. This dissertation is a summation of much of his efforts towards a doctoral degree in the Department of Bioengineering at the University of Washington. As a member of the Center for Sensorimotor Neural Engineering, his current research focuses on optimizing electrocorticographic brain-computer interfaces for cognitive and motor rehabilitation. He is a student member of BMES, IEEE, and SfN. More information can be found at: bodhabuddhi.com